Gamma-ray Signals from Gravitino Dark Matter Decaying to Massive Vector Bosons

Paul Christoph Bätzing
Department of Physics
University of Oslo

A thesis submitted for the degree of
Master of Physics

June 2012

Abstract

In this thesis the width of the gravitino under radiative loop decays $\tilde{G} \to Z^0\nu$ and $\tilde{G} \to W^+l^-$ in R-parity violating SUSY with trilinear R-parity violating couplings is calculated. It is compared to other decay channels [1, 2] and used to set limits on the R-parity violating couplings. It is found that in scenarios with third generation fermions in the loop radiative decays dominate over tree level decays for high sfermion masses and that decays to massive vector bosons can dominate for high sfermion masses and left-right mass splitting. However, the thesis concludes with that including massive vector boson decays changes the limits set on the R-parity violating couplings from the extra-galactic photon spectrum only to a limited degree, even in scenarios where these decay channels dominate.

To my wonderful wife Marit Victoria Rosenvinge.
Du er gleden i mitt liv.

Acknowledgements

I would like to acknowledge the extraordinary help of my advisor Are Raklev, without whom I could never have finished the project. I would also like to thank my fellow master students Ola Liabøtrø, Håvard Sannes, Veronica Øverbye and Kristin Ebbesen for listening to my questions until we could come up with an answer. A great many thanks also to the fellow PhD students in the group, Anders Kvellestad, Lars Andreas Dal and Theresa Palmer. Also many thanks to all the teachers I have had in my life and all the professors that have inspired me on my way.

Contents

List of Figures

List of Tables

LIST OF TABLES

1

Introduction

This thesis investigates whether the radiative decay modes of the gravitino $\tilde{G} \to Z^0\nu$ and $\tilde{G} \to W^+l^-$ contribute to the width of the gravitino in R-parity violating scenarios with a single dominant trilinear coupling in a significant way. Additionally, it is investigated how these processes contribute to the extra galactic photon spectrum, assuming that the gravitino constitutes the main contribution to dark matter, and the spectrum is used to find limits on the R-parity breaking couplings. Chapter 2 introduces supersymmetry and the Minimal Supersymmetric Standard Model (MSSM) with and without R-parity conservation. Chapter 3 gives a brief introduction to gravitinos as a result of local supersymmetry and as a possibility for particle dark matter. Chapter 4 contains the calculation of the decay rates $\tilde{G} \to W^+l^-$ and $\tilde{G} \to Z^0\nu$ and a description of how to evaluate these numerically using version 2.7 of the Loop Tools program [3]. Chapter 5 contains a description of how PYTHIA 6.409 [4] is used to obtain the photon spectrum from the width and how one can use the spectrum to set a limit on the relevant coupling. The results are presented in Chapter 6 in comparison to tree level and $\tilde{G} \to \gamma\nu$ decay rates from [1] and [2] respectively. Finally, limits on the R-parity breaking couplings in a scenario where the massive vector boson processes give the biggest contribution to the gravitino width are investigated. Chapter 7 contains the conclusions.

2

Supersymmetry

This chapter contains a brief introduction to supersymmetry, the general supersymmetric Lagrangian and the Minimal Supersymmetric Standard Model (MSSM). It is inspired by Martin [5], Wiedemann and Müller-Kirsten [6] and the lectures in FYS5190 at the University of Oslo. The notation used in this thesis follows closely the one used by Wiedemann and Müller-Kirsten. The conventions and definitions used in this thesis can be found in Appendix A.1.

Supersymmetric (SUSY) field theories are quantum field theories that can be constructed from extending the space-time symmetries to include gauge symmetries. In the following a general supersymmetric Lagrangian is derived, and then the most popular supersymmetric theory, the MSSM, is summarized with the extension of including R-parity breaking terms.

2.1 The Superpoincaré algebra and the general SUSY Lagrangian

2.1.1 Superpoincaré algebra and its representations

The internal symmetries of space-time are contained in the restricted Poincaré group, whose generators are the generators of Lorentz transformations $M^{\mu\nu}$ and the generators for translation P^{μ}, where a general Lorentz transformation $\Lambda^{\mu}{}_{\nu} = [\exp(-\frac{i}{2}\omega^{\rho\sigma}M_{\rho\sigma})]^{\mu}{}_{\nu}$ is restricted to $\det\Lambda = 1$ and $\Lambda^{0}{}_{0} \geq 1$. This removes space reflections and makes sure time moves in the forward direction. The generators of the group fulfill the following

Lie algebra

$$[M_{\mu\nu}, M_{\rho\sigma}] = -i\left(g_{\mu\rho}M_{\nu\sigma} - g_{\mu\sigma}M_{\nu\rho} - g_{\nu\rho}M_{\mu\sigma} + g_{\nu\sigma}M_{\mu\rho}\right), \tag{2.1}$$

$$[P_\mu, P_\nu] = 0, \tag{2.2}$$

$$[M_{\mu\nu}, P_\rho] = -i\left(g_{\mu\rho}P_\nu - g_{\nu\rho}P_\mu\right). \tag{2.3}$$

It was shown by Haag, Lopuszanski and Sohnius [7] that the most general non-trivial way of extending this symmetry is by constructing a graded Lie algebra, or superalgebra. This is done by introducing N new sets of operators, the Majorana spinor charges Q_a^α with $a = 1, 2, 3, 4$ and $\alpha = 1, ..., N$. One can introduce up to $N = 8$ such sets of operators before the theory is not renormalizable as fields with spin larger than two emerge. This thesis looks at $N = 1$ supersymmetry, where only one such set is introduced. These new operators can be constructed with the Weyl spinors Q_A and $\overline{Q}_{\dot{A}}$ where $A, \dot{A} = 1, 2$,

$$Q_a = \begin{pmatrix} Q_A \\ \overline{Q}_{\dot{A}} \end{pmatrix}. \tag{2.4}$$

These spinors fulfill the following algebra:

$$\{Q_A, Q_B\} = \{\overline{Q}_{\dot{A}}, \overline{Q}_{\dot{B}}\} = 0, \tag{2.5}$$

$$\{Q_A, \overline{Q}_{\dot{B}}\} = 2\sigma^\mu{}_{A\dot{B}}P_\mu, \tag{2.6}$$

$$[Q_A, P_\mu] = [\overline{Q}_{\dot{A}}, P_\mu] = 0 \quad \text{and} \tag{2.7}$$

$$[Q_A, M^{\mu\nu}] = i\sigma^{\mu\nu}{}_A{}^B Q_B. \tag{2.8}$$

To find what kind of particles these operators act on, meaning what the properties of the elements in the vector spaces that a given irreducible representation of the algebra act on are, one finds the Casimir operators of the algebra. The Casimir operators are operators that commute with all elements in the algebra. They are

$$P^2 \equiv P_\mu P^\mu, \tag{2.9}$$

and

$$C^2 \equiv C_{\mu\nu}C^{\mu\nu}, \tag{2.10}$$

where

$$C_{\mu\nu} \equiv B_\mu P_\nu - B_\nu P_\mu, \tag{2.11}$$

and where B_μ is given by

$$B_\mu \equiv W_\mu + \frac{1}{4} X_\mu, \tag{2.12}$$

and

$$X_\mu \equiv \overline{Q}_{\dot{B}} \overline{\sigma}_\mu^{\dot{B}A} Q_A. \tag{2.13}$$

Schur's lemma states that in any irreducible representation of a Lie algebra, the Casimir operators are proportional to the identity. The states on which the operators in a given representation act can therefore be classified with respect to the eigenvalues under operations of the Casimir operators. Any state in a given representation can be labeled with an eigenvalue under P^2, labeled m^2, and under C^2, labeled $-m^4 j(j+1)$. The first eigenvalue is interpreted as the mass squared, such that a state in a representation with mass m and quantum number j fulfills

$$P^2|m,j\rangle = m^2|m,j\rangle \quad \text{and} \tag{2.14}$$

$$C^2|m,j\rangle = -m^4 j(j+1)|m,j\rangle. \tag{2.15}$$

The following calculations are done for a massive state in its rest frame. This can be done in a similar way for massless particles, by transforming to a frame that is boosted in one direction. However, since the Casimir operators commute with all elements in the algebra the result below is valid for any state. In the rest frame of the particle P^μ reduces to

$$P^\mu = (m, \vec{0}). \tag{2.16}$$

This leads to

$$C^2 = 2m^2 B^2 - 2m^2 B_0^2 = 2m^2 B_k B^k, \tag{2.17}$$

where

$$B_k = W_k - \frac{1}{4} \overline{Q}_{\dot{B}} \overline{\sigma}_k^{\dot{B}A} Q_A, \tag{2.18}$$

where $J_i = \frac{1}{m} B_i$ is a generalization of the spin operator S_i that fulfills the spin algebra

$$[J_k, J_l] = i\epsilon_{klm} J_m. \tag{2.19}$$

One can show in the rest frame of the particle that $W_i = mS_i$ such that

$$mJ_k = mS_k - \frac{1}{4} \overline{Q}_{\dot{B}} \overline{\sigma}_k^{\dot{B}A} Q_A. \tag{2.20}$$

Because J_k fulfills Eq. (2.19), a general state in a representation with the quantum numbers m and j can now be quantized by the quantum number j_3, where j can take half integer values, while $j_3 = -j, -j+1, ..., j-1, j$. It can be shown that J_k commutes with the operators Q_A and $\overline{Q}_{\dot{A}}$.

For a given state with quantum numbers $|m, j, j_3\rangle$ there exists a state $|\Omega\rangle$, called the Clifford vacuum, which fulfills

$$Q_1|\Omega\rangle = Q_2|\Omega\rangle = 0. \tag{2.21}$$

The definition in Eq. (2.21) in combination with Eq. (2.20) gives that a Clifford vacuum state has

$$J_k|\Omega\rangle = S_k|\Omega\rangle = j_k|\Omega\rangle. \tag{2.22}$$

This means that the state $|\Omega\rangle$ has total spin $s = j$ and spin in a chosen direction $s_3 = j_3$. There exist four different states with the same quantum numbers j, j_3 and m but different quantum numbers s and s_3, from combinations of this state and the operators $\overline{Q}^{\dot{A}}$. These are

$$|\Omega\rangle_{m,j,j_3}, \quad \overline{Q}^{\dot{1}}|\Omega\rangle_{m,j,j_3}, \quad \overline{Q}^{\dot{2}}|\Omega\rangle_{m,j,j_3} \quad \text{and} \quad \overline{Q}^{\dot{1}}\overline{Q}^{\dot{2}}|\Omega\rangle_{m,j,j_3}. \tag{2.23}$$

As J_3 commutes with the spinors, the spin in one direction for the state $\overline{Q}^{\dot{C}}|\Omega\rangle_{m,j,j_3}$ can now be found using the anti-commutation relations for the spinor charges in Eq. (2.6)

$$\begin{aligned}
S_3\overline{Q}^{\dot{C}}|\Omega\rangle_{m,j,j_3} &= J_3\overline{Q}^{\dot{C}}|\Omega\rangle_{m,j,j_3} - \frac{1}{4m}\overline{Q}_{\dot{B}}\sigma_3^{\dot{B}A}Q_A\overline{Q}^{\dot{C}}|\Omega\rangle_{m,j,j_3} \\
&= \overline{Q}^{\dot{C}}J_3|\Omega\rangle_{m,j,j_3} - \frac{1}{4m}(\overline{Q}_{\dot{1}}Q_1 - \overline{Q}_{\dot{2}}Q_2)\overline{Q}^{\dot{C}}|\Omega\rangle_{m,j,j_3} \\
&= \overline{Q}^{\dot{C}}j_3|\Omega\rangle_{m,j,j_3} - \frac{1}{4m}\overline{Q}_{\dot{1}}(\overline{Q}^{\dot{C}}Q_1 - 2m\sigma^0{}_1{}^{\dot{D}}\epsilon^{\dot{D}\dot{C}})|\Omega\rangle_{m,j,j_3} \\
&\quad + \frac{1}{4m}\overline{Q}_{\dot{2}}(\overline{Q}^{\dot{C}}Q_2 - 2m\sigma^0{}_2{}^{\dot{D}}\epsilon^{\dot{D}\dot{C}})|\Omega\rangle_{m,j,j_3} \\
&= j_3\overline{Q}^{\dot{C}}|\Omega\rangle_{m,j,j_3} + \frac{1}{2}(\overline{Q}_{\dot{1}}\sigma^0{}_1{}^{\dot{D}}\epsilon^{\dot{D}\dot{C}} - \overline{Q}_{\dot{2}}\sigma^0{}_2{}^{\dot{D}}\epsilon^{\dot{D}\dot{C}})|\Omega\rangle_{m,j,j_3}.
\end{aligned} \tag{2.24}$$

This gives for the states $\overline{Q}^{\dot{1}}|\Omega\rangle_{m,j,j_3}$ and $\overline{Q}^{\dot{2}}|\Omega\rangle_{m,j,j_3}$:

$$S_3\overline{Q}^{\dot{1}}|\Omega\rangle_{m,j,j_3} = \left(j_3 + \frac{1}{2}\right)\overline{Q}^{\dot{1}}|\Omega\rangle_{m,j,j_3} \tag{2.25}$$

$$S_3\overline{Q}^{\dot{2}}|\Omega\rangle_{m,j,j_3} = \left(j_3 - \frac{1}{2}\right)\overline{Q}^{\dot{2}}|\Omega\rangle_{m,j,j_3}. \tag{2.26}$$

Similarely one can show that

$$S_3\overline{Q}^{\dot{1}}\overline{Q}^{\dot{2}}|\Omega\rangle_{m,j,j_3} = j_3\overline{Q}^{\dot{1}}\overline{Q}^{\dot{2}}|\Omega\rangle_{m,j,j_3}. \tag{2.27}$$

This means that if the states $|\Omega\rangle_{m,j,j_3}$ and $\overline{Q}^{\dot{1}}\overline{Q}^{\dot{2}}|\Omega\rangle_{m,j,j_3}$ are bosonic, then the states $\overline{Q}^{\dot{1}}|\Omega\rangle_{m,j,j_3}$ and $\overline{Q}^{\dot{2}}|\Omega\rangle_{m,j,j_3}$ are fermionic, and vice versa. This means two things. Firstly, the Majorana spinor charges transform between fermionic and bosonic degrees of freedom, and secondly there exist exactly as many fermionic degrees of freedom as bosonic degrees of freedom in any supersymmetric theory.

2.1.2 Superspace and superfields

Salam and Strathdee [8] show that a general element in the coset space of the Super-poincaré group and the Lorentz group SP/L can be expressed by a set of coordinates called superspace coordinates $Z^\pi = (x^\mu, \theta^A, \overline{\theta}^{\dot{A}})$ as follows:

$$L(x,\theta) = \exp[-ix^\mu P_\mu + i\theta^A Q_A + i\overline{\theta}^{\dot{A}}\overline{Q}_{\dot{A}}]. \tag{2.28}$$

Here θ_A and $\overline{\theta}_{\dot{A}}$ are Grassmann numbers that anti-commute. The elements of the algebra that are on the form $L(x_0,\theta)$ where $x_0^\mu = (0,\vec{0})$, are called SUSY transformations. As this are transformations containing only the Majorana spinor charges, they transform between fermionic and bosonic degrees of freedom, as shown in the previous section.

Grassmann calculus, as defined in Appendix A.1, allows any function of superspace coordinates to be expanded in orders of θ as shown in Eq. (A.11). A general function of superspace coordinates is called a superfield. After second quantization it is an operator valued function, that creates and annihilates particles. The component fields in the superfield can be constructed from the states described in the previous section. A general superfield can be written as

$$\begin{aligned}\Phi(x,\theta,\overline{\theta}) = {} & f(x) + \theta^A\varphi_A(x) + \overline{\theta}_{\dot{A}}\overline{\chi}^{\dot{A}}(x) + \theta\theta m(x) + \overline{\theta\theta}n(x) \\ & + \theta\sigma^\mu\overline{\theta}V_\mu(x) + \theta\theta\overline{\theta}_{\dot{A}}\overline{\lambda}^{\dot{A}}(x) + \overline{\theta\theta}\theta^A\psi_A(x) + \theta\theta\overline{\theta\theta}d(x).\end{aligned} \tag{2.29}$$

As shown in the literature, e.g. in Chapter 6.5 of [6], one can find covariant derivatives that commute with all SUSY transformations. These are

$$D_A = \partial_A + i(\sigma^\mu\overline{\theta})_A\partial_\mu \quad \text{and} \tag{2.30}$$

$$\overline{D}_{\dot{A}} = -\partial_{\dot{A}} - i(\theta\sigma^\mu)_{\dot{A}}\partial_\mu. \tag{2.31}$$

One can define two types of superfields that are more restricted than the general superfield. The left handed scalar superfield fulfills

$$\overline{D}_A \Phi(x,\theta,\overline{\theta}) = 0. \tag{2.32}$$

This leads to the general form of a left handed scalar superfield (also called a chiral superfield)

$$\begin{aligned} \Phi(x,\theta,\overline{\theta}) &= A(x) + i(\theta\sigma^\mu\overline{\theta})\partial_\mu A(x) - \frac{1}{4}\theta\theta\overline{\theta}\overline{\theta}\Box A(x) \\ &\quad +\sqrt{2}\theta\psi(x) - \frac{i}{\sqrt{2}}\theta\theta\partial_\mu\psi(x)\sigma^\mu\overline{\theta} + \theta\theta F(x), \end{aligned} \tag{2.33}$$

where $A(x)$ and $F(x)$ are complex scalar fields and $\psi(x)$ is a left handed Weyl spinor field. Taking the Hermitian conjugate of this field one gets a so-called right handed scalar superfield, which contains two scalar fields and one right handed Weyl spinor field.

The vector superfield fulfills

$$\Phi^\dagger(x,\theta,\overline{\theta}) = \Phi(x,\theta,\overline{\theta}). \tag{2.34}$$

Its general form is

$$\begin{aligned} \Phi(x,\theta,\overline{\theta}) &= C(x) + \theta\varphi(x) + \overline{\theta}\overline{\varphi}(x) + \theta\theta M(x) + \overline{\theta}\overline{\theta}M^*(x) \\ &\quad +\theta\sigma^\mu\overline{\theta}V_\mu(x) + \theta\theta\overline{\theta}\overline{\lambda}(x) + \overline{\theta}\overline{\theta}\theta\lambda(x) + \theta\theta\overline{\theta}\overline{\theta}D(x). \end{aligned} \tag{2.35}$$

Here $C(x)$ and $D(x)$ are real scalar fields, $V^\mu(x)$ is a real vector field, $M(x)$ is a complex scalar field and $\varphi(x)$ and $\lambda(x)$ are left handed Weyl spinor fields.

2.1.3 The supergauge transformations

The vector superfield contains a high number of component fields. In order for it to describe a vector boson and its super partner, it should contain no more then one left-handed spinor field and one complex vector field. The highest order auxiliary field $D(x)$ can be removed through the equations of motion, as will be discussed in Section 2.1.5. One can, however, define the abelian supergauge transformation of a vector superfield $V(x,\theta,\overline{\theta})$ as

$$V(x,\theta,\overline{\theta}) \to V'(x,\theta,\overline{\theta}) \equiv V(x,\theta,\overline{\theta}) + \Phi(x,\theta,\overline{\theta}) + \Phi^\dagger(x,\theta,\overline{\theta}), \tag{2.36}$$

where $\Phi(x,\theta,\overline{\theta})$ is a left handed chiral superfield. This leads to the following transformations of the component fields of the vector superfield:

$$C(x) \rightarrow C'(x) = C(x) + A(x) + A^*(x) \tag{2.37}$$

$$\varphi(x) \rightarrow \varphi'(x) = \varphi(x) + \sqrt{2}\Psi(x) \tag{2.38}$$

$$M(x) \rightarrow M'(x) = M(x) + F(x) \tag{2.39}$$

$$V_\mu(x) \rightarrow V'_\mu(x) = V_\mu(x) + i\partial_\mu(A(x) - A^*(x)) \tag{2.40}$$

$$\lambda(x) \rightarrow \lambda'(x) = \lambda(x) \tag{2.41}$$

$$D(x) \rightarrow D'(x) = D(x) \tag{2.42}$$

These transformations can be used to remove degrees of freedom using the Wess-Zumino gauge, where one chooses the scalar field to have the component fields $\psi(x) = -\frac{1}{\sqrt{2}}\varphi(x)$, $F(x) = -M(x)$, $A(x) + A^*(x) = -C(x)$, removing these fields and leaving standard Abelian gauge freedom in terms of $\mathrm{Im}[A(x)]$. This leads to the vector field in the Wess-Zumino gauge.

$$V_{WZ}(x,\theta,\overline{\theta}) = (\theta\sigma^\mu\overline{\theta})[V_\mu(x) + i\partial_\mu(A(x) - A^*(x))] + \theta\theta\overline{\theta\lambda}(x) + \overline{\theta\theta}\theta\lambda(x) + \theta\theta\overline{\theta\theta}D(x). \tag{2.43}$$

The abelian supergauge transformation on a chiral field is defined as

$$\Phi_i \rightarrow \Phi'_i \equiv e^{-i\Lambda(x)q_i}\Phi_i, \tag{2.44}$$

where q_i is the charge of the field under the $U(1)$ transformation. From requiring that Φ'_i is a left handed chiral field, one gets that $\Lambda(x)$ must be a left handed chiral field.

In the more general non-Abelian case, where the gauge group has the generators t_a, the transformation is

$$\Phi \rightarrow \Phi' \equiv e^{-iq\Lambda(x)^a t_a}\Phi, \tag{2.45}$$

where again $\Lambda(x)^a$ is a set of left handed chiral fields. The non-Abelian definition of a supergauge transformation for a vector superfield is the following

$$e^{qV'^a t_a} \equiv e^{q\Phi^{\dagger a}t_a}e^{qV^a t_a}e^{q\Phi^a t_a}, \tag{2.46}$$

and renaming $\Phi^a = i\Lambda^a$ one gets

$$e^{qV'^a t_a} = e^{-iq\Lambda^{\dagger a}t_a}e^{qV^a t_a}e^{iq\Lambda^a t_a}. \tag{2.47}$$

This can again be used to remove the superfluous degrees of freedom from the vector superfield, leaving it in the Wess-Zumino gauge as is shown by Ferrara and Zumino in [9].

2.1.4 A general supersymmetric Lagrangian

Connecting the pieces above, one can write down a general Lagrangian for a supersymmetric theory constructed of superfields. The action $S \equiv \int_R d^4x\mathcal{L}$ is to be invariant under SUSY transformations and under generalized gauge transformations. This is the case, if the Lagrangian density satisfies $\mathcal{L}' = \mathcal{L} + \partial^\mu f(x)$ where $f(x) \to 0$ on the boundaries of R. It can be shown, see e.g. Chapter 6.8 of [6], that the highest order of theta component of any superfield $d(x)$ transforms under global SUSY transformations as

$$d'(x) - d(x) = \frac{i}{2}(\partial_\mu\psi(x)\sigma^\mu\overline{\alpha} - \partial_\mu\overline{\lambda}(x)\sigma^\mu\alpha), \tag{2.48}$$

which is a total derivative. If all components of the Lagrangian are of highest order in θ, one guarantees that the resulting action is invariant under SUSY transformations. Equation (A.13) shows that integrating over a volume element in Grassmann calculus projects out terms that go with highest order in θ, such that one can write a manifestly SUSY invariant Lagrangian as

$$\mathcal{L} = \int d^4\theta\mathfrak{L}. \tag{2.49}$$

Here $\mathfrak{L}$ is the supersymmetric Lagrangian density. It was shown by Wess and Bagger [10] that this density can not contain more than third order in chiral fields for it to be renormalizable. This leaves the following possibilities, using only chiral fields Φ_i,

$$\mathfrak{L} = \Phi_i^\dagger\Phi_i + \theta\theta W[\Phi] + \overline{\theta\theta}W[\Phi^\dagger]. \tag{2.50}$$

Here the first term is called the kinetic term, while W is the superpotential. It is defined as

$$W[\Phi] = g_i\Phi_i + m_{ij}\Phi_i\Phi_j + \lambda_{ijk}\Phi_i\Phi_j\Phi_k, \tag{2.51}$$

where the first term is called the tadpole term, the second is the mass term and the third the Yukawa term. This is to be invariant under the generalized gauge transformations as well. This sets a number of restrictions on the superpotential. They are (for a

general non-Abelian transformation with the matrix representation U_{ij}):

$$g_i = 0 \quad \text{if} \quad g_i U_{ir} \neq g_r, \tag{2.52}$$

$$m_{ij} = 0 \quad \text{if} \quad m_{ij} U_{ir} U_{js} \neq m_{rs}, \tag{2.53}$$

$$\lambda_{ijk} = 0 \quad \text{if} \quad \lambda_{ijk} U_{ir} U_{js} U_{kt} \neq \lambda_{rst}, \tag{2.54}$$

where $U = (e^{-iq\Lambda^a t_a})$. For the kinetic term this is a bit more tricky. It transforms as:

$$\Phi_i'^{\dagger} \Phi_i' = \Phi_i^{\dagger} e^{iq\Lambda^{a\dagger} t_a} e^{-iq\Lambda^a t_a} \Phi_i. \tag{2.55}$$

To compensate for the change in the term, one introduces a set of vector superfields that transform like in Eq. (2.47). This leads to introducing a kinetic term:

$$\Phi^{\dagger} e^{qV^a t_a} \Phi \to \Phi'^{\dagger} e^{qV'^a t_a} \Phi' = \Phi^{\dagger} e^{iq\Lambda^{a\dagger} t_a} e^{-iq\Lambda^{\dagger a} t_a} e^{qV^a t_a} e^{iq\Lambda^a t_a} e^{-iq\Lambda^a t_a} \Phi = \Phi^{\dagger} e^{qV^a t_a} \Phi. \tag{2.56}$$

The field strength terms of the fields V^a can, as shown in the literature, e.g. Chapter 7.3 of [6], be written

$$\frac{1}{2T(R)} \mathrm{Tr}\{W^A W_A\} \overline{\theta\theta}, \tag{2.57}$$

where

$$W_A \equiv -\frac{1}{4} \overline{DD} e^{-V^a t_a} D_A e^{V^a t_a}, \tag{2.58}$$

and where the Dynkin index is given by

$$T(R) \delta_{ab} = \mathrm{Tr}[t_a t_b]. \tag{2.59}$$

The complete Lagrangian density of a supersymmetric theory is then in terms of superfields given as

$$\mathcal{L} = \int d^4\theta \Phi_i^{\dagger} e^{qV^a t_a} \Phi_i + \theta\theta W[\Phi] + \overline{\theta\theta} W[\Phi^{\dagger}] + \frac{1}{2T(R)} \mathrm{Tr}\{W^A W_A\} \overline{\theta\theta}. \tag{2.60}$$

The theory described by this Lagrangian density is by construction invariant under global SUSY transformations.

It was shown by Ferrara *et al.* [11] that the supertrace, which is a weighted sum of eigenvalues of the mass matrix in a SUSY theory, vanishes at tree level. This means that the masses of Standard Model particles and their supersymmetric partners can not be split arbitrarily, which has as a consequence that this theory contains light scalar partners to Standard Model fermions, and light fermionic partners to Standard Model

gauge bosons. This is not observed in experiments. To explain this, supersymmetry must be broken such that the new scalar and fermionic particles gain mass. There have been different schemes proposed to break supersymmetry. All of them introduce so called soft terms, which are called soft because these terms contribute with a factor no worse then logarithmically in divergent loop corrections for scalar masses, as discussed in Section 2.2.4. These soft terms parametrize SUSY-breaking and give additional masses to supersymmetric particles. Their general form is

$$\begin{aligned}\mathfrak{L}_{soft} &= -\frac{1}{4T(R)}M\theta\theta\overline{\theta}\overline{\theta}\mathrm{Tr}\{W^A W_A\} - \frac{1}{6}a_{ijk}\theta\theta\overline{\theta}\overline{\theta}\Phi_i\Phi_j\Phi_k \\ &\quad -\frac{1}{2}b_{ij}\theta\theta\overline{\theta}\overline{\theta}\Phi_i\Phi_j - t_i\theta\theta\overline{\theta}\overline{\theta}\Phi_i + h.c. \\ &\quad -m_{ij}^2\theta\theta\overline{\theta}\overline{\theta}\Phi_i^\dagger\Phi_j. \end{aligned} \tag{2.61}$$

Additionally, there are so-called maybe-soft terms

$$\mathfrak{L}_{maybe-soft} = -\frac{1}{2}c_{ijk}\theta\theta\overline{\theta}\overline{\theta}\Phi_i^\dagger\Phi_j\Phi_k + h.c., \tag{2.62}$$

which are soft as long as none of the scalar superfields is a singlet under all gauge symmetries. In this thesis the details of SUSY breaking are ignored, and the scalar masses are taken to be free parameters. However, the soft-breaking terms are generally thought to be the result of spontaneous SUSY-breaking in a hidden sector that enters at some high scale. It is also important to note that theories with Lagrangians on the same form as shown in Eq. (2.60) are invariant under global SUSY transformations only. If one constructs a theory with local SUSY invariance, one must introduce new fields which lead to supergravity and contain the massive spin-3/2 gravitino, as discussed by Freedman, van Nieuwenhuizen and Ferrara [12]. Chapter 3 contains a more detailed discussion of gravitinos.

2.1.5 Lagrangians of component fields.

It was mentioned above that the auxiliary fields $F(x)$ and $D(x)$ vanish by virtue of the equations of motion for the Lagrangian. In addition, one needs to find the Lagrangian density in terms of component fields to be able to calculate in terms of said component fields. Chapter 8 in Wiedemann and Müller-Kirsten [6] contains explicit derivations of all terms in a general Lagrangian build of vector and chiral fields. To do the derivation

one needs to remember that the only components of the super-Lagrangian that survive the integral are the ones that have highest order in theta.

As an example we can take a general chiral field Φ_i with component fields as in Eq. (2.33) and without any gauge fields to get the Lagrangian density

$$\begin{aligned}\mathcal{L} &= -A_i^*\Box A_i + |F_i|^2 + i(\partial_\mu \psi_i^\dagger)\overline{\sigma}^\mu \psi_i \\ &\quad + [g_i F_i + m_{ij}(A_i F_j + F_i A_j + 2\psi_i \psi_j) \\ &\quad + \lambda_{ijk}(A_i A_j F_k + A_i F_j A_k + F_i A_j A_k \\ &\quad + \psi_i \psi_j A_k + \psi_i A_j \psi_k + A_i \psi_j \psi_k) + h.c.]. \end{aligned} \tag{2.63}$$

Here some total derivatives were removed. Looking on the Euler-Lagrange functions for the auxiliary field $F(x)$ one can see that

$$\frac{\partial_\mu \mathcal{L}}{\partial(\partial_\mu F_i)} - \frac{\partial \mathcal{L}}{\partial F_i} = 0 \quad \text{gives} \tag{2.64}$$

$$2F_i + [g_i + m_{ij}A_j + \lambda_{ijk}A_j A_k + h.c.] = 0. \tag{2.65}$$

This can be solved for F_i to replace all F_i in the Lagrangian, as promised above. This leads to

$$\begin{aligned}\mathcal{L} &= i(\partial_\mu \psi_i^\dagger)\overline{\sigma}^\mu \psi_i - A_i^*\Box A_i \\ &\quad -\frac{1}{2}W_{ij}\psi_i\psi_j - \frac{1}{2}\overline{W}_{ij}\psi_i^\dagger \psi_j^\dagger - |W_i|^2 \end{aligned} \tag{2.66}$$

where

$$W_i = \frac{W[A_1, A_2..., A_n]}{\partial A_i} \tag{2.67}$$

$$W_{ij} = \frac{W[A_1, A_2..., A_n]}{\partial A_i \partial A_j}. \tag{2.68}$$

For the auxiliary field $D(x)$ a similar derivation can be done, such that the auxiliary field $D(x)$ can be replaced in the Lagrangian.

2.2 Building the MSSM

The Lagrangian (2.60) describes a general theory. One would like to construct a theory that contains the fields/particles measured that make up the Standard Model. The Minimal Supersymmetric Standard Model (MSSM) is a minimal version of this theory. It is minimal in the sense that it contains the least amount of superfields with which one can construct a theory containing all fields and couplings of the Standard Model.

2.2.1 The superfields of the MSSM

The superfields needed to construct all Standard Model particles and give them their Standard Model masses are given in Table 2.1 on the facing page and Table 2.2 on page 16. The Standard Model fermion fields emerge as the spin-1/2 components of the left handed scalar superfields L_i, $\overline{E}_i$, Q_i, $\overline{U}_i$ and $\overline{D}_i$. The remaining spin-0 components form the superpartners of these fields, called sleptons, sneutrinos and squarks. The Standard Model gauge fields emerge as the spin-1 parts of the vector superfields B, W^a and C^a. The remaining spin-1/2 components form the superpartners of the gauge fields, called bino, wino and gluino. Note that the bars over the names of the fields do not designate conjugation, but are part of the name of the field. The fields responsible for the Higgs boson are a bit more complicated. Because one can only include chiral left-handed fields in the superpotential, one needs to introduce two Higgs-doublet superfields to be able to give mass to both up-type and down-type quarks. Radiative electroweak symmetry breaking, see e.g. Section 7.1 of Martin [5], leads to the mixing of the scalar component fields of the Higgs superfields as presented in Table 2.1, to mass eigenstates h^0, H^0, $H^\pm$ and A^0. The scalar field h^0 (called the light Higgs field) is the Standard Model equivalent of the Higgs particle. Additionally there exist four fermionic Higgs fields, called Higgsino fields. The bino, wino and Higgsino states that have equal charge mix to mass eigenstates and form four neutralinos and two charginos.

As the Standard Model equivalents have the measured properties of the Standard Model particles, their masses and couplings are given by the Standard Model couplings and masses. Note that as the Higgs fields are constructed in a different way, the couplings of the Higgs fields are not the same as in the Standard Model, but have a direct relation. However, as none of the superpartners are measured to this date, superpartners and the extra Higgs fields need to have considerably higher masses than the Standard Model fields except in certain limited corners of parameter space.

Superfield	Q_e	Y	$SU(2)$	SU(3)	spin-1/2	spin-0
$L_i = \begin{pmatrix} \nu_i \\ l_i \end{pmatrix}$	$\begin{matrix} 0 \\ -1 \end{matrix}$	-1	**2**	**1**	$\begin{pmatrix} \nu_{iL} \\ l_{iL} \end{pmatrix}$	$\begin{pmatrix} \tilde{\nu}_{iL} \\ \tilde{l}_{iL} \end{pmatrix}$
$\overline{E}_i$	1	2	**1**	**1**	$l_{iR}^\dagger$	$\tilde{l}_{iR}^*$
$Q_i = \begin{pmatrix} u_i \\ d_i \end{pmatrix}$	$\begin{matrix} \frac{2}{3} \\ -\frac{1}{3} \end{matrix}$	$\frac{1}{3}$	**2**	**3**	$\begin{pmatrix} u_{iL} \\ d_{iL} \end{pmatrix}$	$\begin{pmatrix} \tilde{u}_{iL} \\ \tilde{d}_{iL} \end{pmatrix}$
$\overline{U}_i$	$-\frac{2}{3}$	$-\frac{4}{3}$	**1**	**3**	$u_{iR}^\dagger$	$\tilde{u}_{iR}^*$
$\overline{D}_i$	$\frac{1}{3}$	$\frac{2}{3}$	**1**	**3**	$d_{iR}^\dagger$	$\tilde{d}_{iR}^*$
$H_u = \begin{pmatrix} H_u^+ \\ H_u^0 \end{pmatrix}$	$\begin{matrix} +1 \\ 0 \end{matrix}$	$+1$	**2**	**1**	$\begin{pmatrix} \tilde{H}_u^+ \\ \tilde{H}_u^0 \end{pmatrix}$	$\begin{pmatrix} H_u^+ \\ H_u^0 \end{pmatrix}$
$H_d = \begin{pmatrix} H_d^0 \\ H_d^- \end{pmatrix}$	$\begin{matrix} 0 \\ -1 \end{matrix}$	-1	**2**	**1**	$\begin{pmatrix} \tilde{H}_d^- \\ \tilde{H}_d^- \end{pmatrix}$	$\begin{pmatrix} H_d^0 \\ H_d^- \end{pmatrix}$

Table 2.1: Chiral fields in the MSSM with all quantum numbers. Under $SU(2)$ **1** represents a singlet while **2** represents a doublet. Under $SU(3)$ **1** represents a singlet while **3** represents a triplet.

2.2.2 The MSSM Lagrangian

Combining these fields with the general Lagrangian as found in Section 2.1 this leads to the kinetic Lagrangian for the MSSM in terms of superfields

$$\begin{aligned} \mathfrak{L}_{kin} &= L_i^\dagger e^{\frac{1}{2}g\sigma_a W^a - \frac{1}{2}g'B} L_i + Q_i^\dagger e^{\frac{1}{2}g_s\lambda_a C^a + \frac{1}{2}g\sigma_a W^a + \frac{1}{2}\frac{1}{3}g'B} Q_i \\ &\quad + \overline{U}_i^\dagger e^{\frac{1}{2}g_s\lambda_a C^a - \frac{4}{3}\cdot\frac{1}{2}g'B} \overline{U}_i + \overline{D}_i^\dagger e^{\frac{1}{2}g_s\lambda_a C^a + \frac{2}{3}\cdot\frac{1}{2}g'B} \overline{D}_i \\ &\quad + \overline{E}_i^\dagger e^{2\frac{1}{2}g'B} \overline{E}_i + H_u^\dagger e^{\frac{1}{2}g\sigma_a W^a + \frac{1}{2}g'B} H_u + H_d^\dagger e^{\frac{1}{2}g\sigma_a W^a - \frac{1}{2}g'B} H_d. \end{aligned} \quad (2.69)$$

Here σ_a and λ_a are the Pauli and the Gell-Mann matrices respectively. g is the coupling constant for the $SU(2)_L$ group, g' is the coupling constant of the $U(1)_Y$ group and g_s

Superfield	Y	SU(2)	SU(3)	spin-1	spin-1/2
B	0	**1**	**1**	B^0	$\tilde{B}^0$
W^a	0	**3**	**1**	$\begin{pmatrix} W^+ \\ W^3 \\ W^- \end{pmatrix}$	$\begin{pmatrix} \tilde{W}^+ \\ \tilde{W}^3 \\ \tilde{W}^- \end{pmatrix}$
C^a	0	**1**	**8**	g	$\tilde{g}$

Table 2.2: Gauge fields in the MSSM with all quantum numbers. Under $SU(2)$ **1** represents a singlet while **3** represents a triplet. Under $SU(3)$ **1** represents a singlet while **8** represents an octet.

is the coupling constant of the $SU(3)_C$ group. The pure gauge terms are

$$\mathfrak{L}_{gauge} = \frac{1}{2}\mathrm{Tr}\{W^A W_A\}\overline{\theta\theta} + \frac{1}{2}\mathrm{Tr}\{C^A C_A\}\overline{\theta\theta} + \frac{1}{4}B^A B_A \overline{\theta\theta}, \tag{2.70}$$

where

$$\begin{aligned} W_A &= -\frac{1}{4}\overline{DD}e^{-W}D_A e^W\ , \qquad W = \frac{1}{2}g\sigma^a W^a, \\ C_A &= -\frac{1}{4}\overline{DD}e^{-C}D_A e^C\ , \qquad C = \frac{1}{2}g_s\lambda^a C^a, \\ B_A &= -\frac{1}{4}\overline{DD}D_A B^0\ , \qquad B^0 = \frac{1}{2}g' B. \end{aligned}$$

There is no singlet under all gauge groups in the MSSM, so the superpotential contains no tadpole terms.

The only mass terms allowed by Eq. (2.53) are:

$$W_m = \mu H_u H_d + \mu'_i L_i H_u, \tag{2.71}$$

where $H_u H_d = H_u^T i\sigma^2 H_d = H_u^+ H_d^- - H_u^0 H_d^0$, and similarly for other $SU(2)$ doublets, is implied. The couplings μ and μ' do not exist in the Standard Model, and can therefore not be deduced by looking at the Standard Model. However, if one requires electroweak symmetry breaking to occur and fixes the Higgs mass, one can find relations between $|\mu|$ and the soft breaking parameters in the Higgs sector. As μ is a mass term that has a priori no connection to a SUSY-breaking scale, and this connection has no theoretical explanation in the MSSM, this is called the μ problem.

The allowed Yukawa terms from Eq. (2.54) are:

$$\begin{aligned} W_y &= y^e_{ij} L_i H_d E_j + y^u_{ij} Q_i H_u \overline{U}_j + y^d_{ij} Q_i H_d \overline{D}_j \\ &\quad + \lambda_{ijk} L_i L_j \overline{E}_k + \lambda'_{ijk} L_i Q_j \overline{D}_k + \lambda''_{ijk} \overline{U}_i \overline{D}_j \overline{D}_k. \end{aligned} \tag{2.72}$$

Since the Standard Model particles have their (measured) masses, one can identify the Yukawa couplings y^e_{ij}, y^u_{ij} and y^d_{ij} with the ones between the corresponding Standard Model fields and the Higgs field. However, the couplings λ_{ijk}, λ'_{ijk} and λ''_{ijk} do not exist in the Standard Model, and can therefore not be deduced by looking at the Standard Model. Additionally, there are soft breaking terms on the form shown in Eq. (2.61). These are not listed here. Instead the masses of the supersymmetric particles are used as free parameters in the calculation in this thesis.

2.2.3 R-parity and alternatives

In the superpotential (2.72), terms in the second line break lepton or baryon number. These allow the proton to decay, and if both a lepton number violating and a baryon number violating coupling exists it can even decay at tree level. As measurements tell us that the proton lifetime is $\tau_p > 2.1 \times 10^{29}$ years [13], the concept of R-parity, a multiplicative conserved quantum number, was introduced by Fayet [14]. This is defined by

$$P_R = (-1)^{2s+3B+L} \tag{2.73}$$

where B is baryon number, L is lepton number and s is the spin of the particle. This forbids the Yukawa terms that have the couplings λ_{ijk}, λ'_{ijk} and λ''_{ijk} and the mass term with the coupling μ' from the superpotential, and has the consequence that the supersymmetric partners in the theory can only be produced and destroyed in pairs. There are, however, few good theoretical arguments within grand unified theories or string theories for R-parity conservation in the MSSM [15]. Additionally, the proton can be made stable by virtue of other symmetries. One can observe that at tree level both baryon and lepton number have to be broken to allow the proton to decay into a lepton and a pion. This means that at least two of the couplings are needed in the decay. As an alternative one can propose lepton or baryon triality [16, 17], where either leptons or baryons get a new parity that is conserved. The consequence of barion triality is that the trilinear couplings λ''_{ijk} are forbidden, while lepton triality forbids μ', λ_{ijk} and λ'_{ijk}. As the decays in this thesis break lepton number, baryon triality allows the couplings used. There are direct limits on individual fermion number violation as well, which limit the extent to which any given lepton number and baryon number can be broken. These can be found in the latest review of particle physics data [13].

2.2.4 Reasons for a supersymmetric model

This far the only reason why one would construct a supersymmetric model quoted is that such a model is the largest possible extension of special relativity. In the following, further indications for SUSY are given.

Already in the 1930s Zwicky [18] observed that the dispersion of the velocities of galaxies can not be explained by visible matter. Since then an overwhelming amount of evidence for this has been found, for which Zwicky coined the term dark matter. Dark matter has no electromagnetic couplings, meaning that any cosmologically stable, neutral and massive particle can in principle be dark matter. The measured dark matter density is $\Omega_{DM}h^2 \equiv (\rho_{DM}/\rho_c)h^2 = 0.1123 \pm 0.0035$ [19] where the critical density is $\rho_c = 1.05 \cdot 10^{-5} h^2 \text{GeV/cm}^3$ and h is the unitless Hubble constant. Many particles have been proposed as candidates for dark matter, see e.g. reviews by Bertone, Hooper and Silk [20], but the only Standard Model candidate are neutrinos. One can set an upper limit on the abundance of Standard Model neutrinos in the universe of $\Omega_\nu h^2 < 0.0067$ at 95% confidence level [20]. This means that the total dark matter content of the universe is not completely explained by the Standard Model.

The MSSM with R-parity conservation intact, however, yields natural candidates if the lightest supersymmetric particle (LSP) has neutral electric charge. In fact, if any weakly interacting massive particle (WIMP) χ exists and is stable, it is automatically a prime dark matter candidate. A particle is weakly interacting if its couplings are on the order of the weak interactions $\alpha_{weak} \approx 10^{-2}$. The reason for this is that the calculated dark matter density from WIMPs, see e.g. [21], is approximately $\Omega_\chi h^2 \approx 0.1 \times (\alpha_{weak}/\alpha)^2$ for a particle with a mass in the order of 100 GeV. This means that the MSSM with a neutralino LSP with a mass of about 100 GeV would lead to about the right dark matter density. This is a strong argument for SUSY. Axinos, the superpartners of axions, sneutrinos and gravitinos are other possible SUSY dark matter candidates. In this thesis gravitino dark matter is discussed in Section 3.3.

From measurements of the properties of the weak interactions one can find that $m_H^2 \sim \mathcal{O}(100 \text{ GeV})$, and the LHC has seen some evidence of Higgs particles with mass at that scale [22, 23, 24]. If one calculates the loop calculations to the Higgs mass Δm_H^2 for a Higgs particle coupling to two fermions f with the coupling λ_f, see e.g. [5], one

gets that the contribution is proportional to the cut-off squared as

$$\Delta m_H^2 = -|\lambda_f|^2 \Lambda_{UV}^2/(8\pi^2) + O(|\lambda_f|^4), \tag{2.74}$$

where Λ_{UV} is the cut off scale, often taken to be the Planck scale $m_P = 2.4 \times 10^{18}$ GeV. In the Standard Model the most important coupling is the top-quark coupling, which is of order of magnitude 1. This leads to corrections that are 10^{16} times bigger than $\mathcal{O}(100$ GeV). This is the so called hierarchy problem. In unbroken SUSY, however, the Higgs mass is protected by scalar particle loops which couple with λ_s. They contribute as

$$\Delta m_H^2 = \lambda_s \Lambda_{UV}^2/(16\pi^2) + O(\lambda_s^2), \tag{2.75}$$

and one has $\lambda_s = |\lambda_f|^2$ and twice as many scalar particles as fermions, such that all contributions cancel exactly.

In theories where SUSY is broken the the Higgs mass gets extra contributions. These are chosen in such a way that a scalar particle with mass m_s contributes with at most

$$\Delta m_H^2 = -(\lambda_s/16\pi^2) m_s^2 \ln \frac{\Lambda_{UV}^2}{m_s^2}, \tag{2.76}$$

Couplings like this are called soft, and the couplings used in softly broken supersymmetric theories are written down in Eq. (2.61) and Eq. (2.62). As long as there is SUSY below the TEV scale, the loop corrections to the Higgs mass are of the order $\sim \mathcal{O}(10$ GeV). This is another strong indication for SUSY at relatively low energies.

2.2.5 MSSM with R-parity violation at particle colliders

As mentioned above, not a single supersymmetric particle has been found in any collider experiment up until now. One can use the non-detection to set limits on the crossection of a given process, and given that one can calculate crossections in the MSSM, one can set limits on the parameters of the MSSM. This turns out to be an extremely hard exercise. The main reason for this is that the parameter space is complex and hard to understand. More constrained models, like the CMSSM, give better limits, but even in these the parameter space can be hard to handle. In R-parity conserving (RPC) supersymmetric theories the experimental signatures are expected to be decay chains which give multiple leptons or quarks and missing energy. This is because any produced SUSY particle cascades to the LSP which is stable.

In R-parity violating (RPV) theories SUSY particles decay in the detector unless the RPV coupling λ is very small. A simple dimensional analysis gives for a massive particle with mass m_s and a dimensionless coupling λ with which it can decay, an approximate decay rate of $\Gamma \sim \lambda^2 m_s$, such that the decay time for $m_s = 100$ GeV can be written as $\tau \sim (10^{-28}/\lambda^2)$ s. The decay length is then given by

$$l = \gamma\tau \sim 10^{-20}/\lambda^2 (E/m_s) \text{ m} \tag{2.77}$$

where E is the energy of the particle in the lab frame. As an example, the ATLAS detector at the LHC has a distance of 5 cm between the beam and the innermost pixel detectors. Assuming that the particle has an energy on the TeV scale, one gets that for $\lambda^2 \gtrsim 10^{-8}$ the particle decays before it hits the pixel detector. A conservative estimate is therefore that with a coupling strength of $\lambda \geq 10^{-6}$, a sparticle with a mass of $\mathcal{O}(100$ GeV) decays promptly, i.e. before it can be seen to have moved away from the interaction point. The collider signature is then multi-lepton/multi-jet events from the LSP decay through the RPV couplings. In particular for models with a gravitino LSP and R-parity violation one expects all heavier particles to decay inside the detector to Standard Model particles as the gravitino inherits its couplings from gravitational theory as presented in Section 3.1 with the consequence that decays to a gravitino LSP are extremely suppressed.

3

The Gravitino

The action of the theory in the previous chapter can be made invariant under local SUSY transformations. This is called supergravity. An important consequence of making the transformations local is the emergence of a massless spin-3/2 Majorana fermion field which is the super partner of the spin-2 graviton, called the gravitino field. That the field is a Majorana field means that its particle is identical to its anti-particle. This field can obtain a mass $m_{\tilde{G}}$ via the so-called super-Higgs mechanism, see e.g. Freedman *et al.* [12], when local SUSY is spontaneously broken.

In this thesis the low-energy phenomenological consequences of the gravitino, irrespective of the supergravity theory and the SUSY-breaking scheme, are investigated. This means that the gravitino mass $m_{\tilde{G}}$ is kept as a free parameter.

3.1 The gravitino Lagrangian

Following Cremmer *et al.* [25] the dimension-5 terms of the effective supergravity Lagrangian are

$$\mathcal{L} = -\frac{i}{\sqrt{2}M}[(D^*_\mu\phi^*)\overline{\psi}_\nu\gamma^\mu\gamma^\nu P_L\chi - (D_\mu\phi)\overline{\chi}P_R\gamma^\nu\gamma^\mu\psi_\mu] - \frac{i}{8M}\overline{\psi}_\mu[\gamma^\nu,\gamma^\rho]\gamma^\mu\lambda^a F^a{}_{\nu\rho}. \quad (3.1)$$

Here χ designate chiral fermion fields, ϕ their superpartners, D_μ is the covariant derivative given by $D_\mu\phi^i = (\partial_\mu\delta^{ij} + igT^a_{ij}A^a_\mu)\phi^j$, $F^a{}_{\mu\nu}$ is the field strength tensor of the gauge fields A^a_μ:

$$F^a{}_{\mu\nu} = \partial_\mu A^a_\nu - \partial_\nu A^a_\mu - gf^{abc}A^b_\mu A^c_\nu, \quad (3.2)$$

where g is the gauge coupling, λ^a are the superpartner gaugino fields, ψ^μ is the gravitino field, and $M = m_{pl}/\sqrt{8\pi}$ where $m_{pl} = \sqrt{\hbar c/G} \approx 1.2209 \times 10^{19}$ GeV is the Planck mass. Higher order terms are suppressed by additional factors of m_{sc}/M in low energy phenomenology, where m_{sc} is a mass scale of particles involved. Standard Model particles and their supersymmetric partners considered in this thesis are much lighter then the Planck scale and the higher order terms are therefore ignored. This is an effective theory and is only valid in the limit where the momentum of the gravitino is small compared to the Planck mass. As this thesis considers gravitinos as cold dark matter that have little kinetic energy, this is not an issue here.

3.2 Spin-3/2 particles

This section is a short introduction to spinor algebra for Majorana spin-3/2 fields. As mentioned above, a spin-3/2 field emerges when supersymmetry is made local. In the notation developed by Rarita and Schwinger [26] one can write the equations of motion for a spin-3/2 field with momentum p and mass $m = \sqrt{p^2}$ as

$$\gamma^\mu \tilde{\psi}_\mu(p) = 0 \tag{3.3}$$

$$(\not{p} - m)\tilde{\psi}_\mu(p) = 0 \tag{3.4}$$

which also yield

$$p^\mu \tilde{\psi}_\mu(p) = 0. \tag{3.5}$$

These are known as the Rarita-Schwinger equations. Here $\tilde{\psi}_\mu$ is a vector-spinor, where the Dirac index is suppressed such that the components of the four vector are Dirac spinors. These vector-spinors can be constructed by combining Dirac spinors for spin-1/2 particles with polarization vectors of massive spin-1 particles as follows (see e.g. Bolz [27] page 6):

$$\psi_\mu^{l+}(P) = \sum_{s,k} C(l,s,k) u^s(p) \epsilon_\mu^k \tag{3.6}$$

$$\psi_\mu^{l-}(P) = \sum_{s,k} C(l,s,k) v^s(p) \epsilon_\mu^k. \tag{3.7}$$

Here $C(l,s,m)$ are Clebsch-Gordon coefficients, $l = +3/2, +1/2, -1/2, -3/2$ is the helicity index of the spin-3/2 particle, $s = \pm 1/2$ is the spinor index of the spinor

and $k = +1, 0, -1$ is the helicity index of the polarization vector. As the field is a Majorana field, the charge conjugated wave function equals the wave function itself. In the following the positive solution will be used, leaving out the + in the equations. A similar derivation can be constructed for the negative solution. The Dirac spinors are normalized as

$$\overline{u}^s u^{s'} = 2m\delta^{ss'}, \tag{3.8}$$

where m is the mass of the spin-3/2 particle and the polarization vectors fulfill

$$\epsilon^k_\mu \epsilon^{k'*\mu} = -\delta^{kk'}. \tag{3.9}$$

This gives

$$\overline{\psi}^l_\mu \psi^{l'\mu} = \sum_{s,k,s',k'} C(l,s,k)C(l',s',k')\overline{u}^s(p)\epsilon^{*k}_\mu u^{s'}(p)\epsilon^{k'\mu}, \tag{3.10}$$

which can be written as

$$\overline{\psi}^l_\mu \psi^{l'\mu} = -2m\sum_{s,k} C(l,s,k)C(l',s,k) = -2m\delta^{ll'}, \tag{3.11}$$

because of the unitarity of Clebsch-Gordon coefficients.

3.2.1 The spin sum for spin-3/2 particles

The calculation performed in Chapter 4 of this thesis will contain squared matrix elements which are summed over all four gravitino polarizations. In the following the polarization tensor for a spin-3/2 field with momentum p and mass m is calculated. The spin sum

$$\Pi_{\mu\nu}(p) = \sum_l \psi^l_\mu(p)\overline{\psi}^l_\nu(p), \tag{3.12}$$

can in general contain any combination of $g_{\mu\nu}$ γ_μ and p_μ, and has units of m since there are no other masses involved. All terms have mass dimension one, as can be seen from Eq. (3.11). This gives that the general structure of the spin-sum is

$$\begin{aligned}\Pi_{\mu\nu}(p) = {} & x_1 m g_{\mu\nu} + x_2 m\gamma_\mu\gamma_\nu + x_3\gamma_\mu p_\nu + x_4 p_\mu\gamma_\nu + x_5\frac{p_\mu p_\nu}{m} \\ & + x_7\not{p}\gamma_\mu\gamma_\nu + x_8\not{p}\gamma_\mu\frac{p_\nu}{m} + x_9\not{p}\frac{p_\mu}{m}\gamma_\nu + x_{10}\not{p}\frac{p_\mu p_\nu}{m^2},\end{aligned} \tag{3.13}$$

where all coefficients are unitless scalars. $\Pi_{\mu\nu}$ must satisfy the equations of motion Eqs. (3.3), (3.4) and (3.5) as ψ^l_μ is a solution of the Rarita-Schwinger equations. Contracting two spin sums and using Eq. (3.11) one gets

$$\begin{aligned}\Pi^\lambda_\mu(p)\Pi_{\lambda\nu}(p) &= \sum_{ll'}\psi^l_\mu(p)\overline{\psi}^{l\lambda}(p)\psi^{l'}_\lambda(p)\overline{\psi}^{l'}_\nu(p)\\ &= -2m\sum_{ll'}\psi^l_\mu(p)\delta^{ll'}\overline{\psi}^{l'}_\nu(p) = -2m\Pi_{\mu\nu}(p). \end{aligned} \tag{3.14}$$

Using Eq. (3.4) one can write

$$\begin{aligned}0 &= \left(\not{p}-m\right)\Big[x_1 m g_{\mu\nu} + x_2 m\gamma_\mu\gamma_\nu + x_3\gamma_\mu p_\nu + x_4 p_\mu\gamma_\nu + x_5\frac{p_\mu p_\nu}{m}\\ &\quad + x_6\not{p}g_{\mu\nu} + x_7\not{p}\gamma_\mu\gamma_\nu + x_8\not{p}\gamma_\mu\frac{p_\nu}{m} + x_9\not{p}\frac{p_\mu}{m}\gamma_\nu + x_{10}\not{p}\frac{p_\mu p_\nu}{m^2}\Big].\end{aligned} \tag{3.15}$$

Splitting the sum gives

$$\begin{aligned}0 &= \left(m\not{p}-m^2\right)\left[x_1 g_{\mu\nu} + x_2\gamma_\mu\gamma_\nu\right]\\ &\quad + \left(\not{p}^2 - m\not{p}\right)\left[x_6 g_{\mu\nu} + x_7\gamma_\mu\gamma_\nu + x_8\gamma_\mu\frac{p_\nu}{m} + x_9\frac{p_\mu}{m}\gamma_\nu + x_{10}\frac{p_\mu p_\nu}{m^2}\right]\\ &\quad + \left(m\not{p}-m^2\right)\left[x_3\gamma_\mu\frac{p_\nu}{m} + x_4\frac{p_\mu}{m}\gamma_\nu + x_5\frac{p_\mu p_\nu}{m^2}\right].\end{aligned} \tag{3.16}$$

One can now use that $\not{p}^2 = p^2 = m^2$ and collect terms to get

$$\begin{aligned}0 &= m\left(\not{p}-m\right)\Big[(x_1-x_6)g_{\mu\nu} + (x_2-x_7)\gamma_\mu\gamma_\nu - (x_8-x_3)\gamma_\mu\frac{p_\nu}{m}\\ &\quad -(x_9-x_4)\frac{p_\mu}{m}\gamma_\nu - (x_{10}-x_5)\frac{p_\mu p_\nu}{m^2}\Big].\end{aligned} \tag{3.17}$$

This requires that $x_1 = x_6$, $x_2 = x_7$, $x_3 = x_8$, $x_4 = x_9$ and $x_5 = x_{10}$, which reduces the expression for the spin sum to

$$\Pi_{\mu\nu}(p) = \left(\not{p}+m\right)\left[x_1 g_{\mu\nu} + x_2\gamma_\mu\gamma_\nu + x_3\frac{\gamma_\mu p_\nu}{m} + x_4\frac{p_\mu\gamma_\nu}{m} + x_5\frac{p_\mu p_\nu}{m^2}\right]. \tag{3.18}$$

Using Eq. (3.3) one can write

$$0 = \gamma^\mu\left(\not{p}+m\right)\left[x_1 g_{\mu\nu} + x_2\gamma_\mu\gamma_\nu + x_3\frac{\gamma_\mu p_\nu}{m} + x_4\frac{p_\mu\gamma_\nu}{m} + x_5\frac{p_\mu p_\nu}{m^2}\right]. \tag{3.19}$$

Commuting γ_μ with $\left(\not{p}+m\right)$ gives

$$0 = \left(2p_\mu - \not{p}\gamma^\mu + m\gamma^\mu\right)\left[x_1 g_{\mu\nu} + x_2\gamma_\mu\gamma_\nu + x_3\frac{\gamma_\mu p_\nu}{m} + x_4\frac{p_\mu\gamma_\nu}{m} + x_5\frac{p_\mu p_\nu}{m^2}\right]. \tag{3.20}$$

Contracting μ in this and simplifying one can write this as

$$\begin{aligned} 0 &= (2x_1 + x_5 + 4x_3)\, p_\nu + (x_4 + x_1 + 4x_2)\, m\gamma_\nu \\ &\quad + (-2x_2 + x_4 - x_1)\, \not{p}\gamma_\nu + (-2x_3 + x_5)\, \not{p}\frac{p_\nu}{m}. \end{aligned} \tag{3.21}$$

This gives the four equations

$$0 = 2x_1 + x_5 + 4x_3, \tag{3.22}$$

$$0 = x_4 + x_1 + 4x_2, \tag{3.23}$$

$$0 = -2x_2 + x_4 - x_1 \quad \text{and} \tag{3.24}$$

$$0 = -2x_3 + x_5. \tag{3.25}$$

Solving the set of Eqs. (3.22)–(3.25) yields

$$x_2 = -\frac{1}{3}x_1, \tag{3.26}$$

$$x_3 = -\frac{1}{3}x_1, \tag{3.27}$$

$$x_4 = \frac{1}{3}x_1 \quad \text{and} \tag{3.28}$$

$$x_5 = -\frac{2}{3}x_1. \tag{3.29}$$

This can be used to write the spin sum as a function of x_1:

$$\Pi_{\mu\nu}(p) = x_1 \left(\not{p} + m\right) \left[g_{\mu\nu} - \frac{p_\mu p_\nu}{m^2} - \frac{1}{3}\left(\gamma_\mu\gamma_\nu + m\frac{\gamma_\mu p_\nu}{m^2} - m\frac{p_\mu\gamma_\nu}{m^2} - \frac{p_\mu p_\nu}{m^2}\right)\right]. \tag{3.30}$$

This can be rewritten using the commutation relations of gamma matrices and a lot of algebra as

$$\Pi_{\mu\nu}(p) = x_1 \left(\not{p} + m\right) \left[g_{\mu\nu} - \frac{p_\mu p_\nu}{m^2} - \frac{1}{3}\left(g_{\mu\rho} - \frac{p_\mu p_\rho}{m^2}\right)\left(g_{\nu\sigma} - \frac{p_\nu p_\sigma}{m^2}\right)\gamma^\rho\gamma^\sigma\right]. \tag{3.31}$$

It remains to find the absolute normalization in x_1. Equation (3.14) can be written as

$$\begin{aligned} -2m\Pi_{\mu\nu}(p) &= x_1^2 \left(\not{p} + m\right)^2 \left[g_\mu{}^\lambda - \frac{p_\mu p^\lambda}{m^2} - \frac{1}{3}\left(g_{\mu\rho} - \frac{p_\mu p_\rho}{m^2}\right)\left(g^\lambda{}_\sigma - \frac{p^\lambda p_\sigma}{m^2}\right)\gamma^\rho\gamma^\sigma\right] \\ &\quad \left[g_{\lambda\nu} - \frac{p_\lambda p_\nu}{m^2} - \frac{1}{3}\left(g_{\lambda\rho'} - \frac{p_\lambda p_{\rho'}}{m^2}\right)\left(g_{\nu\sigma'} - \frac{p_\nu p_{\sigma'}}{m^2}\right)\gamma^{\rho'}\gamma^{\sigma'}\right], \end{aligned} \tag{3.32}$$

where it was used that $\gamma^\rho\gamma^\sigma\not{p} = -\gamma^\rho\not{p}\gamma^\sigma + 2\gamma^\rho p^\sigma = \not{p}\gamma^\rho\gamma^\sigma + 2\gamma^\rho p^\sigma - 2p^\rho\gamma^\sigma$ and that $\left(g^\lambda{}_\sigma - p^\lambda p_\sigma/m^2\right)p^\sigma = 0$ such that

$$\left(g_{\mu\rho} - \frac{p_\mu p_\rho}{m^2}\right)\left(g^\lambda{}_\sigma - \frac{p^\lambda p_\sigma}{m^2}\right)\gamma^\rho\gamma^\sigma\not{p} = \not{p}\left(g_{\mu\rho} - \frac{p_\mu p_\rho}{m^2}\right)\left(g^\lambda{}_\sigma - \frac{p^\lambda p_\sigma}{m^2}\right)\gamma^\rho\gamma^\sigma.$$

Contracting λ yields

$$\begin{aligned} -2m\Pi_{\mu\nu}(p) &= 2mx_1^2\left(\not{p}+m\right)\left[g_{\mu\nu}-\frac{p_\mu p_\nu}{m^2}-\frac{1}{3}\left(g_{\mu\rho}-\frac{p_\mu p_\rho}{m^2}\right)\left(g_{\nu\sigma}-\frac{p_\nu p_\sigma}{m^2}\right)\gamma^\rho\gamma^\sigma\right. \\ &\quad -\frac{1}{3}\left(g_{\mu\rho'}-\frac{p_\mu p_{\rho'}}{m^2}\right)\left(g_{\nu\sigma'}-\frac{p_\nu p_{\sigma'}}{m^2}\right)\gamma^{\rho'}\gamma^{\sigma'} \\ &\quad \left.+\frac{1}{9}\left(g_{\mu\rho}-\frac{p_\mu p_\rho}{m^2}\right)\gamma^\rho\gamma^\sigma\left(g_{\sigma\rho'}-\frac{p_\sigma p_{\rho'}}{m^2}\right)\left(\gamma^{\rho'}\gamma_\nu-\gamma^{\rho'}\frac{p_\nu}{m^2}\not{p}\right)\right]. \quad (3.33) \end{aligned}$$

Here the last term can be multiplied out to give

$$\begin{aligned} -2m\Pi_{\mu\nu}(p) &= 2mx_1^2\left(\not{p}+m\right)\left[g_{\mu\nu}-\frac{p_\mu p_\nu}{m^2}-\frac{1}{3}\left(g_{\mu\rho}-\frac{p_\mu p_\rho}{m^2}\right)\left(g_{\nu\sigma}-\frac{p_\nu p_\sigma}{m^2}\right)\gamma^\rho\gamma^\sigma\right. \\ &\quad -\frac{1}{3}\left(g_{\mu\rho'}-\frac{p_\mu p_{\rho'}}{m^2}\right)\left(g_{\nu\sigma'}-\frac{p_\nu p_{\sigma'}}{m^2}\right)\gamma^{\rho'}\gamma^{\sigma'} \\ &\quad \left.+\frac{1}{3}\left(g_{\mu\rho}-\frac{p_\mu p_\rho}{m^2}\right)\left(g_{\nu\sigma}-\frac{p_\nu p_\sigma}{m^2}\right)\gamma^\rho\gamma^\sigma\right]. \quad (3.34) \end{aligned}$$

The right hand side now gives

$$-2m\Pi_{\mu\nu}(p) = 2mx_1\Pi_{\mu\nu}(p). \quad (3.35)$$

This means that $x_1 = -1$. The final result is:

$$\Pi_{\mu\nu}(p) = -\left(\not{p}+m\right)\left[g_{\mu\nu}-\frac{p_\mu p_\nu}{m^2}-\frac{1}{3}\left(g_{\mu\rho}-\frac{p_\mu p_\rho}{m^2}\right)\left(g_{\nu\sigma}-\frac{p_\nu p_\sigma}{m^2}\right)\gamma^\rho\gamma^\sigma\right]. \quad (3.36)$$

3.3 Gravitino dark matter

In Section 2.2.4 dark matter and WIMPs were discussed. In this section gravitino dark matter will be discussed. Gravitino LSPs are very "dark" dark matter candidates, because all their effective couplings are much smaller then the weak scale, as they are suppressed by the Planck scale. Gravitino LSPs can be realized in various supersymmetric models. Bolz, Brandenburg and Buchmüller [28] treat thermal production of a gravitino LSP. They find that the density of gravitino dark matter from thermal production can be expressed by

$$\Omega_{\tilde{G}}h^2 = 0.27\left(\frac{T_R}{10^{10}\text{ GeV}}\right)\left(\frac{100\text{ GeV}}{m_{\tilde{G}}}\right)^2\left(\frac{m_{\tilde{g}}(\mu)}{1\text{ TeV}}\right)^2. \quad (3.37)$$

Here T_R is the reheating temperature of the universe and $m_{\tilde{g}}$ is the mass of the gluino.

For high reheating temperatures $T_R \sim 10^{10}$ GeV, a gluino mass on the TeV scale and a gravitino mass on the 100 GeV scale, this gives a prediction that is on the right

order of magnitude compared to the experimental value $\Omega_{DM}h^2 = 0.1123 \pm 0.0035$. The reheating temperature is dependent on which model is used for inflation and is unknown, so one can in principle adjust it to get the right amount of gravitinos to constitute cold dark matter. Reheating temperatures on such a scale are required by theories that realize baryogenesis by thermal leptogenesis [29].

In R-parity conserving theories a gravitino LSP is absolutely stable. There is however a problem with this. As the next to LSP (NLSP) can only decay into gravitinos with a strongly suppressed decay rate, the NLSP can be relatively long lived. This creates problems for nucleosynthesis models [30]. In scenarios where R-parity is violated the NLSP would decay mainly through direct R-parity violating processes, as the decay to the LSP is suppressed, saving nucleosynthesis. One would still need to require the lifetime of the gravitino to be on the scale of the age of the universe or higher such that the dark matter density does not decay to a too low value or causes problems with the history of the Universe. Such decays are discussed in the section below, and how one can use these decays to detect gravitino dark matter is discussed in Section 3.5.

3.4 Gravitino decays

In R-parity violating scenarios gravitino LSPs can decay. As the supergravity Lagrangian does not include any direct R-parity violating terms, the decay has to go through a virtual sparticle. For the trilinear R-parity breaking couplings, one can construct such decays either at tree level or over a radiative loop. Tree level decays for the gravitino in R-parity violating scenarios with trilinear couplings with three leptons, three quarks and two quarks and a lepton in the final state were studied by Moreau and Chemtob [1], while Lola, Osland and Raklev [2] studied radiative decays with a photon-neutrino final state. In both cases one-coupling dominance was assumed, meaning that only one R-parity violating coupling is significant. Lola *et al.* showed that radiative decays can dominate for low gravitino masses and that one can get a big enough lifetime for the gravitino for it to be a viable dark matter candidate even with R-parity violating couplings of order $\mathcal{O}(10^{-3})$ for a wide range of gravitino masses. This thesis extends this work for the case of $Z^0\nu$ and W^+l^- final states.

The other possibility to make a gravitino decay is to mix charginos with leptons and neutrinos with neutralinos with bilinear R-parity breaking terms. Tran and Ibarra

[31] studied gravitino decays in the channels $\tilde{G} \to \gamma\nu$, $\tilde{G} \to Z^0\nu$ and $\tilde{G} \to W^+l^-$ in scenarios with bilinear RPV couplings and found that the last two processes are especially important as sources of cosmic anti-matter for gravitino masses bigger then the Z^0 mass.

3.5 Detecting gravitino dark matter

Any type of dark matter has at most three ways of being detected. These are direct detection, where one tries do detect interactions of a detector with dark matter particles, indirect detection, where one tries to detect the end products of decaying or annihilating dark matter and production/evidence at particle colliders. For gravitinos the coupling to matter is very small, and the hope of directly detecting gravitino dark matter is slim. Stable gravitinos allow massive metastable charged particles (MMCPs) in some scenarios which would in principle be observable at collider experiments, but this would not be conclusive evidence for a gravitino as there are several other scenarios allowing MMCPs, for a review see e.g. [32]. Directly produced gravitinos would only be seen as missing energy at colliders and determining what kind of particle is responsible for the missing energy is nontrivial.

Indirect detection has the advantage that one can use the whole universe as the production area for the detected particles. For dark matter particle models that assume the particles to only be produced and destroyed in pairs, the detection rate is proportional to the density of dark matter squared. Models where the dark matter particles decay, however, have a detection rate proportional to the density of dark matter. This is especially good for detecting dark matter in parts of the universe that have a lower density of dark matter, which usually are the parts where the background is lowest as well. Decay modes that contain photons are especially good for this kind of detection, as photons are not affected by the magnetic fields of the galaxy and point to their origin. This means that one can focus searches on areas of the universe that have a high dark matter density, or on areas that have little or no known background photons.

As the background inside our galaxy is very big, this thesis will look at the extragalactic photon flux measured by Fermi-LAT as presented in [33]. No clear signals have been seen in indirect detection experiments. One can, however, use measured spectra to

set limits on the decay rates of the dark matter candidates. In this thesis the gravitinos are unstable, such that one can use the extragalactic photons to set limits on the RPV couplings. The details on how to do this are discussed in Chapter 5. In addition to that one could use the anti-matter created in gravitino decays to set limits, however, as detectable anti-matter usually is charged its propagation through the galactic magnetic field must be included, which makes the calculation of the flux at the Earth is much more complicated.

4

Calculation of the Width of the Gravitino

In this chapter the partial widths of the gravitino in the decay channels $\tilde{G} \to Z^0\nu$ and $\tilde{G} \to W^+l^-$ for trilinear R-parity violating couplings are calculated. Note that the Hermitian conjugated processes $\tilde{G} \to Z^0\overline{\nu}$ and $\tilde{G} \to W^-l^+$ give the same contribution because the gravitino is a Majorana particle.

In Section 4.1 the kinematics of the two-body decay of the gravitino are discussed and the width of the gravitino for a given Feynman amplitude is calculated. Section 4.2 introduces the Passarino-Veltman integral decomposition used in the following sections. Section 4.3 contains the calculation of the spin averaged Feynman amplitude in a generic 2-body gravitino decay process. Section 4.4 contains the calculation of the width in the $Z^0\nu$ channel, first Subsection 4.4.1 shows the construction of the Feynman amplitudes for each diagram, Subsection 4.4.2 calculates the total amplitude for all diagrams and finally Subsection 4.4.3 contains the combination of all parts to the total width in the channel. Similarely Section 4.5 contains the calculation of the width in the W^+l^- channel. Finally Section 4.6 contains a description of how computational tools are used to evaluate the width numerically.

4.1 Two body decay of a gravitino

Before we can start calculating the width, the kinematics of the decay must be discussed. We are discussing a two body decay of a gravitino with mass $m_{\tilde{G}}$ and four momentum

p decaying into two particles with mass and four-momentum m_B, k and m_l, q. The four-momentums satisfy

$$p^2 = m_{\tilde{G}}^2, \quad k^2 = m_B^2 \quad \text{and} \quad q^2 = m_l^2. \tag{4.1}$$

As the four-momentums have to be conserved in the collision one can find

$$q = p - k. \tag{4.2}$$

Eqs. (4.1) and (4.2) give in combination that

$$p \cdot k = \frac{1}{2}\left(m_{\tilde{G}}^2 + m_B^2 - m_l^2\right). \tag{4.3}$$

As the three-momentums are conserved as well, one can find in the rest frame of the decaying particle that

$$|\mathbf{k}| = |\mathbf{q}| = \frac{m_+ m_-}{2m_{\tilde{G}}}. \tag{4.4}$$

where

$$m_+^2 = m_{\tilde{G}}^2 - (m_B + m_l)^2 \quad \text{and} \quad m_-^2 = m_{\tilde{G}}^2 - (m_B - m_l)^2. \tag{4.5}$$

A two body decay for a given spin configuration in the rest frame of the decaying particle has the differential decay width

$$d\Gamma = \frac{1}{32\pi^2}|\mathcal{M}|^2 \frac{|\mathbf{k}|}{m_{\tilde{G}}^2} d\Omega. \tag{4.6}$$

Here $\mathcal{M}$ is the Feynman amplitude for the process and $\mathbf{k}$ is the three-momentum of the first final state particle.

To get the total decay width for any spin state, the initial spins are averaged over while the final spins are summed over. The gravitino has four spin states, so to average these we sum over all spin states s_G of the gravitino and multiply by 1/4. In the final state we sum over the final fermion spin states s and the polarization states of the final boson l. The spin averaged amplitude of the process is then

$$\overline{|\mathcal{M}|^2} = \frac{1}{4}\sum_{s_G,s,l} |\mathcal{M}|^2. \tag{4.7}$$

In the rest frame of the decaying particle there can not be any preferred direction after spin averaging and the solid angle can be integrated out to give 4π. This gives together with Eq. (4.4)

$$\Gamma = \frac{1}{16\pi}\frac{m_+ m_-}{m_{\tilde{G}}^3}\overline{|\mathcal{M}|^2}. \tag{4.8}$$

4.2 The Passarino-Veltman integral decomposition

In this thesis the techniques of Passarino-Veltman (PaVe) integral decomposition [34] are used to remove divergences and the package LoopTools 2.7 [3] is used for numerical calculation. This section will introduce the integrals used in this work and which divergences they have. Then they are decomposed into their tensor components. Appendix B contains explicit decompositions of the tensor integrals used in this work. The notation used is consistent with the definitions of the LoopTools package. The definitions below are meant as integral definitions, interpretations of these as diagrams can be found in Section 4.4 and Section 4.5.

In this thesis two and three point integrals, meaning diagrams with two or three propagators, are used. In the standard definitions for Passerino-Veltman integrals the general scalar two point integral is written as

$$B_0(p10^2, m_1^2, m_2^2) = \frac{(2\pi\mu)^{(4-d)}}{i\pi^2} \int \frac{d^d q}{\left(q^2 - m_1^2\right)\left((q+p_1)^2 - m_2^2\right)}, \tag{4.9}$$

where $pij = (p_i - p_j)$ and $p_0 = (0, \vec{0})$. Here p_i are external momenta, while q is the loop momentum to be integrated over. Note that the integral is done in $d = 4 - \epsilon$ dimensions, and that an anomalous mass dimension μ is introduced to keep the mass dimension of the integral independent of ϵ. The physical limit $\epsilon \to 0$ is taken in the end. Similarly the general scalar three point function is written as

$$\begin{aligned} &C_0(p10^2, p12^2, p20^2, m_1^2, m_2^2, m_3^2) = \\ &\frac{(2\pi\mu)^{(4-d)}}{i\pi^2} \int \frac{d^d q}{\left(q^2 - m_1^2\right)\left((q+p_1)^2 - m_2^2\right)\left((q+p_2)^2 - m_3^2\right)}. \end{aligned} \tag{4.10}$$

The general scalar n-point function is designated by the nth letter in the alphabet with index 0.

In the same notation tensor three point integrals can be written as

$$C^{\mu} = \frac{(2\pi\mu)^{(4-d)}}{i\pi^2} \int \frac{q^{\mu} d^d q}{\left(q^2 - m_1^2\right)\left((q+p_1)^2 - m_2^2\right)\left((q+p_2)^2 - m_3^2\right)}, \tag{4.11}$$

and

$$C^{\mu\nu} = \frac{(2\pi\mu)^{(4-d)}}{i\pi^2} \int \frac{q^{\mu} q^{\nu} d^d q}{\left(q^2 - m_1^2\right)\left((q+p_1)^2 - m_2^2\right)\left((q+p_2)^2 - m_3^2\right)}, \tag{4.12}$$

where we have omitted the parameters $(p10^2, p12^2, p20^2, m_1^2, m_2^2, m_3^2)$ on the left hand side for simplicity. Because of Lorentz invariance these can be decomposed in their tensor-structure as

$$C^\mu = p_1^\mu C_{p1} + p_2^\mu C_{p2}, \tag{4.13}$$

and

$$C^{\mu\nu} = g^{\mu\nu} C_{00} + p_1^\mu p_1^\nu C_{p_1p_1} + p_2^\mu p_2^\nu C_{p_2p_2} + (p_1^\mu p_2^\nu + p_2^\mu p_1^\nu) C_{p_1p_2}. \tag{4.14}$$

The constants C_i and C_{ij} can again be decomposed into the scalar two and three point functions above.

While the scalar three point function C_0 in Eq. (4.10) has no divergences, the scalar two-point function in Eq. (4.9) diverges as

$$\mathrm{Div}[B_0(p10^2, m_1^2, m_2^2)] = \frac{2}{\epsilon} \tag{4.15}$$

where ϵ is the anomalous dimension. As the divergence is independent of the masses in the loop and the masses of the external particles, any difference between two scalar two-point functions is finite.

For the diagrams in the discussed processes the external momenta will be defined as follows: $p_1 = -p$, $p_2 = -k$ with $p^2 = m_{\tilde{G}}^2$, $k^2 = m_B^2$ and $(p-k)^2 = m_l^2$. Here $m_{\tilde{G}}$ is the gravitino mass and p its four-momentum, m_B is the gauge boson mass and k its four-momentum and m_l is the mass of the final lepton (either a charged lepton or a neutrino) which has a four momentum of $p-k$. The loop masses vary from diagram to diagram.

In Appendix B the constants C_i and C_{ij} are written down explicitly in terms of scalar PaVe integrals and the external momenta with generic loop masses m_1, m_2 and m_3. For $m_{\tilde{G}}^2 \neq 0$ and $m_B^2 \neq 0$ Eqs. (B.11) and (B.12) contain the finite expressions for the scalar constants for the tensor three point integral with one free tensor index in Eq. (4.13), which are rewritten in a dimensionless form in Eqs. (B.13) and (B.14) respectively. The constants for the tensor three point integral with two free tensor indices in Eq. (4.14) have a finite part and a divergent part. They are given in Eqs. (B.17), (B.19),(B.21) and (B.23). They can be rewritten as finite dimensionless constants C'_{00}, C'_{pp}, C'_{kk} and C'_{pk} plus a second divergent part as shown in Eqs. (B.18), (B.20), (B.22) and (B.24) respectively. From these we see that C_{00} diverges as $2/\epsilon$, while C_{pp}, C_{kk} and C_{pk} contain a term that goes as $1/m_l^2$. In cases where $m_l \to 0$ the latter terms manifest

as a superficial divergence, and one has to cancel them explicitly before evaluating the constants numerically.

4.3 Calculation of $\overline{|\mathcal{M}|^2}$

In this section, the averaged amplitude is calculated. Below, e.g. Eq. (4.92), the form of the amplitude $\mathcal{M}$ for all radiative processes involved will be found to be

$$\mathcal{M} = -i\frac{\lambda e}{2\sin\theta_W}\frac{m_{fd}m_{\tilde{G}}}{16\pi^2\sqrt{2}M}\mathcal{F}. \tag{4.16}$$

Here λ is the R-parity violating coupling involved, θ_W is the weak mixing angle, $m_{\tilde{G}}$ is the mass of the gravitino, m_{fd} is the mass of the down type fermion in the loop and M is the reduced Planck mass. The reduced amplitude $\mathcal{F}$ is on the form

$$\mathcal{F} = \epsilon^*(k)^\rho\overline{u}(p-k)\mathrm{P_R}\left\{(C_{Ppk}p_\rho + C_{P\gamma k}\gamma_\rho + C_{Pkk}k_\rho)k_\mu + C_{Pg}g_{\rho\mu}\right\}\psi^\mu(p), \tag{4.17}$$

where k_ρ is the 4-momentum of the final state boson, p_ρ is the 4-momentum of the gravitino, $\epsilon(k)$ is the polarization vector of the gauge boson, $\overline{u}(p-k)$ is the spinor of the final state lepton and $\psi^\mu(p)$ is the vector-spinor of the gravitino. The constants C_{Pij} contain combinations of the constants C_i and C_{ij} introduced in Section 4.2. The reason for this structure is that the equations of motion of the gravitino, Eqs. (3.3)–(3.5), eliminate occurrences of $p_\mu\psi^\mu(p)$ and $\gamma_\mu\psi^\mu(p)$.

Writing down $\overline{|\mathcal{M}|^2}$, the absolute square of the Feynman amplitude averaged over spin states of the gravitino, in terms of the reduced amplitude, one gets

$$\overline{|\mathcal{M}|^2} = \frac{\alpha\lambda^2 m_{\tilde{G}}^2}{512\pi^3\sin^2\theta_W}\frac{m_{fd}^2}{M^2}\overline{|\mathcal{F}|^2}, \tag{4.18}$$

where

$$\overline{|\mathcal{F}|^2} = \frac{1}{4}\sum_{s_G,s,l}\mathcal{F}\mathcal{F}^\dagger, \tag{4.19}$$

is the spin averaged reduced amplitude. This can be written

$$\begin{aligned}\overline{|\mathcal{F}|^2} = \frac{1}{4}\sum_{s_G,s,l}&\epsilon_l^*(k)^\rho\epsilon_l(k)^\eta \\ &\times\overline{u}_s(p-k)\mathrm{P_R}\left\{(C_{Ppk}p_\rho + C_{P\gamma k}\gamma_\rho + C_{Pkk}k_\rho)k_\mu + C_{Pg}g_{\mu\rho}\right\}\psi^\mu_{s_G}(p) \\ &\times\overline{\psi}^\pi_{s_G}(p)\left\{(C^*_{Ppk}p_\eta + C^*_{P\gamma k}\gamma_\eta + C^*_{Pkk}k_\eta)k_\pi + C^*_{Pg}g_{\eta\pi}\right\}\mathrm{P_L}u_s(p-k).\end{aligned} \tag{4.20}$$

We now use the spin polarization sum for the gravitino found in Eq. (3.36) and the polarization sum for the boson in Eq. (A.14) to replace the polarization vectors ϵ and vector-spinors ψ in this expression:

$$\begin{aligned}\overline{|\mathcal{F}|^2} &= \frac{1}{4}\sum_s \left(-(g^{\rho\eta}-k^\rho k^\eta/m_B^2)\right)\\ &\times\overline{u}_s(p-k)\mathrm{P_R}\left\{(C_{Ppk}p_\rho+C_{P\gamma k}\gamma_\rho+C_{Pkk}k_\rho)k_\mu+C_{Pg}g_{\mu\rho}\right\}\\ &\times(-1)\left(\not{p}+m_{\tilde{G}}\right)\left[\left(g^{\mu\pi}-\frac{p^\mu p^\pi}{m_{\tilde{G}}^2}\right)-\frac{1}{3}\left(g^{\mu\alpha}-\frac{p^\mu p^\alpha}{m_{\tilde{G}}^2}\right)\left(g^{\pi\beta}-\frac{p^\pi p^\beta}{m_{\tilde{G}}^2}\right)\gamma_\alpha\gamma_\beta\right]\\ &\times\left\{(C^*_{Ppk}p_\eta+C^*_{P\gamma k}\gamma_\eta+C^*_{Pkk}k_\eta)k_\pi+C^*_{Pg}g_{\eta\pi}\right\}\mathrm{P_L}u_s(p-k),\end{aligned} \tag{4.21}$$

where $m_B^2=k^2$ is the mass of the final state boson.

Because

$$\left(g^{\rho\eta}-x^\rho x^\eta/x^2\right)x_\rho=\left(g^{\rho\eta}-x^\rho x^\eta/x^2\right)x_\eta=0, \tag{4.22}$$

all terms that contain k_ρ or k_η, in other words the C_{kk} terms, will not contribute and are removed. Using the spin sum for a fermion in Eq. (A.15) for a massive lepton with mass m_l one can replace the spinors with a trace over the Dirac matrices and get

$$\overline{|\mathcal{F}|}^2 = \frac{1}{4}\left(g^{\rho\eta}-k^\rho k^\eta/m_B^2\right)T_{\rho\eta}. \tag{4.23}$$

Here we have defined the trace

$$\begin{aligned}T_{\rho\eta} &= \mathrm{Tr}[(\not{p}-\not{k}+m_l)\mathrm{P_R}\left\{(C_{Ppk}p_\rho+C_{P\gamma k}\gamma_\rho)k_\mu+C_{Pg}g_{\mu\rho}\right\}\\ &\times\left(\not{p}+m_{\tilde{G}}\right)\left[\left(g^{\mu\pi}-\frac{p^\mu p^\pi}{m_{\tilde{G}}^2}\right)-\frac{1}{3}\left(g^{\mu\alpha}-\frac{p^\mu p^\alpha}{m_{\tilde{G}}^2}\right)\left(g^{\pi\beta}-\frac{p^\pi p^\beta}{m_{\tilde{G}}^2}\right)\gamma_\alpha\gamma_\beta\right]\\ &\times\left\{(C^*_{Ppk}p_\eta+C^*_{P\gamma k}\gamma_\eta)k_\pi+C^*_{Pg}g_{\eta\pi}\right\}\mathrm{P_L}].\end{aligned} \tag{4.24}$$

Again because of Eq. (4.22) terms in $T_{\rho\eta}$ that contain k_ρ or k_η will not contribute and can be removed. The trace $T_{\rho\eta}$ is calculated in Appendix C. Equation (C.35) contains the complete expression for $T_{\rho\eta}$. The kinematics as described in Section 4.1 and the $m_\pm$ notation defined in Eq. (4.5) used in combination with the spin sum for the boson in Eq. (A.14) give

$$\left(g^{\rho\eta}-k^\rho k^\eta/m_B^2\right)g_{\rho\eta} = \left(4-k^2/m_B^2\right)=3 \quad \text{and} \tag{4.25}$$

$$\left(g^{\rho\eta}-k^\rho k^\eta/m_B^2\right)p_\rho p_\eta = \frac{m_{\tilde{G}}^2m_B^2-\frac{1}{4}\left(m_{\tilde{G}}^2+m_B^2-m_l^2\right)^2}{m_B^2}, \tag{4.26}$$

such that, using Eq. (C.35), Eq. (4.23) can be written

$$\begin{aligned}
\overline{|\mathcal{F}|^2} &= \frac{1}{96}|C_{Ppk}|^2\frac{(m_{\tilde{G}}^2-m_B^2+m_l^2)}{m_{\tilde{G}}^2m_B^2}m_-^4m_+^4 \\
&+\frac{1}{24}|C_{P\gamma k}|^2\frac{m_-^2m_+^2}{m_{\tilde{G}}^2m_B^2}[m_-^2m_+^2+3(m_{\tilde{G}}^2-m_B^2+m_l^2)m_B^2] \\
&+\frac{1}{24}|C_{Pg}|^2\frac{(m_{\tilde{G}}^2-m_B^2+m_l^2)}{m_{\tilde{G}}^2m_B^2}(m_{\tilde{G}}^4+2(5m_B^2-m_l^2)m_{\tilde{G}}^2+(m_B^2-m_l^2)^2) \\
&+\frac{1}{24}\mathrm{Re}\{C_{Ppk}C_{Pg}^*\}\frac{(m_{\tilde{G}}^4-(m_B^2-m_l^2)^2)}{m_{\tilde{G}}^2m_B^2}m_+^2m_-^2 \\
&+\frac{1}{24}\mathrm{Re}\{C_{P\gamma k}C_{Ppk}^*\}\frac{m_-^4m_+^4}{m_{\tilde{G}}m_B^2} \\
&+\frac{1}{12}\mathrm{Re}\{C_{P\gamma k}C_{Pg}^*\}m_-^2m_+^2\frac{(m_{\tilde{G}}^2+3m_B^2-m_l^2)}{m_{\tilde{G}}m_B^2}. \qquad (4.27)
\end{aligned}$$

However, the constants C_{Ppk}, $C_{P\gamma k}$ and C_{Pg} do not have zero mass dimension. Additionally, parts of the expression will cancel when using the explicit expressions for the constants C_i and C_{ij} that can be found in Appendix B. To make the cancellations explicit and simplify numerical calculations we define the following constants

$$K_1 = C_{pk}\frac{m_-^2m_+^2}{m_{\tilde{G}}}, \qquad (4.28)$$

$$K_2 = C_{\gamma k}\frac{m_-^2m_+^2}{m_{\tilde{G}}^2} \text{ and} \qquad (4.29)$$

$$K_3 = C_g m_{\tilde{G}}. \qquad (4.30)$$

Using these constants Eq. (4.27) can be written

$$\begin{aligned}
\overline{|\mathcal{F}|^2} &= \frac{1}{96}|K_1|^2\frac{(m_{\tilde{G}}^2 - m_B^2 + m_l^2)}{m_B^2} \\
&+\frac{1}{24}|K_2|^2\frac{m_{\tilde{G}}^2}{m_B^2}\left[1 + 3\frac{(m_{\tilde{G}}^2 - m_B^2 + m_l^2)m_B^2}{m_-^2 m_+^2}\right] \\
&+\frac{1}{24}|K_3|^2\frac{(m_{\tilde{G}}^2 - m_B^2 + m_l^2)}{m_{\tilde{G}}^2}\left(\frac{m_{\tilde{G}}^2}{m_B^2} + 2\frac{(5m_B^2 - m_l^2)}{m_B^2} + \frac{(m_B^2 - m_l^2)^2}{m_{\tilde{G}}^2 m_B^2}\right) \\
&+\frac{1}{24}\mathrm{Re}\{K_1 K_3^*\}\left(\frac{m_{\tilde{G}}^2}{m_B^2} - \frac{(m_B^2 - m_l^2)^2}{m_{\tilde{G}}^2 m_B^2}\right) \\
&+\frac{1}{24}\mathrm{Re}\{K_1 K_2^*\}\frac{m_{\tilde{G}}^2}{m_B^2} \\
&+\frac{1}{12}\mathrm{Re}\{K_2 K_3^*\}\frac{(m_{\tilde{G}}^2 + 3m_B^2 - m_l^2)}{m_B^2}. \qquad (4.31)
\end{aligned}$$

We have now found an expression for $\overline{|\mathcal{F}|^2}$, given a reduced amplitude $\mathcal{F}$ on the form of Eq. (4.17). It remains to demonstrate that Eq. (4.17) is correct and to find explicit expressions for the constants K_1, K_2 and K_3 for the two processes discussed.

4.4 $\tilde{G} \to Z^0\nu$

In the following the width of the gravitino in the radiative decay mode $\tilde{G} \to Z^0\nu$ will be calculated. There will be contributions from the trilinear couplings λ_{ijk} and λ'_{ijk} in the superpotential in Eq. (2.72). However, as decays through λ''_{ijk} always have a quark in the final state these couplings can not contribute to this process at lowest order. To do the calculation the amplitudes for the involved diagrams are found, combined and brought on the form shown in Eq. (4.16). Then the result from Section 4.3 is used to calculate the spin averaged squared amplitude for the process, and finally Eq. (4.8) is used to find the width.

In this section p designates the four-momentum of the gravitino, k is the four-momentum of the Z boson and $p - k$ is the four-momentum of the neutrino. The neutrino is assumed to be massless and the equation of motion for a massless spin-1/2 spinor with the 4-momentum $p^\mu - k^\mu$ is used, which is

$$(\not{p} - \not{k})u(p - k) = 0. \qquad (4.32)$$

The kinematics are given in Section 4.1 where one can replace $m_B = m_Z$ and $m_l = 0$.

4.4.1 Diagrams and amplitudes

The contributing diagrams are shown in Figs. 4.1–4.6 and are divided into three types of diagrams. Type 1 diagrams, shown in Figs. 4.1 and 4.2 on the following page, are the diagrams where the boson radiates of the fermion in the loop. Type 2 diagrams, shown in Figs. 4.3 on page 42 and 4.4 on page 43, are the diagrams where the boson radiates off the sfermion in the loop. Type 3 diagrams, shown in Figs 4.5 on page 44 and 4.6 on page 45, are the diagrams that contain the four-particle couplings. All diagrams come in two versions, one where the scalar particles in the loop are the superpartners of the left handed fermions, which we call the left handed diagrams, and one where the scalar particles in the loop are the superpartners of the right handed fermions, which we call the right handed diagrams. The right handed diagrams have reversed fermion number flow in the loop, compared to the left handed diagrams. In all diagrams the loop particles with an index L are understood to be contained in a SU(2) doublet of superfields with weak hypercharge Y_L. The additional index $u(d)$ designates that the particle is contained in the upper (lower) component of the doublet. Similarly, all loop particles with an index R are understood to be contained in an SU(2) singlet superfield with weak hypercharge Y_R. Here the additional index $u(d)$ indicates which $SU(2)$ singlet superfield the particle is contained in.

As the Z-couplings as well as the gravitino-couplings do not violate fermion flavor, while the R-parity violating interaction does, all the (s)fermions in the loops in the diagrams must have the same flavor. As $\lambda_{iik} = 0$ because of $SU(2)$ symmetry, the neutrino must have a different flavor than the ones in the leptonic loop. This is not the case for quark-squark loops. For simplicity λ will designate both λ_{ijk} and λ'_{ijk} and flavor indices will be omitted in the following.

The Feynman rules and conventions used in this part are given in Appendix A. All momenta are defined to flow left to right. Note that diagrams with colored particles have to be multiplied by a color factor 3 because quarks exist in three colors, such that three copies of the diagram exist. The loop masses are labeled by the name of the particle, e.g. $m_{\tilde{f}dL}$ is the mass of the down type sfermion belonging to the SU(2) doublet. The dimensionless constants

$$a = \frac{[1 - (1 - Y_L)\sin^2\theta_W]}{\cos\theta_W} \quad \text{and} \quad b = \frac{[Y_R \sin^2\theta_W]}{\cos\theta_W}, \tag{4.33}$$

are used to separate the different structures of the amplitudes for this process.

4.4.1.1 Type 1 diagrams

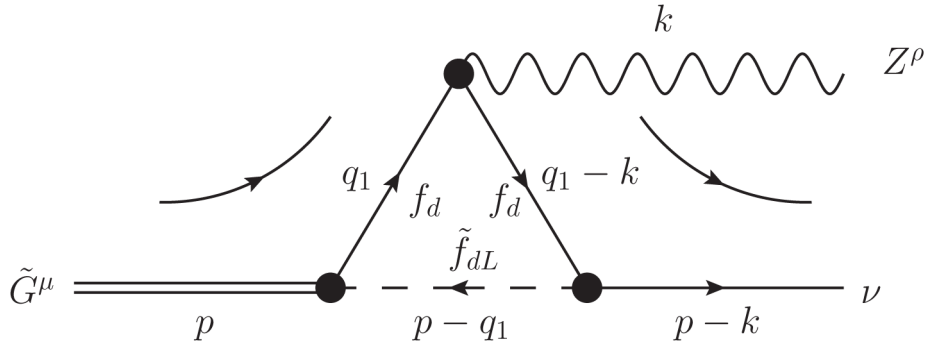

Figure 4.1: Diagram 1L for the radiative gravitino decay $\tilde{G} \to Z^0\nu$. The external arrows specify the reading direction for the fermion lines in the diagram. The arrows on the lines represent fermion number flow. All momenta are defined left-to-right.

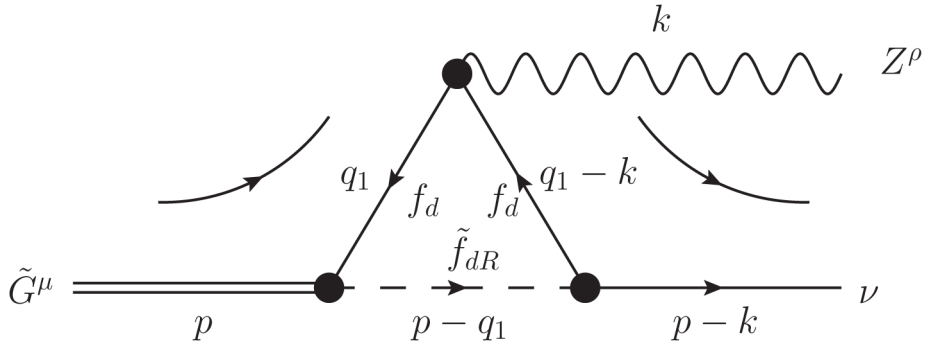

Figure 4.2: Diagram 1R for the radiative gravitino decay $\tilde{G} \to Z^0\nu$. See caption of Fig. 4.1 for details.

Using the Feynman rules in Figs. A.10 on page 92 and A.11 on page 94 in combination with the R-parity violating Feynman rules of Section A.3.1, Diagram 1L in Fig. 4.1 gives the Feynman amplitude

$$\begin{aligned}
\mathcal{M}_{1LZ} &= \int \frac{d^4q_1}{(2\pi)^4}\overline{u}(p-k)\,(-i\lambda \mathrm{P_R})\,\frac{i(\not{q}_1 - \not{k} + m_{fd})}{(q_1-k)^2 - m_{fd}^2} \\
&\quad \times \left(i\gamma_\rho \frac{e(a\mathrm{P_L} + b\mathrm{P_R})}{2\sin\theta_W}\right)\frac{i(\not{q}_1 + m_{fd})}{q_1^2 - m_{fd}^2} \\
&\quad \times \left[\frac{-i}{\sqrt{2}M}\mathrm{P_R}\gamma_\mu\left(\not{p} - \not{q}_1\right)\right]\psi^\mu(P)\frac{i}{(p-q_1)^2 - m_{\tilde{f}dL}^2}\epsilon^*(k)^\rho, \qquad (4.34)
\end{aligned}$$

which can be rewritten, using the commutation relations for $\mathrm{P_R}$ and gamma matrices, as

$$\begin{aligned}\mathcal{M}_{1LZ} &= -\frac{\lambda e}{2\sqrt{2}\sin\theta_W}\frac{m_{fd}}{M}\epsilon^*(k)^\rho\overline{u}(p-k)\mathrm{P_R}\int\frac{d^4q_1}{(2\pi)^4} \\ &\times\frac{a\gamma_\rho\not{q}_1+b(\not{q}_1-\not{k})\gamma_\rho}{(q_1^2-m_{fd}^2)((q_1-p)^2-m_{\tilde{f}dL}^2)((q_1-k)^2-m_{fd}^2)}\gamma_\mu\left(\not{p}-\not{q}_1\right)\psi^\mu(P). \quad (4.35)\end{aligned}$$

Using the same Feynman rules, Diagram 1R in Fig. 4.2 on the facing page, gives the Feynman amplitude

$$\begin{aligned}\mathcal{M}_{1RZ} &= \int\frac{d^4q_1}{(2\pi)^4}\overline{u}(p-k)\left(-i\lambda\mathrm{P_R}\right)\frac{i(\not{q}_1-\not{k}+m_{fd})}{(q_1-k)^2-m_{fd}^2} \\ &\times\left(-i\gamma_\rho\frac{e(a\mathrm{P_R}+b\mathrm{P_L})}{2\sin\theta_W}\right)\frac{i(\not{q}_1+m_{fd})}{q_1^2-m_{fd}^2} \\ &\times\left[\frac{i}{\sqrt{2}M}\mathrm{P_R}\gamma_\mu\left(\not{p}-\not{q}_1\right)\right]\psi^\mu(p)\frac{i}{(p-q_1)^2-m_{\tilde{f}dR}^2}\epsilon^*(k)^\rho, \quad (4.36)\end{aligned}$$

which can be rewritten as

$$\begin{aligned}\mathcal{M}_{1RZ} &= -\frac{e\lambda}{2\sqrt{2}\sin\theta_W}\frac{m_{fd}}{M}\epsilon^*(k)^\rho\overline{u}(p-k)\mathrm{P_R}\int\frac{d^4q_1}{(2\pi)^4} \\ &\times\frac{a(\not{q}_1-\not{k})\gamma_\rho+b\gamma_\rho\not{q}_1}{(q_1^2-m_{fd}^2)((q_1-p)^2-m_{\tilde{f}dR}^2)((q_1-k)^2-m_{fd}^2)}\gamma_\mu(\not{p}-\not{q}_1)\psi^\mu(p). \quad (4.37)\end{aligned}$$

This gives that the total Feynman amplitude for the two Diagrams 1L and 1R defined as

$$\mathcal{M}_{1Z} \equiv \mathcal{M}_{1LZ}+\mathcal{M}_{1RZ}, \quad (4.38)$$

can be written

$$\begin{aligned}\mathcal{M}_{1Z} &= -\frac{e\lambda}{2\sqrt{2}\sin\theta_W}\frac{m_{fd}}{M}\epsilon^*(k)^\rho\overline{u}(p-k)\mathrm{P_R}\int\frac{d^4q_1}{(2\pi)^4} \\ &\times\left\{a\left(\frac{\gamma_\rho\not{q}_1}{d_{1ZL}}+\frac{(\not{q}_1-\not{k})\gamma_\rho}{d_{1ZR}}\right)+b\left(\frac{(\not{q}_1-\not{k})\gamma_\rho}{d_{1ZL}}+\frac{\gamma_\rho\not{q}_1}{d_{1ZR}}\right)\right\} \\ &\times\gamma_\mu\left(\not{p}-\not{q}_1\right)\psi^\mu(p), \quad (4.39)\end{aligned}$$

where

$$d_{1ZL/R} = \left(q_1^2-m_{fd}^2\right)\left((q_1-p)^2-m_{\tilde{f}dL/R}^2\right)\left((q_1-k)^2-m_{fd}^2\right). \quad (4.40)$$

As a shorthand, one can write this as

$$\mathcal{M}_{1Z} = -i\frac{e\lambda}{2\sin\theta_W}\frac{m_{fd}m_{\tilde{G}}}{16\pi^2\sqrt{2}M}\{a\mathcal{F}_{1aZ}+b\mathcal{F}_{1bZ}\}, \quad (4.41)$$

where the reduced amplitudes $\mathcal{F}_{1aZ}$ and $\mathcal{F}_{1bZ}$ are given by

$$\begin{aligned}\mathcal{F}_{1aZ} &= \left[\frac{16\pi^2}{im_{\tilde{G}}}\right]\epsilon^*(k)^\rho\overline{u}(p-k)\\ &\quad \mathrm{P_R}\int\frac{d^4q_1}{(2\pi)^4}\left(\frac{\gamma_\rho \not{q}_1}{d_{1ZL}}+\frac{(\not{q}_1-\not{k})\gamma_\rho}{d_{1ZR}}\right)\gamma_\mu(\not{p}-\not{q}_1)\psi^\mu(p) \qquad (4.42)\end{aligned}$$

and

$$\begin{aligned}\mathcal{F}_{1bZ} &= \left[\frac{16\pi^2}{im_{\tilde{G}}}\right]\epsilon^*(k)^\rho\overline{u}(p-k)\\ &\quad \mathrm{P_R}\int\frac{d^4q_1}{(2\pi)^4}\left(\frac{(\not{q}_1-\not{k})\gamma_\rho}{d_{1ZL}}+\frac{\gamma_\rho \not{q}_1}{d_{1ZR}}\right)\gamma_\mu(\not{p}-\not{q}_1)\psi^\mu(p). \qquad (4.43)\end{aligned}$$

Here $\mathcal{F}_{1aZ}$ and $\mathcal{F}_{1bZ}$ do not correspond to the left and right handed diagrams respectively, but mix these. However, as the only difference between $\mathcal{F}_{1aZ}$ and $\mathcal{F}_{1bZ}$ are the denominators, one can see that $\mathcal{F}_{1bZ}$ is recovered when replacing $L \leftrightarrow R$ in the scalar mass in $\mathcal{F}_{1aZ}$.

4.4.1.2 Type 2 diagrams

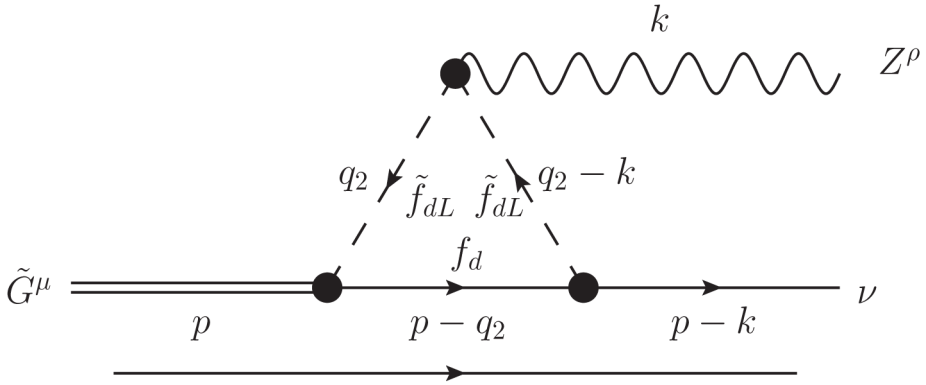

Figure 4.3: Diagram 2L for the radiative gravitino decay $\tilde{G} \to Z^0\nu$. See caption of Fig. 4.1 for details.

Using the Feynman rules in Figs. A.10 on page 92 and A.12 on page 95 in combination with the R-parity violating Feynman rules of Section A.3.1, Diagram 2L in Fig. 4.3 gives the Feynman amplitude

$$\begin{aligned}\mathcal{M}_{2LZ} &= \int\frac{d^4q_2}{(2\pi)^4}\overline{u}(p-k)\,(-i\lambda\mathrm{P_R})\,\frac{i(\not{p}-\not{q}_2+m_{fd})}{(p-q_2)^2-m_{fd}^2}\left(\frac{-i}{\sqrt{2}M}\mathrm{P_R}\gamma_\mu\not{q}_2\right)\psi^\mu(p)\\ &\quad\times\frac{i}{q_2^2-m_{\tilde{f}dL}^2}\left(-ie\frac{a}{2\sin\theta_W}\right)(2q_2-k)_\rho\frac{i}{(q_2-k)^2-m_{\tilde{f}dL}^2}\epsilon^*(k)^\rho, \qquad (4.44)\end{aligned}$$

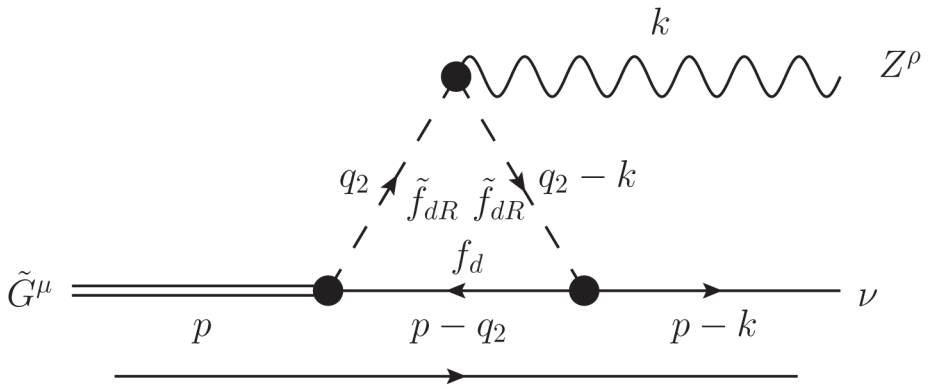

Figure 4.4: Diagram 2R for the radiative gravitino decay $\tilde{G} \to Z^0\nu$. See caption of Fig. 4.1 for details.

which can be written as

$$\mathcal{M}_{2LZ} = -i\frac{\lambda e}{2\sin\theta_W}\frac{m_{fd}m_{\tilde{G}}}{16\pi^2\sqrt{2}M}a\mathcal{F}_{2aZ}, \tag{4.45}$$

where

$$\mathcal{F}_{2aZ} = \left[\frac{16\pi^2}{im_{\tilde{G}}}\right]\epsilon^*(k)^\rho\overline{u}(p-k)\mathrm{P_R}\int\frac{d^4q_2}{(2\pi)^4}\frac{-(2q_2-k)_\rho\gamma_\mu\not{q}_2}{d_{2LZ}}\psi^\mu(p), \tag{4.46}$$

and

$$d_{2L/RZ} = (q_2^2 - m^2_{\tilde{f}dL/R})((q_2-p)^2 - m^2_{fd})((q_2-k)^2 - m^2_{\tilde{f}dL/R}). \tag{4.47}$$

Using the same Feynman rules, Diagram 2R in Fig. 4.4 gives the Feynman amplitude

$$\begin{aligned}\mathcal{M}_{2RZ} = &\int\frac{d^4q_2}{(2\pi)^4}\overline{u}(p-k)\,(-i\lambda\mathrm{P_R})\,\frac{i(\not{p}-\not{q}_2+m_{fd})}{(p-q_2)^2-m^2_{fd}}\left(\frac{i}{\sqrt{2}M}\mathrm{P_R}\gamma_\mu\not{q}_2\right)\psi^\mu(p)\\ &\times\frac{i}{q_2^2-m^2_{\tilde{f}dR}}\left(ie\frac{Y_R\sin^2\theta_W}{2\sin\theta_W\cos\theta_W}\right)(2q_2-k)_\rho\frac{i}{(q_2-k)^2-m^2_{\tilde{f}dR}}\epsilon^*(k)^\rho,\end{aligned} \tag{4.48}$$

which can be written as

$$\mathcal{M}_{2RZ} = -i\frac{\lambda e}{2\sin\theta_W}\frac{m_{fd}m_{\tilde{G}}}{16\pi^2\sqrt{2}M}b\mathcal{F}_{2bZ}, \tag{4.49}$$

where

$$\mathcal{F}_{2bZ} = \left[\frac{16\pi^2}{im_{\tilde{G}}}\right]\epsilon^*(k)^\rho\overline{u}(p-k)\mathrm{P_R}\int\frac{d^4q_2}{(2\pi)^4}\frac{-(2q_2-k)_\rho\gamma_\mu\not{q}_2}{d_{2RZ}}\psi^\mu(p). \tag{4.50}$$

This gives that the total Feynman amplitude for the two Diagrams 2L and 2R defined as

$$\mathcal{M}_{2Z} \equiv \mathcal{M}_{2LZ} + \mathcal{M}_{2RZ}, \tag{4.51}$$

can be written as

$$\mathcal{M}_{2Z} = -i\frac{\lambda e}{2\sin\theta_W}\frac{m_{fd}m_{\tilde{G}}}{16\pi^2\sqrt{2}M}(a\mathcal{F}_{2aZ} + b\mathcal{F}_{2bZ}). \tag{4.52}$$

Here $\mathcal{F}_{2aZ}$ and $\mathcal{F}_{2bZ}$ do correspond to the left and right handed diagrams respectively, and we can again recover $\mathcal{F}_{2bZ}$ from replacing $L \leftrightarrow R$ in all scalar masses in $\mathcal{F}_{2aZ}$.

4.4.1.3 Type 3 diagrams

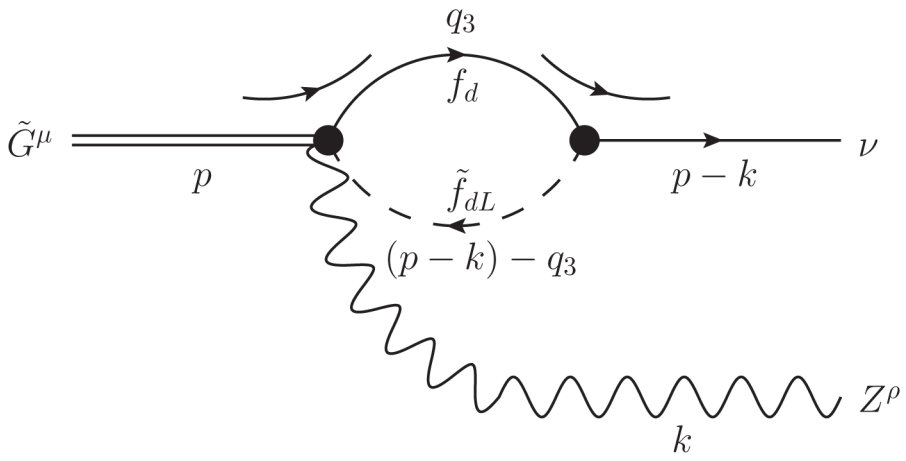

Figure 4.5: Diagram 3L for the radiative gravitino decay $\tilde{G} \to Z^0\nu$. See caption of Fig. 4.1 for details.

Using the Feynman rules in Fig. A.13 on page 96 and the R-parity violating Feynman rules of Section A.3.1, Diagram 3L in Fig. 4.5 gives the Feynman amplitude

$$\begin{aligned}\mathcal{M}_{3LZ} &= \int \frac{d^4q_3}{(2\pi)^4}\overline{u}(p-k)\,(-i\lambda \mathrm{P_R})\,\frac{i(\not{q}_3 + m_{fd})}{q_3^2 - m_{fd}^2}\left(\frac{ie}{\sqrt{2}M}\frac{a}{2\sin\theta_W}\mathrm{P_R}\gamma_\mu\gamma_\rho\right)\psi^\mu(p) \\ &\quad \times\frac{i}{(p-k-q_3)^2 - m^2_{\tilde{f}dL}}\epsilon^*(k)^\rho,\end{aligned} \tag{4.53}$$

which can be written as

$$\mathcal{M}_{3LZ} = -i\frac{\lambda e}{2\sin\theta_W}\frac{m_{fd}m_{\tilde{G}}}{16\pi^2\sqrt{2}M}a\mathcal{F}_{3aZ}. \tag{4.54}$$

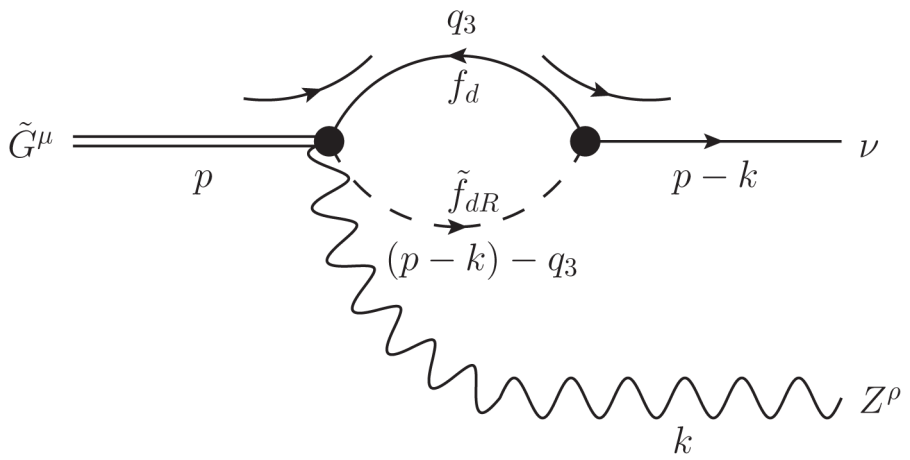

Figure 4.6: Diagram 3R for the radiative gravitino decay $\tilde{G} \to Z^0\nu$. See caption of Fig. 4.1 for details.

Here

$$\mathcal{F}_{3aZ} = \left[\frac{16\pi^2}{im_{\tilde{G}}}\right] \epsilon^*(k)^\rho \overline{u}(p-k) \mathrm{P_R} \int \frac{d^4q_3}{(2\pi)^4} \frac{\gamma_\mu \gamma_\rho}{d_{3LZ}} \psi^\mu(p), \tag{4.55}$$

and

$$d_{3L/RZ} = (q_3^2 - m_{fd}^2)((q_3 - p + k)^2 - m_{\tilde{f}dL/R}^2). \tag{4.56}$$

The same Feynman rules used on Diagram 3R in Fig. 4.6 give the Feynman amplitude

$$\begin{aligned} \mathcal{M}_{3RZ} &= \int \frac{d^4q_3}{(2\pi)^4} \overline{u}(p-k)\,(-i\lambda \mathrm{P_R})\, \frac{i(\not{q}_3 + m_{fd})}{q_3^2 - m_{fd}^2} \left(\frac{ie}{\sqrt{2}M} \frac{b}{2\sin\theta_W} \mathrm{P_R}\gamma_\mu\gamma_\rho\right) \psi^\mu(p) \\ &\quad \times \frac{i}{(p-k-q_3)^2 - m_{\tilde{f}d}^2} \epsilon^*(k)^\rho, \end{aligned} \tag{4.57}$$

which can be written as

$$\mathcal{M}_{3RZ} = -i \frac{\lambda e}{2\sin\theta_W} \frac{m_{fd} m_{\tilde{G}}}{16\pi^2\sqrt{2}M} b \mathcal{F}_{3bZ}, \tag{4.58}$$

where

$$\mathcal{F}_{3bZ} = \left[\frac{16\pi^2}{im_{\tilde{G}}}\right] \epsilon^*(k)^\rho \overline{u}(p-k) \mathrm{P_R} \int \frac{d^4q_3}{(2\pi)^4} \frac{\gamma_\mu \gamma_\rho}{d_{3RZ}} \psi^\mu(p). \tag{4.59}$$

This gives the total Feynman amplitude for the two Diagrams 3L and 3R, defined by

$$\mathcal{M}_{3Z} \equiv \mathcal{M}_{3LZ} + \mathcal{M}_{3RZ}, \tag{4.60}$$

as

$$\mathcal{M}_{3Z} = -i\frac{\lambda e}{2\sin\theta_W}\frac{m_{fd}m_{\tilde{G}}}{16\pi^2\sqrt{2}M}(a\mathcal{F}_{3aZ}+b\mathcal{F}_{3bZ}). \tag{4.61}$$

Again, $\mathcal{F}_{3aZ}$ and $\mathcal{F}_{3bZ}$ correspond to the left and right handed diagram respectively, and are interchanged when switching L and R for the scalar mass in the propagator.

4.4.2 The total amplitude

Now the amplitudes for each type of diagram are combined below to the total amplitude in the radiative process $\tilde{G}\to Z^0\nu$. To do this, all the amplitudes above are added. Then the equations of motion for the gravitino, the neutrino and the Z-boson are used to bring the expression on the form of Eq. (4.17), such that the results of Section 4.3 can be used.

Combining the results from the three sections above, one can write the total amplitude for the radiative decay $\tilde{G}\to Z^0\nu$ at one loop level as

$$\mathcal{M}_Z = \mathcal{M}_{1Z}+\mathcal{M}_{2Z}+\mathcal{M}_{3Z}, \tag{4.62}$$

which can be written in terms of the reduced amplitudes $\mathcal{F}_{aZ}$ and $\mathcal{F}_{bZ}$ as

$$\mathcal{M}_Z = -i\frac{\lambda e}{2\sin\theta_W}\frac{m_{fd}m_{\tilde{G}}}{16\pi^2\sqrt{2}M}(a\mathcal{F}_{aZ}+b\mathcal{F}_{bZ}), \tag{4.63}$$

where

$$\mathcal{F}_{a/bZ} = \mathcal{F}_{1a/bZ}+\mathcal{F}_{2a/bZ}+\mathcal{F}_{3a/bZ}. \tag{4.64}$$

As mentioned in the previous three subsections, one recovers $\mathcal{F}_{ibZ}$ by replacing $L\leftrightarrow R$ in all scalar masses in $\mathcal{F}_{iaZ}$. Since $\mathcal{F}_{a/bZ}$ is just the sum of these the calculation will be done only for $\mathcal{F}_{aZ}$. $\mathcal{F}_{bZ}$ can then be recovered by replacing the scalar masses in the result.

We use the notation in Eqs. (4.9)–(4.14) with indices on the PaVe integrals to specify which set off masses m_1, m_2 and m_3 to use, as shown in Table 4.1 on the facing page. Replacing these in $\mathcal{F}_{aZ}$ the expression can be written as

$$\begin{aligned}\mathcal{F}_{aZ} = &\left[\frac{1}{m_{\tilde{G}}}\right]\epsilon^*(k)^\rho\overline{u}(p-k)\mathrm{P_R}\{-C_{1RZ}\not{k}\gamma_\rho\gamma_\mu\not{p}+(C^\eta_{1LZ}\gamma_\rho\gamma_\eta+C^\eta_{1RZ}\gamma_\eta\gamma_\rho)\gamma_\mu\not{p}\\
&+C^\eta_{1RZ}\not{k}\gamma_\rho\gamma_\mu\gamma_\eta-C^{\eta\pi}_{1LZ}\gamma_\rho\gamma_\eta\gamma_\mu\gamma_\pi-C^{\eta\pi}_{1RZ}\gamma_\eta\gamma_\rho\gamma_\mu\gamma_\pi\\
&+C^\eta_{2LZ}\gamma_\mu\gamma_\eta k_\rho-2C_{2LZ}{}^\eta\gamma_\rho\gamma_\mu\gamma_\eta+B_0(0,m^2_{fd},m^2_{\tilde{f}dL})\gamma_\mu\gamma_\rho\}\psi^\mu(p).\end{aligned} \tag{4.65}$$

PaVe	m_B	m_l	m_1	m_2	m_3
C_{1RZ}	m_Z	0	m_{fd}	$m_{\tilde{f}dR}$	m_{fd}
C_{1LZ}	m_Z	0	m_{fd}	$m_{\tilde{f}dL}$	m_{fd}
C_{2RZ}	m_Z	0	$m_{\tilde{f}dR}$	m_{fd}	$m_{\tilde{f}dR}$
C_{2LZ}	m_Z	0	$m_{\tilde{f}dL}$	m_{fd}	$m_{\tilde{f}dL}$

Table 4.1: Masses to replace for different indices on the PaVe integrals for the $Z^0\nu$ diagrams.

Here both $B_0(0, m_{fd}^2, m_{\tilde{f}dL}^2)$ and $C_i^{\eta\pi}$ contain divergences. To simplify the expression the equations of motion for the gravitino, Eqs. (3.3)–(3.5), as well as the equation of motion for a massless neutrino, Eq. (4.32), are used to eliminate terms that do not contribute. Before expanding the integrals in terms of scalar functions, Eqs. (3.3) and (3.4) are used to remove constructions of $\gamma_\mu \not{p} \psi^\mu(p) = m_{\tilde{G}} \gamma_\mu \psi^\mu(p)$, while Eq. (A.1) is used in combination with Eq. (3.3) to replace $(\gamma_\mu\gamma_\eta)\psi^\mu(p) = 2g_{\mu\eta}\psi^\mu(p) - \gamma_\eta\gamma_\mu\psi^\mu(p) = 2g_{\mu\eta}\psi^\mu(p)$. This yields

$$\begin{aligned}\mathcal{F}_{aZ} &= \left[\frac{2}{m_{\tilde{G}}}\right] \epsilon^*(k)^\rho \overline{u}(p-k) \mathrm{P_R} \{ C_{1RZ\mu} \not{k} \gamma_\rho - C_{1LZ\mu}^\eta \gamma_\rho \gamma_\eta - C_{1RZ\mu}^\eta \gamma_\eta \gamma_\rho \\ &\quad + C_{2LZ\mu} k_\rho - 2C_{2LZ\mu\rho} + B_0(0, m_{fd}^2, m_{\tilde{f}dL}^2) g_{\mu\rho} \} \psi^\mu(p). \end{aligned} \tag{4.66}$$

Expanding the tensor integrals in $\mathcal{F}_{aZ}$ in terms of scalar components defined in Eqs. (4.13) and (4.14) gives

$$\begin{aligned}\mathcal{F}_{aZ} &= \left[\frac{2}{m_{\tilde{G}}}\right] \epsilon^*(k)^\rho \overline{u}(p-k) \mathrm{P_R} \{ C_{1RZp} \not{k} \gamma_\rho p_\mu + C_{1RZk} \not{k} \gamma_\rho k_\mu \\ &\quad - C_{1LZ00} \gamma_\rho \gamma_\mu - C_{1LZpp} \gamma_\rho \not{p} p_\mu - C_{1LZkk} \gamma_\rho \not{k} k_\mu - C_{1LZkp} (\gamma_\rho \not{p} k_\mu + \gamma_\rho \not{k} p_\mu) \\ &\quad - C_{1RZ00} \gamma_\mu \gamma_\rho - C_{1RZpp} \not{p} \gamma_\rho p_\mu - C_{1RZkk} \not{k} \gamma_\rho k_\mu - C_{1RZpk} (\not{p} \gamma_\rho k_\mu + \not{k} \gamma_\rho p_\mu) \\ &\quad + C_{2LZp} k_\rho p_\mu + C_{2LZk} k_\rho k_\mu - 2C_{2LZ00} g_{\mu\rho} - 2C_{2LZpp} p_\rho p_\mu - 2C_{2LZkk} k_\rho k_\mu \\ &\quad - 2C_{2LZpk} (p_\rho k_\mu + k_\rho p_\mu) + B_0(0, m_{fd}^2, m_{\tilde{f}dL}^2) g_{\mu\rho} \} \psi^\mu(p). \end{aligned} \tag{4.67}$$

Equation (3.3) is again used to remove all occurences of $\gamma_\mu\psi^\mu(p)$ and Eq. (3.5) is used to remove all occurences of $p_\mu\psi^\mu(p)$. Then Eq. (4.32) is used to write

$$\overline{u}(p-k) \not{k} \gamma_\rho = \overline{u}(p-k) \not{p} \gamma_\rho = \overline{u}(p-k)(2p_\rho - \gamma_\rho \not{p}). \tag{4.68}$$

Finally Eq. (3.4) is used to replace $\not{p}\psi^\mu(p) = m_{\tilde{G}}\psi^\mu(p)$. This gives

$$\begin{aligned}\mathcal{F}_{aZ} &= \left[\frac{2}{m_{\tilde{G}}}\right]\epsilon^*(k)^\rho\overline{u}(p-k)\mathrm{P_R}\{C_{1RZk}(2p_\rho-\gamma_\rho m_{\tilde{G}})k_\mu \\ &\quad -C_{1LZkk}(2k_\rho-2p_\rho+\gamma_\rho m_{\tilde{G}})k_\mu - C_{1LZkp}\gamma_\rho m_{\tilde{G}}k_\mu \\ &\quad -2C_{1RZ00}g_{\rho\mu} - C_{1RZkk}(2p_\rho-\gamma_\rho m_{\tilde{G}})k_\mu - C_{1RZpk}(2p_\rho-\gamma_\rho m_{\tilde{G}})k_\mu \\ &\quad +C_{2LZk}k_\rho k_\mu - 2C_{2LZ00}g_{\mu\rho} - 2C_{2LZkk}k_\rho k_\mu \\ &\quad -2C_{2LZpk}p_\rho k_\mu + B_0(0,m_{fd}^2,m_{\tilde{f}dL}^2)g_{\mu\rho}\}\psi^\mu(p). \end{aligned} \tag{4.69}$$

However, the $k_\mu k_\rho$ part here will not contribute to the final result, as shown in Section 4.3. Using this one can sort the expression in terms of tensor structure as

$$\begin{aligned}\mathcal{F}_{aZ} &= \left[\frac{2}{m_{\tilde{G}}}\right]\epsilon^*(k)^\rho\overline{u}(p-k)\mathrm{P_R}\{ \\ &\quad \times 2p_\rho k_\mu(C_{1LZkk}-C_{1RZkk}-C_{1RZpk}-C_{2LZpk}+C_{1RZk}) \\ &\quad +m_{\tilde{G}}\gamma_\rho k_\mu(C_{1RZkk}-C_{1LZkk}+C_{1RZpk}-C_{1LZpk}-C_{1RZk}) \\ &\quad +g_{\rho\mu}(B_0(0,m_{fd}^2,m_{\tilde{f}dL}^2)-2C_{2LZ00}-2C_{1RZ00})\}\psi^\mu(p). \end{aligned} \tag{4.70}$$

One can now write down the set of constants on the form of the ones in Eq. (4.17) as

$$C_{aZpk} = \frac{4}{m_{\tilde{G}}}(C_{1LZkk}-C_{1RZkk}-C_{1RZpk}-C_{2LZpk}+C_{1RZk}) \tag{4.71}$$

$$C_{aZg} = \frac{2}{m_{\tilde{G}}}(B_0(0,m_{fd}^2,m_{\tilde{f}dL}^2)-2C_{2LZ00}-2C_{1RZ00}) \tag{4.72}$$

$$C_{aZ\gamma k} = 2(C_{1RZkk}-C_{1LZkk}+C_{1RZpk}-C_{1LZpk}-C_{1RZk}). \tag{4.73}$$

To retrieve the constants for the b case, replace all $L \leftrightarrow R$. Using Eqs. (B.18)–(B.24) one can write Eq. (4.71) in terms of the dimensionless constants defined in Appendix B. Doing this all $1/m_\nu^2$ divergent terms cancel and leave an expression without superficial divergences:

$$C_{aZpk} = -\frac{4m_{\tilde{G}}(C'_{1LZkk}-C'_{1RZkk}-C'_{1RZpk}-C'_{2LZpk}+C'_{1RZk})}{(m_{\tilde{G}}^2-m_Z^2)^2}. \tag{4.74}$$

For Eq. (4.72) this leaves

$$\begin{aligned}C_{aZg} &= \frac{1}{m_{\tilde{G}}}(2B_0(0,m_{fd}^2,m_{\tilde{f}dL}^2)-B_0(m_{\tilde{G}}^2,m_{\tilde{f}dL},m_{fd}^2)-B_0(m_{\tilde{G}}^2,m_{fd}^2,m_{\tilde{f}dR}^2) \\ &\quad -4C'_{2LZ00}-4C'_{1RZ00}). \end{aligned} \tag{4.75}$$

Here $B_0(0, m^2_{fd}, m^2_{\tilde{f}dL})$, $B_0(m^2_{\tilde{G}}, m_{\tilde{f}dL}, m^2_{fd})$ and $B_0(m^2_{\tilde{G}}, m^2_{fd}, m^2_{\tilde{f}dR})$ each diverge with $1/\epsilon$, but the dimensionless constant is finite as the divergences cancel exactly. As $B_0(0, m^2_{fd}, m^2_{\tilde{f}dL})$ comes from diagrams of type three, while the two canceling terms come from diagrams of type two and type one respectively, this shows that the divergences cancel between all three types of diagrams.

For Eq. (4.73) all terms containing $1/m^2_\nu$ divergences cancel as well and leave

$$C_{aZ\gamma k} = -\frac{2m^2_{\tilde{G}}(C'_{1RZkk} - C'_{1LZkk} + C'_{1RZpk} - C'_{1LZpk} - C'_{1RZk})}{(m^2_{\tilde{G}} - m^2_Z)^2}. \quad (4.76)$$

Taken together the results in this section give that the total amplitude of the process $\tilde{G} \to Z^0\nu$ at lowest order can be written on the form of Eq. (4.16) and Eq. (4.17) where one can identify

$$C_{Zpk} = aC_{aZpk} + bC_{bZpk}, \quad (4.77)$$

$$C_{Zg} = aC_{aZg} + bC_{bZg} \quad \text{and} \quad (4.78)$$

$$C_{Z\gamma k} = aC_{aZ\gamma k} + bC_{bZ\gamma k}. \quad (4.79)$$

Instead of this choice of constants, one can use the dimensionless constants defined in Eqs. (4.28)–(4.30) which are

$$\begin{aligned} K_{1Z} = {} & 4[a(C'_{1LZkk} - C'_{1RZkk} - C'_{1RZpk} - C'_{2LZpk} + C'_{1RZk}) \\ & + b(C'_{1RZkk} - C'_{1LZkk} - C'_{1LZpk} - C'_{2RZpk} + C'_{1LZk})], \end{aligned} \quad (4.80)$$

and

$$\begin{aligned} K_{2Z} = {} & 2[a(C'_{1RZkk} - C'_{1LZkk} + C'_{1RZpk} - C'_{1LZpk} - C'_{1RZk}) \\ & + b(C'_{1LZkk} - C'_{1RZkk} + C'_{1LZpk} - C'_{1RZpk} - C'_{1LZk})], \end{aligned} \quad (4.81)$$

and

$$\begin{aligned} K_{3Z} = {} & [a(2B_0(0, m^2_{fd}, m^2_{\tilde{f}dL}) - B_0(m^2_{\tilde{G}}, m_{\tilde{f}dL}, m^2_{fd}) - B_0(m^2_{\tilde{G}}, m^2_{fd}, m^2_{\tilde{f}dR}) \\ & - 4C'_{2LZ00} - 4C'_{1RZ00}) \\ & + b(2B_0(0, m^2_{fd}, m^2_{\tilde{f}dR}) - B_0(m^2_{\tilde{G}}, m_{\tilde{f}dR}, m^2_{fd}) - B_0(m^2_{\tilde{G}}, m^2_{fd}, m^2_{\tilde{f}dL}) \\ & - 4C'_{2RZ00} - 4C'_{1LZ00})], \end{aligned} \quad (4.82)$$

where the dimensionless constants can be found from Appendix B by replacing the masses as in Table 4.1.

4.4.3 The width in the channel $Z^0\nu$

In this section the results from the previous two sections are combined. As shown in Eq. (4.8) together with Eq. (4.17), one can write the width of the gravitino in the radiative decay $\tilde{G} \to Z\nu$ as

$$\Gamma_{\tilde{G}\to Z^0\nu} = \frac{1}{16}\frac{\alpha\lambda^2 m_{\tilde{G}}}{512\pi^4 \sin^2\theta_W}\frac{m_{fd}^2}{M^2}\frac{(m_{\tilde{G}}^2 - m_Z^2)}{m_{\tilde{G}}^2}\overline{|\mathcal{F}|^2}. \tag{4.83}$$

The general form of $\overline{|\mathcal{F}|^2}$ is shown in Eq. (4.31), which can be written for the special case of $m_B = m_Z$ and $m_l = 0$ as

$$\begin{aligned}
\overline{|\mathcal{F}|^2} &= \frac{1}{96}|K_{1Z}|^2\left(\frac{m_{\tilde{G}}^2}{m_Z^2} - 1\right) + \frac{1}{24}|K_{2Z}|^2\left[\frac{m_{\tilde{G}}^2}{m_Z^2} + 3\frac{m_{\tilde{G}}^2}{(m_{\tilde{G}}^2 - m_Z^2)}\right] \\
&+ \frac{1}{24}|K_{3Z}|^2\left(1 - \frac{m_Z^2}{m_{\tilde{G}}^2}\right)\left(10 + \frac{m_{\tilde{G}}^2}{m_Z^2} + \frac{m_Z^2}{m_{\tilde{G}}^2}\right) \\
&+ \frac{1}{24}\mathrm{Re}\{K_{1Z}K_{3Z}^*\}\left(\frac{m_{\tilde{G}}^2}{m_Z^2} - \frac{m_Z^2}{m_{\tilde{G}}^2}\right) \\
&+ \frac{1}{24}\mathrm{Re}\{K_{1Z}K_{2Z}^*\}\frac{m_{\tilde{G}}^2}{m_Z^2} + \frac{1}{12}\mathrm{Re}\{K_{2Z}K_{3Z}^*\}\left(3 + \frac{m_{\tilde{G}}^2}{m_Z^2}\right).
\end{aligned} \tag{4.84}$$

K_{1Z}, K_{2Z} and K_{3Z} have been written down in Eqs. (4.80)–(4.82).

4.5 $\tilde{G} \to W^+l^-$

In the following the width of the gravitino in the radiative decay mode $\tilde{G} \to W^+l^-$ will be calculated. There will again be contributions from the trilinear couplings λ_{ijk} and λ'_{ijk} in the superpotential in Eq. (2.72). Again, contributions of the involved diagrams are found, combined and brought on the form shown in Eq. (4.16). Then the result of Section 4.3 is used to calculate the spin averaged squared amplitude for the process, and Eq. (4.8) is used to find the width. The particles are designated by indices as presented in Section 4.4. The main difference to the Z-case is that the final state lepton has mass. For the lepton we will in the following use the equation of motion for a massive spin-1/2 spinor with the four momentum $p^\mu - k^\mu$ and mass m_l, which is

$$(\not{p} - \not{k})u(p-k) = m_l u(p-k). \tag{4.85}$$

The kinematics in Section 4.1 are used, where one can replace $m_B = m_W$.

4.5.1 Diagrams and amplitudes

The gravitino-couplings do not violate fermion flavor, while the R-parity breaking interaction does. However, for quark couplings there is the complication that the W^+ couplings can also violate fermion flavor. As this is CKM-suppressed, it is ignored in this thesis. All the (s)fermions in the loops in the diagrams therefore be of the same generation. As $\lambda_{iik} = 0$ because of $SU(2)$ symmetry, the final state lepton must be of a different generation than the ones in the leptonic loop. This is not the case for quark-squark loops. For simplicity λ will designate $-\lambda_{ijk}$ and $-\lambda'_{ijk}$[1], and flavor indices will be omitted in the following.

The relevant diagrams are shown in Figs. 4.7–4.10 and are again divided into three types of diagrams in the same way as discussed in Section 4.4.1. There are still two versions of the first type where one has reversed fermion number flow in the loop compared to the other. However, as the W^+ particle does not couple to singlet superfields there are no right handed versions of the second and third type. The Feynman rules and conventions used in this part are given in Appendix A. The loop particles carry the same indices as described in Section 4.4.1 to designate which field they belong to.

4.5.1.1 Type 1 diagrams

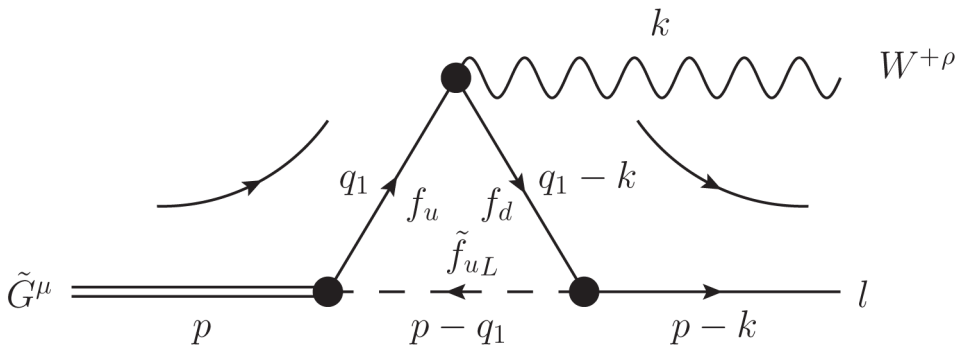

Figure 4.7: Diagram 1L for the radiative gravitino decay $\tilde{G} \to W^+ l^-$. See caption of Fig. 4.1 for details.

Using the Feynman rules in Figs. A.10 on page 92 and A.14 on page 97 in combination with the R-parity violating Feynman rules of Section A.3.1, Diagram 1L in

[1]The extra sign change is made to get the amplitude on the same form as in the $Z^0\nu$ case. As the coupling only occurs squared in the final result, this is only cosmetic.

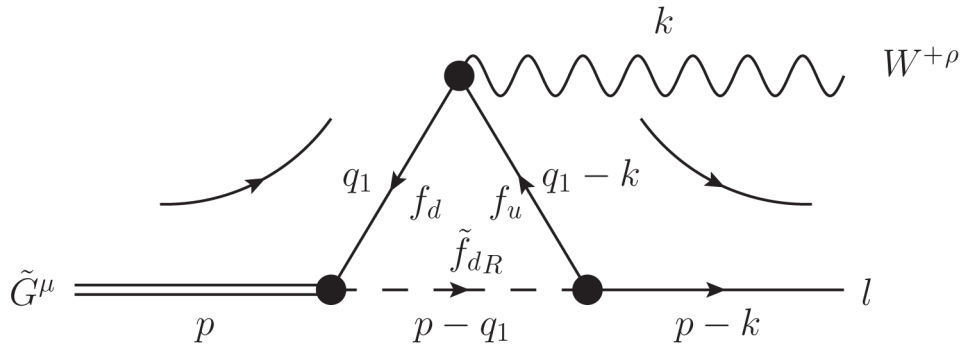

Figure 4.8: Diagram 1R for the radiative gravitino decay $\tilde{G} \to W^+ l^-$. See caption of Fig. 4.1 for details.

Fig. 4.1 on page 40 gives the Feynman amplitude

$$\begin{aligned}\mathcal{M}_{1LW} &= \int \frac{d^4q_1}{(2\pi)^4}\overline{u}(p-k)\,(-i\lambda \mathrm{P_R})\,\frac{i(\not{q}_1 - \not{k} + m_{fd})}{(q_1-k)^2 - m_{fd}^2}\left(\frac{-i\gamma_\rho e}{\sqrt{2}\sin\theta_W}\mathrm{P_L}\right)\frac{i(\not{q}_1 + m_{fu})}{q_1^2 - m_{fu}^2} \\ &\quad \times\left[\frac{-i}{\sqrt{2}M}\mathrm{P_R}\gamma_\mu\left(\not{p} - \not{q}_1\right)\right]\psi^\mu(P)\frac{i}{(p-q_1)^2 - m^2_{\tilde{f}uL}}\epsilon^*(k)^\rho, \qquad (4.86)\end{aligned}$$

which can be rewritten, using the commutation relations for $\mathrm{P_R}$ and gamma matrices, as

$$\mathcal{M}_{1LW} = \frac{\lambda e}{2\sin\theta_W}\frac{m_{fd}}{M}\epsilon^*(k)^\rho\overline{u}(p-k)\mathrm{P_R}\int\frac{d^4q_1}{(2\pi)^4}\frac{\gamma_\rho\not{q}_1\gamma_\mu\left(\not{p}-\not{q}_1\right)}{d_{1LW}}\psi^\mu(P), \quad (4.87)$$

where

$$d_{1LW} = (q_1^2 - m_{fu}^2)((q_1-p)^2 - m^2_{\tilde{f}uL})((q_1-k)^2 - m_{fd}^2). \qquad (4.88)$$

Using the same Feynman rules, Diagram 1R in Fig. 4.8, gives the Feynman amplitude

$$\begin{aligned}\mathcal{M}_{1RW} &= \int \frac{d^4q_1}{(2\pi)^4}\overline{u}(p-k)\,(-i\lambda \mathrm{P_R})\,\frac{i(\not{q}_1 - \not{k} + m_{fu})}{(q_1-k)^2 - m_{fu}^2}\left(\frac{i\gamma_\rho e}{\sqrt{2}\sin\theta_W}\mathrm{P_R}\right)\frac{i(\not{q}_1 + m_{fd})}{q_1^2 - m_{fd}^2} \\ &\quad \times\left[\frac{i}{\sqrt{2}M}\mathrm{P_R}\gamma_\mu\left(\not{p} - \not{q}_1\right)\right]\psi^\mu(p)\frac{i}{(p-q_1)^2 - m^2_{\tilde{f}dR}}\epsilon^*(k)^\rho, \qquad (4.89)\end{aligned}$$

which can be rewritten as

$$\begin{aligned}\mathcal{M}_{1RW} &= \frac{\lambda e}{2\sin\theta_W}\frac{m_{fd}}{M}\epsilon^*(k)^\rho\overline{u}(p-k) \\ &\quad \times\mathrm{P_R}\int\frac{d^4q_1}{(2\pi)^4}\frac{(\not{q}_1 - \not{k})\gamma_\rho\gamma_\mu\left(\not{p}-\not{q}_1\right)}{d_{1RW}}\psi^\mu(p), \qquad (4.90)\end{aligned}$$

where

$$d_{1RW} = (q_1^2 - m_{fd}^2)((q_1 - p)^2 - m_{\tilde{f}dR}^2)((q_1 - k)^2 - m_{fu}^2). \tag{4.91}$$

Thus, the sum of both diagrams can be written as

$$\mathcal{M}_{1W} = -i\frac{\lambda e}{2\sin\theta_W}\frac{m_{fd}m_{\tilde{G}}}{16\pi^2\sqrt{2}M}\mathcal{F}_{1W}, \tag{4.92}$$

where

$$\begin{aligned}\mathcal{F}_{1W} &= \left[\frac{16\pi^2\sqrt{2}}{im_{\tilde{G}}}\right]\epsilon^*(k)^\rho\overline{u}(p-k)\mathrm{P_R}\int\frac{d^4q_1}{(2\pi)^4} \\ &\times\left(\frac{\gamma_\rho \not{q}_1\gamma_\mu(\not{q}_1 - \not{p})}{d_{1LW}} + \frac{(\not{q}_1 - \not{k})\gamma_\rho\gamma_\mu(\not{q}_1 - \not{p})}{d_{1RW}}\right)\psi^\mu(p).\end{aligned} \tag{4.93}$$

4.5.1.2 Type 2 diagram

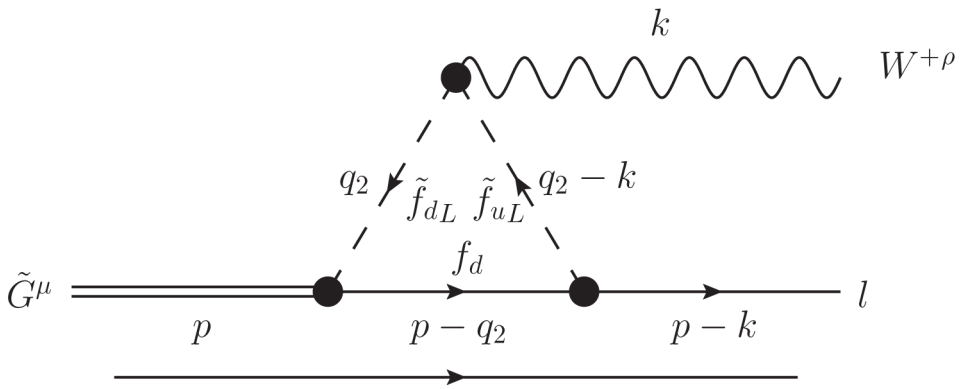

Figure 4.9: Diagram 2 for the radiative gravitino decay $\tilde{G} \to W^+ l^-$. See caption of Fig. 4.1 for details.

Using the Feynman rules in Figs. A.10 on page 92 and A.15 on page 97 in combination with the R-parity violating Feynman rules of Section A.3.1, Diagram 2 in Fig. 4.9, gives the Feynman amplitude

$$\begin{aligned}\mathcal{M}_{2W} &= \int\frac{d^4q_2}{(2\pi)^4}\overline{u}(p-k)\,(-i\lambda\mathrm{P_R})\,\frac{i(\not{p} - \not{q}_2 + m_{fd})}{(p-q_2)^2 - m_{fd}^2}\left(\frac{-i}{\sqrt{2}M}\mathrm{P_R}\gamma_\mu\not{q}_2\right)\psi^\mu(p) \\ &\times\frac{i}{q_2^2 - m_{\tilde{f}dL}^2}\left(\frac{ie}{\sqrt{2}\sin\theta_W}\right)(2q_2 - k)_\rho\frac{i}{(q_2-k)^2 - m_{\tilde{f}uL}^2}\epsilon^*(k)^\rho.\end{aligned} \tag{4.94}$$

The amplitude can be rewritten

$$\begin{aligned}\mathcal{M}_{2W} &= -\frac{\lambda e}{2\sin\theta_W}\frac{m_{fd}}{M}\epsilon^*(k)^\rho\overline{u}(p-k)\mathrm{P_R}\int\frac{d^4q_2}{(2\pi)^4}\\ &\times\frac{\gamma_\mu\not{q}_2(2q_2-k)_\rho}{(q_2^2-m^2_{\tilde{f}dL})((q_2-k)^2-m^2_{\tilde{f}uL})((p-q_2)^2-m^2_{fd})}\psi^\mu(p),\end{aligned}\tag{4.95}$$

which we can write as

$$\mathcal{M}_{2W} = -i\frac{\lambda e}{2\sin\theta_W}\frac{m_{fd}m_{\tilde{G}}}{16\pi^2\sqrt{2}M}\mathcal{F}_{2W},\tag{4.96}$$

where

$$\mathcal{F}_{2W} = \left[\frac{16\pi\sqrt{2}}{im_{\tilde{G}}}\right]\epsilon^*(k)^\rho\overline{u}(p-k)\mathrm{P_R}\int\frac{d^4q_2}{(2\pi)^4}\frac{\gamma_\mu\not{q}_2(2q_2-k)_\rho}{d_{2W}}\psi^\mu(p).\tag{4.97}$$

Here

$$d_{2W} = (q_2^2-m^2_{\tilde{f}dL})((q_2-p)^2-m^2_{fd})((q_2-k)^2-m^2_{\tilde{f}uL}).\tag{4.98}$$

4.5.1.3 Type 3 diagram

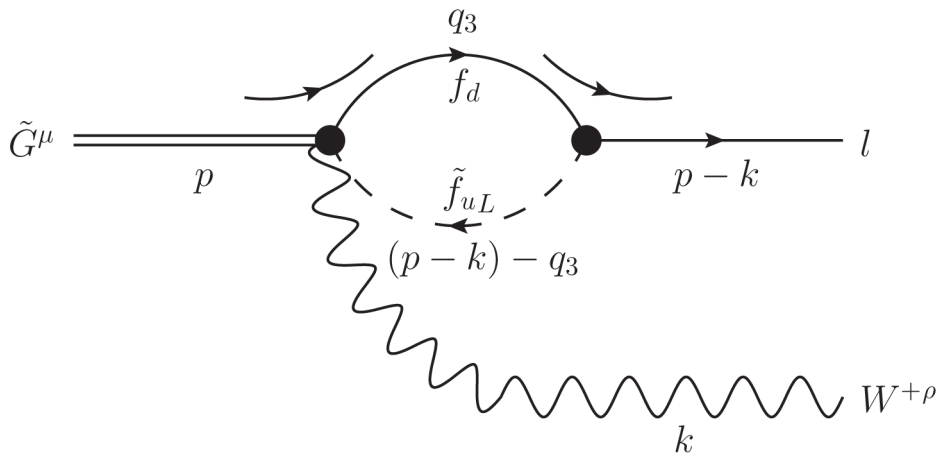

Figure 4.10: Diagram 3 for the radiative gravitino decay $\tilde{G}\to W^+l^-$. See caption of Fig. 4.1 for details.

Using the Feynman rules in Fig. A.16 on page 98 and the R-parity violating Feynman rules of section A.3.1, Diagram 3 in Fig. 4.10, gives the Feynman amplitude

$$\begin{aligned}\mathcal{M}_{3W} &= \int\frac{d^4q_3}{(2\pi)^4}\overline{u}(p-k)\left(-i\lambda\mathrm{P_R}\right)\frac{i(\not{q}_3+m_{fd})}{q_3^2-m^2_{fd}}\left(-\frac{ie}{2\sin\theta_W M}\mathrm{P_R}\gamma_\mu\gamma_\rho\right)\psi^\mu(p)\\ &\times\frac{i}{(p-k-q_3)^2-m^2_{\tilde{f}uL}}\epsilon^*(k)^\rho,\end{aligned}\tag{4.99}$$

which can again be rewritten using the commutation relations for projection operators and gamma matrices as

$$\begin{aligned}\mathcal{M}_{3W} &= \frac{\lambda e}{2\sin\theta_W}\frac{1}{M}\epsilon^*(k)^\rho \overline{u}(p-k)\mathrm{P_R}\int\frac{d^4q_3}{(2\pi)^4}\frac{(\not{q}_3+m_{fd})}{q_3^2-m_{fd}^2}\mathrm{P_R}\gamma_\mu\gamma_\rho \\ &\quad\times\frac{1}{(p-k-q_3)^2-m_{\tilde{f}uL}^2}\psi^\mu(p). \end{aligned} \tag{4.100}$$

This amplitude can also be written in terms of a reduced amplitude $\mathcal{F}_{3W}$

$$\mathcal{M}_{3W} = -i\frac{\lambda e}{2\sin\theta_W}\frac{m_{fd}m_{\tilde{G}}}{16\pi^2\sqrt{2}M}\mathcal{F}_{3W}, \tag{4.101}$$

where

$$\mathcal{F}_{3W} = \left[\frac{16\pi^2\sqrt{2}}{im_{\tilde{G}}}\right]\epsilon^*(k)^\rho\overline{u}(p-k)\mathrm{P_R}\int\frac{d^4q_3}{(2\pi)^4}\frac{-\gamma_\mu\gamma_\rho}{d_{3W}}\psi^\mu(p). \tag{4.102}$$

Here

$$d_{3W} = (q_3^2-m_{fd}^2)((q_3-p+k)^2-m_{\tilde{f}uL}^2). \tag{4.103}$$

4.5.2 The total amplitude

In this section the amplitudes of the three types of diagrams are combined to give the total amplitude of the radiative process $\tilde{G} \to W^+ l^-$ to lowest perturbation order. The equations of motion for the gravitino, the lepton and the gauge boson are then used to bring the expression on the form of Eq. (4.16), such that the results of Section 4.3 can be used.

Combining the results from the three subsections above, one can write the total amplitude for the radiative decay $\tilde{G} \to W^+ l^-$ at one loop level as

$$\mathcal{M}_W = \mathcal{M}_{1W} + \mathcal{M}_{2W} + \mathcal{M}_{3W}, \tag{4.104}$$

which can be written in terms of the reduced amplitude $\mathcal{F}_W$ as

$$\mathcal{M}_W = -i\frac{\lambda e}{2\sin\theta_W}\frac{m_{fd}m_{\tilde{G}}}{16\pi^2\sqrt{2}M}\mathcal{F}_W, \tag{4.105}$$

where

$$\mathcal{F}_W = \mathcal{F}_{1W} + \mathcal{F}_{2W} + \mathcal{F}_{3W}. \tag{4.106}$$

PaVe	m_B	m_l	m_1	m_2	m_3
C_{1LW}	m_W	m_l	m_{fu}	$m_{\tilde{f}uL}$	m_{fd}
C_{1RW}	m_W	m_l	m_{fd}	$m_{\tilde{f}dR}$	m_{fu}
C_{2W}	m_W	m_l	$m_{\tilde{f}dL}$	m_{fd}	$m_{\tilde{f}uL}$

Table 4.2: Masses to replace for different indices on the PaVe integrals for the W^+l^- diagrams.

We use the notation in Eqs. (4.9)–(4.14) with indices to specify which set of masses m_1, m_2 and m_3 to use, specified in Table 4.2. Substituting these in $\mathcal{F}_W$ the expression can be written as

$$\begin{aligned}\mathcal{F}_W &= \left[\frac{\sqrt{2}}{m_{\tilde{G}}}\right]\epsilon^*(k)^\rho\overline{u}(p-k)\mathrm{P_R}[(C_{1LW}{}^{\alpha\beta}\gamma_\rho\gamma_\alpha + C_{1RW}{}^{\alpha\beta}\gamma_\alpha\gamma_\rho)\gamma_\mu\gamma_\beta \\ &\quad -C_{1LW}{}^{\alpha}\gamma_\rho\gamma_\alpha\gamma_\mu\not{p} - C_{1RW}{}^{\alpha}(\gamma_\alpha\gamma_\rho\gamma_\mu\not{p} - \not{k}\gamma_\rho\gamma_\mu\gamma_\alpha) - C_{01RW}\not{k}\gamma_\rho\gamma_\mu\not{p} \\ &\quad +2C_{2W}{}^{\alpha}{}_\rho\gamma_\mu\gamma_\alpha - C_{2W}{}^{\alpha}\gamma_\mu\gamma_\alpha k_\rho - B_0(m_l^2, m_{fd}^2, m_{\tilde{f}uL}^2)\gamma_\mu\gamma_\rho]\psi^\mu(p). \quad (4.107)\end{aligned}$$

To simplify this expression the equations of motion for the gravitino, Eqs. (3.3)–(3.5), as well as the equation of motion for a lepton in Eq. (4.85), are used to eliminate terms that do not contribute and to replace $\overline{u}(p-k)\not{k} = \overline{u}(p-k)(\not{p} - m_l)$. Before expanding the integrals in terms of scalar functions, Eqs. (3.3) and (3.4) are used to remove constructions of $\gamma_\mu\not{p}\psi^\mu(p) = m_{\tilde{G}}\gamma_\mu\psi^\mu(p)$, while Eq. (A.1) is used in combination with Eq. (3.3) to replace $\gamma_\mu\gamma_\eta\psi^\mu(p) = 2g_{\mu\eta}\psi^\mu(p)$. This yields

$$\begin{aligned}\mathcal{F}_W &= \left[\frac{2\sqrt{2}}{m_{\tilde{G}}}\right]\epsilon^*(k)^\rho\overline{u}(p-k)\mathrm{P_R}[C_{1LW}{}^{\alpha}{}_\mu\gamma_\rho\gamma_\alpha + C_{1RW}{}^{\alpha}{}_\mu\gamma_\alpha\gamma_\rho \\ &\quad +C_{1RW\,\mu}(\not{p} - m_l)\gamma_\rho \\ &\quad +2C_{2W\,\mu\rho} - C_{2W\,\mu}k_\rho - B_0(m_l^2, m_{fd}^2, m_{\tilde{f}uL}^2)g_{\mu\rho}]\psi^\mu(p). \quad (4.108)\end{aligned}$$

Expanding the tensor integrals in $\mathcal{F}_W$ in terms of scalar components defined in Eqs. (4.13)

and (4.14) gives

$$\begin{aligned}
\mathcal{F}_W &= \left[\frac{2\sqrt{2}}{m_{\tilde{G}}}\right] \epsilon^*(k)^\rho \overline{u}(p-k) \mathrm{P_R} [C_{1LW00}\gamma_\rho\gamma_\mu \\
&+C_{1LWpp}\gamma_\rho \not{p} p_\mu + C_{1LWkk}\gamma_\rho \not{k} k_\mu + C_{1LWpk}\gamma_\rho(k_\mu \not{p} + \not{k} p_\mu) \\
&+C_{1RW00}\gamma_\mu\gamma_\rho + C_{1RWpp}\not{p}\gamma_\rho p_\mu + C_{1RWkk}\not{k}\gamma_\rho k_\mu + C_{1RWpk}(\not{p} k_\mu + \not{k} p_\mu)\gamma_\rho \\
&+(C_{1RWp}p_\mu + C_{1RWk}k_\mu)(\not{p} - m_l)\gamma_\rho \\
&+2(C_{2W00}g_{\mu\rho} + C_{2Wpp}p_\mu p_\rho + C_{2Wkk}k_\mu k_\rho + C_{2Wpk}(k_\mu p_\rho + p_\mu k_\rho)) \\
&-(C_{2Wp}p_\mu + C_{2Wk}k_\mu)k_\rho - B_0(m_l^2, m_{fd}^2, m_{\tilde{f}uL}^2) g_{\mu\rho}] \psi^\mu(p). \qquad (4.109)
\end{aligned}$$

Equation (3.3) is then used to remove all occurences of $\gamma_\mu\psi^\mu(p)$ and Eq. (3.5) to remove $p_\mu\psi^\mu(p)$. Then Eq. (4.85) is used to rewrite $\overline{u}(p-k)\not{k}\gamma_\rho = \overline{u}(p-k)(\not{p} - m_l)\gamma_\rho = \overline{u}(p-k)(2p_\rho - \gamma_\rho\not{p} - m_l\gamma_\rho)$. Finally Eq. (3.4) is used to replace $\not{p}\psi^\mu(p) = m_{\tilde{G}}\psi^\mu(p)$. The result is

$$\begin{aligned}
\mathcal{F}_W &= \left[\frac{2\sqrt{2}}{m_{\tilde{G}}}\right] \epsilon^*(k)^\rho \overline{u}(p-k) \mathrm{P_R} [2C_{1LWkk}k_\rho k_\mu - C_{1LWkk}(2p_\rho - \gamma_\rho(m_{\tilde{G}} + m_l))k_\mu \\
&+C_{1LWpk}m_{\tilde{G}}\gamma_\rho k_\mu + 2C_{1RW00}g_{\mu\rho} + C_{1RWkk}(2p_\rho - \gamma_\rho(m_{\tilde{G}} + m_l))k_\mu \\
&+C_{1RWpk}(2p_\rho - \gamma_\rho m_{\tilde{G}})k_\mu + C_{1bWk}(2p_\rho - \gamma_\rho(m_{\tilde{G}} + m_l))k_\mu \\
&+2(C_{2W00}g_{\mu\rho} + C_{2Wkk}k_\mu k_\rho + C_{2Wpk}k_\mu p_\rho) \\
&-C_{2Wk}k_\mu k_\rho - B_0(m_l^2, m_{fd}^2, m_{\tilde{f}uL}^2) g_{\mu\rho}] \psi^\mu(p). \qquad (4.110)
\end{aligned}$$

However, the $k_\mu k_\rho$ part will not contribute to the amplitude, as shown in Section 4.3. Using this one can write

$$\begin{aligned}
\mathcal{F}_W &= \left[\frac{2\sqrt{2}}{m_{\tilde{G}}}\right] \epsilon^*(k)^\rho \overline{u}(p-k) \mathrm{P_R} \{[(C_{1LWpk} - C_{1RWpk})m_{\tilde{G}} \\
&+(C_{1LWkk} - C_{1RWkk} - C_{1RWk})(m_{\tilde{G}} + m_l)]\gamma_\rho k_\mu \\
&+2(C_{1RWpk} + C_{2Wpk} + C_{1RWkk} - C_{1LWkk} + C_{1RWk})p_\rho k_\mu \\
&+[2C_{2W00} + 2C_{1RW00} - B_0(m_l^2, m_{fd}^2, m_{\tilde{f}uL}^2)] g_{\mu\rho}\} \psi^\mu(p). \qquad (4.111)
\end{aligned}$$

One can now write down the set of constants on the form of Eq. (4.17) as

$$C_{Wpk} = \frac{4\sqrt{2}}{m_{\tilde{G}}}(C_{1bWpk} + C_{2Wpk} + C_{1bWkk} - C_{1aWkk} + C_{1bWk}) \quad (4.112)$$

$$C_{Wg} = \frac{2\sqrt{2}}{m_{\tilde{G}}}(2C_{2W0} + 2C_{1bW0} - B_0(m_l^2, m_{fd}^2, m_{\tilde{f}uL}^2)) \quad (4.113)$$

$$C_{W\gamma k} = 2\sqrt{2}\Big[(C_{1aWpk} - C_{1bWpk}) + (C_{1aWkk} - C_{1bWkk} - C_{1bWk})\left(1 + \frac{m_l}{m_{\tilde{G}}}\right)\Big]. \quad (4.114)$$

Using Eqs. (B.18)–(B.24) one can write these constants in terms of the dimensionless constants defined in Appendix B. For Eq. (4.112) all the $1/m_l^2$ terms cancel and this gives

$$C_{Wpk} = \frac{\sqrt{32}m_{\tilde{G}}(-C'_{1bWpk} - C'_{2Wpk} + C'_{1bWkk} - C'_{1aWkk} - C'_{1bWk})}{(m_{\tilde{G}}^2 - (m_W + m_l)^2)(m_{\tilde{G}}^2 - (m_W - m_l)^2)} + \frac{\sqrt{32}\left[(m_{\tilde{f}dR}^2 - m_{fu}^2)\Delta B_0^{(gusdW)} - (m_{\tilde{f}uL}^2 - m_{fd}^2)\Delta B_0^{(gdsuW)}\right]}{m_{\tilde{G}}(m_{\tilde{G}}^2 - (m_W + m_l)^2)(m_{\tilde{G}}^2 + (m_W - m_l)^2)}, \quad (4.115)$$

where

$$\Delta B_0^{(gusdW)} = B_0(m_l^2, m_{fu}^2, m_{\tilde{f}dR}^2) - B_0(0, m_{fu}^2, m_{\tilde{f}dR}^2), \quad (4.116)$$

and

$$\Delta B_0^{(gdsuW)} = B_0(m_l^2, m_{fd}^2, m_{\tilde{f}uL}^2) - B_0(0, m_{fd}^2, m_{\tilde{f}uL}^2), \quad (4.117)$$

are finite differences of two-point functions.

For Eq. (4.113) we have

$$C_{Wg} = \frac{\sqrt{8}}{m_{\tilde{G}}}\Big(2C'_{2W0} + 2C'_{1bW0} + \frac{1}{2}B_0(m_{\tilde{G}}^2, m_{fd}^2, m_{\tilde{f}dR}^2) + \frac{1}{2}B_0(m_{\tilde{G}}^2, m_{\tilde{f}dL}^2, m_{fd}^2) - B_0(m_l, m_{fd}^2, m_{\tilde{f}uL}^2)\Big) \quad (4.118)$$

Again, the divergences in the two point function $B_0(m_l, m_{fd}^2, m_{\tilde{f}uL}^2)$ cancel against the divergences in $B_0(m_{\tilde{G}}^2, m_{\tilde{f}dL}^2, m_{fd}^2)$ and $B_0(m_{\tilde{G}}^2, m_{fd}^2, m_{\tilde{f}dR}^2)$.

For Eq. (4.114) we finally have

$$\begin{aligned} C_{W\gamma k} &= \frac{\sqrt{8} m_{\tilde{G}} [(C'_{1bWpk} - C'_{1aWpk}) m_{\tilde{G}} + (C'_{1aWkk} - C'_{1bWkk} + C'_{1bWk})(m_{\tilde{G}} + m_l)]}{((m^2_{\tilde{G}} - (m_B + m_l)^2)(m^2_{\tilde{G}} - (m_B - m_l)^2))} \\ &+ \frac{\sqrt{2}(m^2_{\tilde{f}uL} - m^2_{fd})(m^2_{\tilde{G}} - m^2_W + m^2_l)}{m_{\tilde{G}}(m^2_{\tilde{G}} - (m_W + m_l)^2)(m^2_{\tilde{G}} + (m_W - m_l)^2)} \frac{\Delta B_0^{(gdsuW)}}{m_l} \\ &- \frac{\sqrt{2}(m^2_{\tilde{f}dR} - m^2_{fu})(m^2_{\tilde{G}} - m^2_W + m^2_l)}{m_{\tilde{G}}(m^2_{\tilde{G}} - (m_W + m_l)^2)(m^2_{\tilde{G}} + (m_W - m_l)^2)} \frac{\Delta B_0^{(gusdW)}}{m_l} \\ &- \frac{\sqrt{8}[(m^2_{\tilde{f}dR} - m^2_{fu}) \Delta B_0^{(gusdW)} - (m^2_{\tilde{f}uL} - m^2_{fd}) \Delta B_0^{(gdsuW)}]}{(m^2_{\tilde{G}} - (m_W + m_l)^2)(m^2_{\tilde{G}} + (m_W - m_l)^2)}. \end{aligned} \tag{4.119}$$

Here the second and third term go as $\Delta B_0^{(gdsuW)}/m_l$ and $\Delta B_0^{(gusdW)}/m_l$ respectively. Even though this seems to be divergent in the limit $m_l \to 0$ at first glance, however, Eqs. (4.116) and (4.117) give that

$$\lim_{m_l \to 0} \Delta B_0^{(gdsuW)} = 0 \quad \text{and} \quad \lim_{m_l \to 0} \Delta B_0^{(gusdW)} = 0 \tag{4.120}$$

respectively, such that $C_{W\gamma k}$ is protected for divergences, even if we approximate leptons to be massless.

Instead of this choice of constants, one can use the dimensionless constants defined in Eqs. (4.28)–(4.30) which are

$$\begin{aligned} K_{1W} &= \sqrt{32}(-C'_{1bWpk} - C'_{2Wpk} + C'_{1bWkk} - C'_{1aWkk} - C'_{1bWk} \\ &+ \frac{[(m^2_{fu} - m^2_{\tilde{f}dR}) \Delta B_0^{(gusdW)} - (m^2_{fd} - m^2_{\tilde{f}uL}) \Delta B_0^{(gdsuW)}]}{m^2_{\tilde{G}}}), \end{aligned} \tag{4.121}$$

$$\begin{aligned} K_{2W} &= \sqrt{8}[(C'_{1bWpk} - C'_{1aWpk}) + (C'_{1aWkk} - C'_{1bWkk} + C'_{1bWk})(1 + \frac{m_l}{m_{\tilde{G}}})] \\ &+ \frac{\sqrt{2}(m^2_{\tilde{f}uL} - m^2_{fd})(m^2_W - m^2_l - m^2_{\tilde{G}})}{m^3_{\tilde{G}}} \frac{\Delta B_0^{(gdsuW)}}{m_l} \\ &- \frac{\sqrt{2}(m^2_{\tilde{f}dR} - m^2_{fu})(m^2_W - m^2_l - m^2_{\tilde{G}})}{m^3_{\tilde{G}}} \frac{\Delta B_0^{(gusdW)}}{m_l} \\ &- \frac{\sqrt{8}[(m^2_{\tilde{f}uL} - m^2_{fd}) \Delta B_0^{(gdsuW)} - (m^2_{\tilde{f}dR} - m^2_{fu}) \Delta B_0^{(gusdW)}]}{m^2_{\tilde{G}}}, \end{aligned} \tag{4.122}$$

$$\begin{aligned} K_{3W} &= \sqrt{8}(2C'_{2W0} + 2C'_{1bW0} + \frac{1}{2} B_0(m^2_{\tilde{G}}, m^2_{fd}, m^2_{\tilde{f}dR}) \\ &+ \frac{1}{2} B_0(m^2_{\tilde{G}}, m^2_{\tilde{f}dL}, m^2_{fd}) - B_0(m_l, m^2_{fd}, m^2_{\tilde{f}uL})), \end{aligned} \tag{4.123}$$

where the dimensionless constants C'_{index} can be found by replacing the masses in Appendix B following Table 4.2.

4.5.3 The width in the channel W^+l^-

In this section the results from the previous two subsections are combined. As shown in Eq. (4.8) together with Eq. (4.17), one can write the width of the gravitino in the radiative decay $\tilde{G} \to W^+l^-$ as

$$\begin{aligned}\Gamma_{\tilde{G}\to W^+l^-} &= \frac{1}{16}\frac{\alpha\lambda^2 m_{\tilde{G}}}{512\pi^4\sin^2\theta_W}\frac{m_{fd}^2}{M^2} \\ &\quad\times\frac{[(m_{\tilde{G}}^2-(m_W-m_l)^2)(m_{\tilde{G}}^2-(m_W+m_l)^2)]^{1/2}}{m_{\tilde{G}}^2}\overline{|\mathcal{F}|}^2. \quad (4.124)\end{aligned}$$

The general form of $\overline{|\mathcal{F}|}^2$ has been calculated above and presented in Eq. (4.31), which can be written for the special case of $m_B = m_W$ as

$$\begin{aligned}\overline{|\mathcal{F}|}^2 &= \frac{1}{96}|K_{1W}|^2\frac{(m_{\tilde{G}}^2-m_W^2+m_l^2)}{m_W^2} \\ &\quad+\frac{1}{24}|K_{2W}|^2\left[\frac{m_{\tilde{G}}^2}{m_W^2}+3\frac{(m_{\tilde{G}}^2-m_W^2+m_l^2)m_{\tilde{G}}^2}{(m_{\tilde{G}}^2-(m_W-m_l)^2)(m_{\tilde{G}}^2-(m_W+m_l)^2)}\right] \\ &\quad+\frac{1}{24}|K_{3W}|^2\frac{(m_{\tilde{G}}^2-m_W^2+m_l^2)}{m_{\tilde{G}}^2} \\ &\quad\times\left(\frac{m_{\tilde{G}}^2}{m_W^2}+2\left(5-\frac{m_l^2}{m_W^2}\right)+\frac{(m_W^2-m_l^2)^2}{m_{\tilde{G}}^2m_W^2}\right) \\ &\quad+\frac{1}{24}\mathrm{Re}\{K_{1W}K_{3W}^*\}\left(\frac{m_{\tilde{G}}^2}{m_W^2}-\frac{(m_W^2-m_l^2)^2}{m_{\tilde{G}}^2m_W^2}\right) \\ &\quad+\frac{1}{24}\mathrm{Re}\{K_{1W}K_{2W}^*\}\frac{m_{\tilde{G}}^2}{m_W^2} \\ &\quad+\frac{1}{12}\mathrm{Re}\{K_{2W}K_{3W}^*\}\frac{(m_{\tilde{G}}^2+3m_W^2-m_l^2)}{m_W^2}. \quad (4.125)\end{aligned}$$

K_{1W}, K_{2W} and K_{3W} were presented in Eqs. (4.121)–(4.123).

4.6 Numerical evaluation of the width in FORTRAN

The sections above, in combination with Appendix B, contain all the information one needs to evaluate the numerical value of the width of the gravitino in its respective decay

channels for a given scenario. One has, however, to be careful to make sure that the assumptions made under the calculations are followed. The massive bosons are assumed to be on-shell particles with a well defined mass. In practice this is equivalent to the narrow width approximation, where the masses are assumed to take the central value of the distribution. This is a problem only for gravitino masses near the kinematical limit, where the decay channels becomes kinematically accessible. Because of this the program is set to return zero for the width in the respective channel when the gravitino mass is close to the kinematical limit.

The numerical calculations in this work were done in Fortran 77, using LoopTools 2.7 by Hahn and Perez-Victoria [3]. First subroutines calculate the variables C'_k as given in Eq. (B.14), C'_{00} as given in Eq. (B.17), C'_{kk} as given in Eq. (B.21) and C'_{pk} as given in Eq. (B.23), for a given set of loop-particle masses m_1, m_2 and m_3 and the masses of the final state m_B and m_l. Then a subroutine takes the gravitino mass and the masses of the involved particles and checks the kinematical limit and returns zero for the width $\tilde{G} \to W^+ l^-$ when $m_{\tilde{G}} < m_W + m_l + \frac{\Gamma_W}{2}$ where Γ_W is the width of the W boson. If the kinematical limit is passed it then calculates K_{1W} as given in Eq. (4.121), K_{2W} as given in Eq. (4.122) and K_{3W} as given in Eq. (4.123) and combines these to $\overline{|\mathcal{F}|}^2$ as given in Eq. (4.125). Finally, the width of the gravitino in the decay channel $\tilde{G} \to W^+ l^-$ as given in Eq. (4.124) is evaluated. Similarly there is a subroutine that takes the gravitino mass and the masses of the involved particles and checks the kinematical limit and returns zero for the width $\tilde{G} \to Z^0 \nu$ when $m_{\tilde{G}} < m_Z + m_l + \frac{\Gamma_Z}{2}$ where Γ_Z is the width of the Z boson. If the kinematical limit is exceeded it then calculates $K_{1Za/b}$ as given in Eq. (4.80), $K_{2Za/b}$ as given in Eq. (4.81) and $K_{3Za/b}$ as given in Eq. (4.82). These are then combined to K_{1Z}–K_{3Z} by using Eqs. (4.80)–(4.82), which in turn are combined to $\overline{|\mathcal{F}|}^2$ as given in Eq. (4.84). Finally, the width of the gravitino in the decay channel $\tilde{G} \to Z^0 \nu$, as given in Eq. (4.83), is calculated. All these subroutines are listed in Appendix D.

To collect the widths of the gravitino for different scenarios, including the radiative process $\tilde{G} \to \gamma\nu$ calculated by Lola, Osland and Raklev [2], and the tree level processes calculated by Moreau and Chemtob [1], these subroutines have been inserted into the program DoG [35]. A description of how these widths are further used to calculate the extragalactic γ-spectrum from gravitino decays, and how one can use this spectrum to set limits on the R-parity violating couplings, can be found in Chapter 5.

5

The Extragalactic Photon Spectrum

In this chapter it is first shown how one can calculate the photon spectrum from a decaying gravitino at rest using PYTHIA 6.409 [4]. Then it is discussed how one can use this spectrum to extract the extragalactic photon spectrum from gravitino dark matter decays, how to smear the result according to the resolution of the Fermi-LAT experiment [33] and finally how to use the resulting spectrum to set limits on R-parity breaking couplings by performing a least square fit.

The extra galactic photon spectrum is the spectrum of photons that come from outside our galaxy. It is found by measuring the photon spectrum at earth coming from high latitude as compared to the galactic plane and then subtracting known galactic backgrounds. A detailed description of the backgrounds used by the Fermi-LAT experiment can be found in [33].

5.1 Red-shifting and smearing the spectrum

In Chapter 4 the decay width of the gravitino in the decay modes $Z^0\nu$ and W^+l^- was calculated and a program to calculate the total width of the gravitino and the branching ratios in all decay channels is described. One of the outputs of the program is a SLHA [36] file, which is a file that can be used to simulate decays in the PYTHIA Monte Carlo event generator, containing the total width of the gravitino and the branching ratios in the respective channels. The event generator is then used to generate $N_{ev} =$

30000 gravitinos at rest and to let them decay according to the SLHA file in both the decay channels calculated in Chapter 4 as well as the tree level decay channels [1] and the $\gamma\nu$ decay channel [2]. It is set up to let all unstable particles decay, and collect all final state photons, produced mainly by Bremsstrahlung and in pion decays, in an array.

To find the extragalactic photon spectrum from gravitino dark matter one needs to redshift the spectrum. The diffuse extra-galactic gamma ray flux of energy E from the gravitino decays is described by a integral over red-shift z given by [37]

$$F(E) = E^2 \frac{dJ}{dE} = \frac{2E^2}{m_{\tilde{G}}} C_\gamma \int_1^\infty dy \frac{dN_\gamma}{d(Ey)} \frac{y^{-3/2}}{\sqrt{1+\kappa y^{-3}}}, \tag{5.1}$$

where $y = 1 + z$ and dN_γ/dEy is the gamma ray spectrum from a decaying gravitino at rest in units of [GeV^{-1}], and dJ/dE is the spectrum measured at earth in units of [GeV^{-1}cm^{-2}sr^{-1}s^{-1}]. Additionally, we define

$$C_\gamma = \frac{\Omega_{\tilde{G}\rho_c}}{8\pi\tau_{\tilde{G}} H_0 \Omega_M^{1/2}} \quad \text{and} \quad \kappa = \frac{\Omega_\Lambda}{\Omega_M}. \tag{5.2}$$

Here $\Omega_{\tilde{G}}$ is the density of gravitinos in terms of the critical density ρ_c. In this thesis the gravitino is assumed to be the main contribution to dark matter, so that $\Omega_{\tilde{G}} = \Omega_{DM}$. $\tau_{\tilde{G}}$ is the lifetime of the gravitino, H_0 is the Hubble expansion rate, Ω_Λ is the density of dark energy and Ω_M is the density of matter. With current values for the cosmological parameters [13] this gives

$$C_\gamma = 1.06 \left(\frac{10^{21} s}{\tau_{\tilde{G}}}\right) \text{cm}^{-2}\text{sr}^{-1}\text{s}^{-1} \text{ and } \quad \kappa \approx 2.85. \tag{5.3}$$

The spectrum is smeared by the detector resolution and binned as in the experimental data shown in Table 5.1. The smeared spectrum $F(x)$ for a detector with the resolution R from a spectrum $G(y)$ is given as

$$F(x) = \frac{1}{\sqrt{2\pi}\sigma_R} \int_{-\infty}^{\infty} G(y) e^{-\frac{(x-y)^2}{2\sigma_R^2}} dy, \tag{5.4}$$

where $\sigma_R = E \cdot R$. For the Fermi-LAT experiment the resolution is energy dependent, we use an average in the energy range of the extra galactic background of 15% [38].

5.2 Setting limits

This spectrum can now be compared to the data for the extra galactic background (EGB) flux taken from [33]. This is done as a least square analysis, as described e.g. by Cowan [39]. As the width of the process goes as λ^2 the normalization of the spectrum has to be proportional to λ^2 as well. The background is assumed to follow a power law distribution

$$F(E) = I_{BG}(\frac{E}{1\text{GeV}})^{-\gamma_{BG}}. \tag{5.5}$$

To analyze how well the theoretical calculation fits the data one calculates the least squares function $\chi^2(\lambda, I_{BG}, \gamma_{BG})$ which can be expressed as

$$\chi^2(\lambda, I_{BG}, \gamma_{BG}) = \sum_i \left(\frac{y_i^{obs} - y_i^{th}(\lambda, I_{BG}, \gamma_{BG})}{\sigma_i} \right)^2, \tag{5.6}$$

where y_i^{obs} is the measured value in the ith bin with an experimental error of σ_i and can be found in Table 5.1, while $y_i^{th} = y_i^{\tilde{G}} \cdot \lambda^2 + y_i^{BG}(I_{BG}, \gamma_{BG})$ is the theoretical prediction, where $y_i^{BG}(I_{BG}, \gamma_{BG})$ is the background for given parameters and $y_i^{\tilde{G}}$ is the signal prediction in the ith bin from the gravitino decay for $\lambda = 1$. The theoretical error is assumed to be smaller than the experimental error and is ignored.

To set a limit on the coupling λ one calculates

$$\Delta\chi^2(\lambda) = \chi^2(\lambda, \hat{I}_{BG\lambda}, \hat{\gamma}_{BG\lambda}) - \chi^2(0, \hat{I}_{BG}, \hat{\gamma}_{BG}), \tag{5.7}$$

where $\hat{I}_{BG}$ and $\hat{\gamma}_{BG}$ are chosen such that the function is minimized for the case with only background, while $\hat{I}_{BG\lambda}$ and $\hat{\gamma}_{BG\lambda}$ are chosen such that the distribution is minimized for a given coupling λ. Using the one sided chi-squared distribution the upper limit for the coupling is then given by the coupling where $\Delta\chi^2(\lambda_{max}) = 3.84$ at a confidence level of 95%. The results of this analysis are shown in Section 6.3.

Center of bin energy E [GeV]	Bin width ΔE [GeV]	EGB intensity $E^2 dN/dE$ [GeV cm^{-2}s^{-1}sr^{-1}]
0.3	0.2	$(1.08 \pm 0.27) \times 10^{-6}$
0.6	0.4	$(8.37 \pm 1.62) \times 10^{-7}$
1.2	0.8	$(6.3 \pm 1.08) \times 10^{-7}$
2.4	1.6	$(4.572 \pm 0.756) \times 10^{-7}$
4.8	3.2	$(3.6 \pm 0.72) \times 10^{-7}$
9.6	6.4	$(2.0592 \pm 0.576) \times 10^{-7}$
19.2	12.8	$(1.8144 \pm 0.432) \times 10^{-7}$
38.4	25.6	$(1.4976 \pm 0.4032) \times 10^{-7}$
76.8	51.2	$(1.27872 \pm 0.33408) \times 10^{-7}$

Table 5.1: The extra galactic background flux as measured by Fermi-LAT [33].

6

Results and Discussion

In the following the results found in Chapters 4 and 5 are presented together with the decay modes $\tilde{G} \to \gamma\nu$ calculated by Lola, Osland and Raklev [2] and the tree level decay modes found by Moreau and Chemtob [1] for comparison. First the results are investigated for mass and flavor dependence, then the stability of the gravitino in one scenario is discussed and finally limits are set on the R-parity violating coupling for interesting scenarios.

Note that the widths below are only plotted for one final state. As the gravitino is a Majorana particle there exists charge conjugated processes, $Z^0\overline{\nu}$ for $Z^0\nu$ and W^-l^+ for W^+l^-, which give the same result. To get the total width one has to multiply the sum of all channels by two. Note also that the width in all channels is proportional to the R-parity breaking coupling squared, so that one can rescale the result for a given coupling λ by multiplying by λ^2/λ_u^2 where λ_u is the coupling used in the plots. The width plots are all plotted in units of GeV$/\lambda^2$, so that one can easily rescale the result by multiplying by λ^2.

As the calculations done in this thesis are only valid for gravitino masses larger than the sum of the final state particle masses and because it is found in this thesis that tree level processes dominate for gravitino masses much bigger than the gauge boson mass, the mass range considered in the following discussion is 50 GeV $\leq m_{\tilde{G}} \leq$ 250 GeV. In the following one-coupling dominance is also assumed, meaning that only one of the trilinear R-parity violating couplings is significant at a time.

6.1 Flavor and mass dependence of the width

This section discusses the dependence of the gravitino width on the sfermion masses for a given coupling and gravitino mass. As the radiative diagrams all go as m_{fd}^2/M^2 where m_{fd} is the mass of the down type fermion in the loop and M is the reduced Planck mass, the most important diagrams are the ones where the loop particles are third generation fermions as they have the highest masses. This means that scenarios where λ_{i33} or λ'_{i33} have the largest contribution from radiative processes. As mentioned in Chapter 4, the λ''_{ijk} trilinear R-parity violating couplings do not lead to radiative processes as studied in this thesis and are therefore not considered.

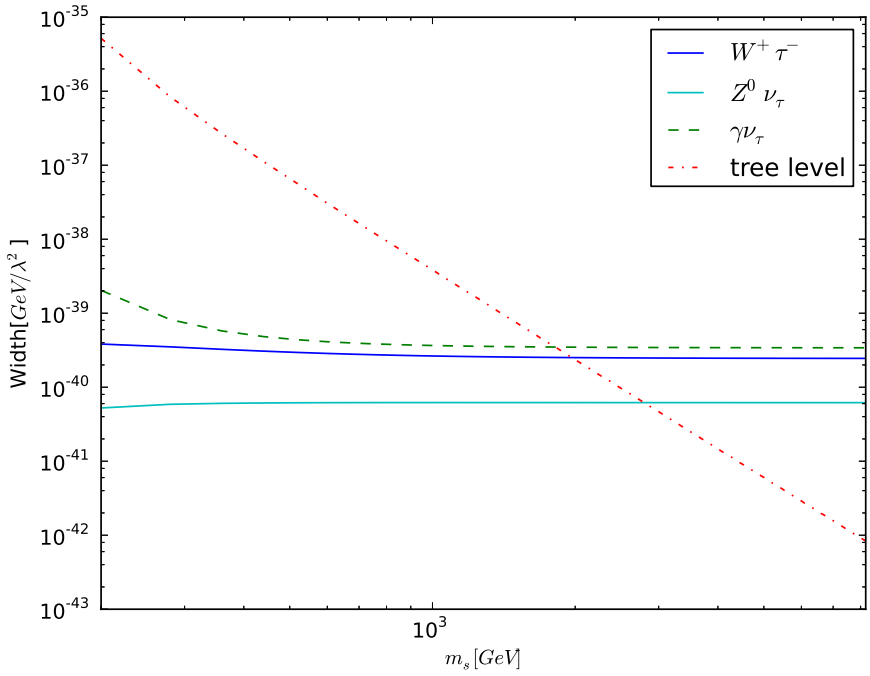

Figure 6.1: Width of the gravitino in different decay channels when λ'_{333} is the dominating coupling, plotted against the sfermion mass scale m_s, where $m_{\tilde{f}L} = m_{\tilde{f}R} = m_s$ and $m_{\tilde{G}} = 190GeV$.

Figure 6.1 shows the width of different channels of the gravitino decay for λ'_{333} for a fixed gravitino mass $m_{\tilde{G}}$ plotted against a scalar mass scale m_s where all sfermion masses are fixed to $m_{\tilde{f}L} = m_{\tilde{f}R} = m_s$. One can see that the tree-level processes decreases with $1/m_s^4$ as expected, while the radiative channels are approximately constant

for high scalar masses. The reason for this is that the gravitino coupling is proportional to the momentum of one of the particles it couples to. In the tree level case, one can always replace the momentum with an external momentum, but in the radiative case the momentum is always proportional to the biggest mass in the loop, so that the coupling compensates for the propagators. This means that radiative processes dominate over tree level processes for high sfermion mass scales. One can in particular see that radiative processes have width on the same scale as the tree level processes for $m_s \sim 2$ TeV for a gravitino mass of $m_{\tilde{G}} = 190$ GeV for λ'_{333}.

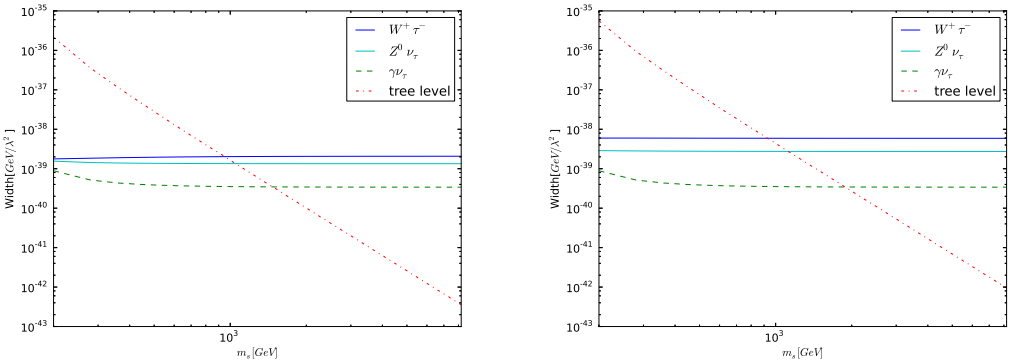

(a) $m_{\tilde{f}L} = 50 \times m_s$ and $m_{\tilde{f}R} = m_s$

(b) $m_{\tilde{f}L} = m_s$ and $m_{\tilde{f}R} = 50 \times m_s$

Figure 6.2: Width of decay channels for the gravitino for a dominant λ'_{333} plotted in units of GeV/λ^2 as a function of the scalar mass scale m_s, where $m_{\tilde{f}L} = 50 \times m_s$ and $m_{\tilde{f}R} = m_s$ (left figure) and $m_{\tilde{f}L} = m_s$ and $m_{\tilde{f}R} = 50 \times m_s$ (right figure). In both plots $m_{\tilde{G}} = 190$ GeV.

As the $\tilde{G} \to Z^0\nu$ and $\tilde{G} \to W^+l^-$ processes mix diagrams containing sfermion partners of left and right handed fermions, meaning that both left and right handed sfermion masses appear in the expressions, and since significant parts of the constants K_{1Z}, K_{2Z} and K_{3Z} in Eqs. (4.80)–(4.82) and in the constants K_{1W}, K_{2W} and K_{3W} in Eqs. (4.121)–(4.123) cancel exactly for $m_{\tilde{f}L} = m_{\tilde{f}R}$, it is interesting to look at the case where the left and right sfermion masses are split. Fig. 6.2 shows the different channels of the gravitino decay for $\lambda'_{333} > 0$ for a fixed gravitino mass $m_{\tilde{G}}$ plotted against a sfermion mass scale m_s, where all sfermion masses are fixed to $m_{\tilde{f}L} = 50 \times m_s$ and $m_{\tilde{f}R} = m_s$ in Fig. 6.2(a) and fixed to $m_{\tilde{f}R} = 50 \times m_s$ and $m_{\tilde{f}L} = m_s$ in Fig. 6.2(b).

Again, one can see that the tree-level processes decreases with $1/m_s^4$, and are about halved compared to Fig. 6.1 as diagrams with one handedness decouple. The process $\tilde{G} \to \gamma\nu$ is left right symmetric, and is not changed much compared to Fig. 6.1. The reason for this is that all diagrams in this process are approximately constant for high scalar masses. The processes $\tilde{G} \to Z^0\nu$ and $\tilde{G} \to W^+l^-$, however, are in comparison enhanced and still approximately constant for high scalar masses. The main contribution for the $Z^0\nu$ process is through the factor K_{3Z} given in Eq. (4.82), where

$$a[B_0(m^2_{\tilde{G}}, m^2_{\tilde{f}L}, m^2_{fd}) + B_0(m^2_{\tilde{G}}, m^2_{fd}, m^2_{\tilde{f}R}) - 2B_0(0, m^2_{fd}, m^2_{\tilde{f}L})] \tag{6.1}$$

dominates for large splittings between left and right handed sfermion masses. The main contribution for the W^+l^- process is through the factor K_{3W} given in Eq. (4.123), where similarly

$$B_0(m^2_{\tilde{G}}, m^2_{fd}, m^2_{\tilde{f}dR}) + B_0(m^2_{\tilde{G}}, m^2_{\tilde{f}dL}, m^2_{fd}) - 2B_0(0, m^2_{fd}, m^2_{\tilde{f}uL}) \tag{6.2}$$

dominates for large mass splittings between left and right handed sfermions. Figure 6.2(a) and Fig. 6.2(b) also show that the processes are significantly more enhanced for heavier right handed sparticles then for heavier left handed sparticles. The reason for this is that the expressions in Eqs. (6.1) and (6.2) are bigger for $m_{\tilde{f}R} > m_{\tilde{f}L}$. Figure 6.1 and Fig. 6.2 look at the effect of a dominant λ'_{333} only. For a general λ'_{ijj} and λ_{ijj} the results are quite similar to the discussed case with the exception of fermion mass effects. Such effects are discussed in the following paragraphs.

Now a sfermion mass scale of $m_s = 1$ TeV is chosen to show the dependence of the width on the gravitino mass. Figure 6.3 shows the width for the leptonic loops with third generation leptons in the loop, while Fig. 6.4 shows the width for quark loops with third generation quarks in the loop. As lepton masses are small compared to the scale of the W and Z masses, the width does not depend noticeably on the generation of the final state lepton. Because of this the case where λ_{133} dominates is equal to the case where λ_{233} dominates, shown in the figure, to a very good approximation. Similarly the case where λ'_{133} dominates and the case where λ'_{233} dominates gives indistinguishable results to the case where λ'_{333} dominates. However, the generation of the loop particles is of great importance. Figure 6.5 on page 73 compares the width in all channels for λ_{133} to the case where λ_{122} dominates. One can see that the radiative processes scale with the loop lepton mass squared, while the tree level processes for both scenarios are

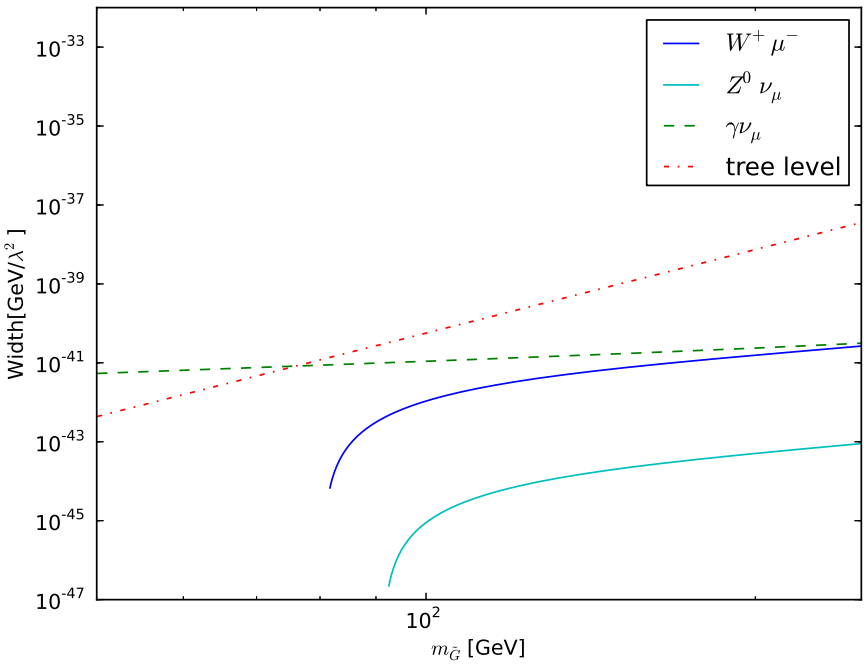

Figure 6.3: Width of decay channels for the gravitino plotted as a function of the gravitino mass, where λ_{233} is the dominating RPV coupling. Here all sfermions have a mass $m_s = 1$ TeV.

plotted on top of each other and are indistinguishable. Figure 6.6 on page 74 compares λ'_{333} domination to λ'_{233} domination. The radiative processes scale with the loop quark mass squared in this case also, but additionally the third generation tree level decay width is decreased as the tree level decay channel with a final state top quark is not kinematically accessible for gravitinos that are lighter then $m_{\tilde{G}} < m_t + m_b + m_\tau$. However, in all cases one can see that the decay channels to massive vector bosons are dominated by the tree level decays and by the photon channel.

As shown in Fig. 6.2 and discussed above the decay channels to massive vector bosons are enhanced by introducing a mass splitting between left handed and right handed sparticles. In particular, a splitting between $m_{\tilde{f}dL}$ and $m_{\tilde{f}dR}$ is enough to enhance the processes as a splitting between the first and the second terms in Eqs. (6.1) and (6.2) gives the biggest effect. Because of that, scenarios where $m_{\tilde{b}L}$ and $m_{\tilde{b}R}$ have different masses are considered in this paragraph. The decay width in the tree-level

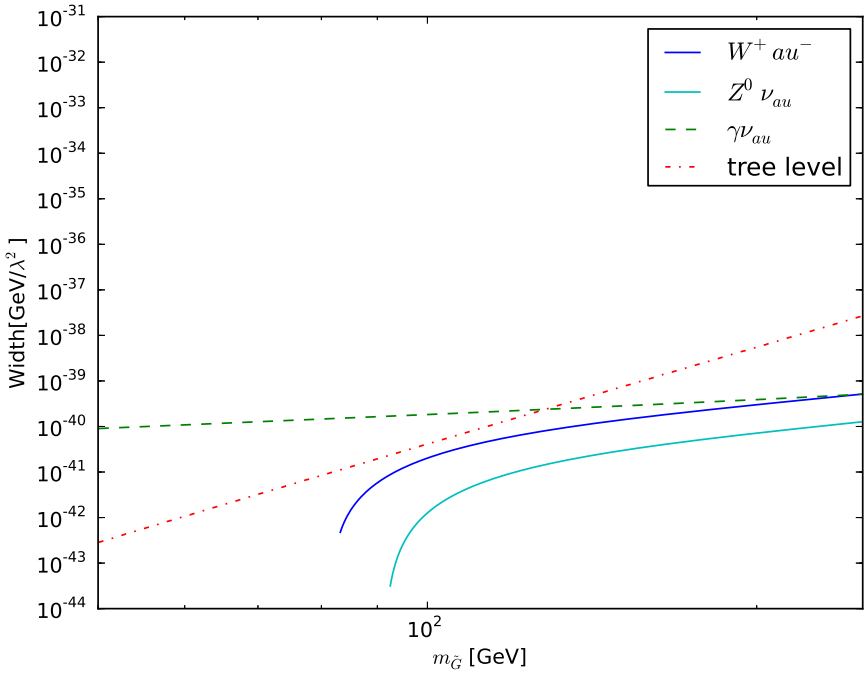

Figure 6.4: Width of decay channels for the gravitino plotted as a function of the gravitino mass, where λ'_{333} is the dominating RPV coupling. Here all sfermions have a mass m_s = 1 TeV.

channels and the $\gamma\nu$ channel are plotted for $m_{\tilde{b}L} = m_{\tilde{b}R} = m_s = 1$TeV for comparison. As discussed above, the $\gamma\nu$ process does not change for mass splitting, while the tree-level processes are halved in the decoupled limit. Figure 6.7(a) on page 75 shows the decay channels for $m_{\tilde{b}R} = 1$ TeV compared to $m_{\tilde{b}R} = 100$ TeV for λ'_{333} and with $m_{\tilde{b}L} = 1$ TeV. Figure 6.7(b) shows the decay channels for $m_{\tilde{b}L} = 1$ TeV compared to $m_{\tilde{b}L} = 100$ TeV for λ'_{333} with $m_{\tilde{b}R} = 1$ TeV. In both cases one can see that in the case where the left and right sbottom masses are split, the $W^+\tau^-$ process gives the biggest contribution to the gravitino width in a mass range between $m_{\tilde{G}} \approx 90$ GeV–210 GeV, while the $Z^0\nu_\tau$ width is bigger than the tree level width and the $\gamma\nu_\tau$ width for a mass in the range $m_{\tilde{G}} \approx 110$ GeV–190 GeV. Figure 6.8 on page 75 shows how the width of the decay channel $\tilde{G} \to W^+\tau^-$ varies with different $m_{\tilde{b}R}$ and $m_{\tilde{b}L}$. One can see that there are gravitino masses where the $W^+\tau^-$ decay mode gives the biggest contribution already for $m_{\tilde{b}R/L} = 3 \times m_{\tilde{b}L/R}$, and that for $m_{\tilde{b}R/L} = 10 \times m_{\tilde{b}L/R}$ there is a considerable

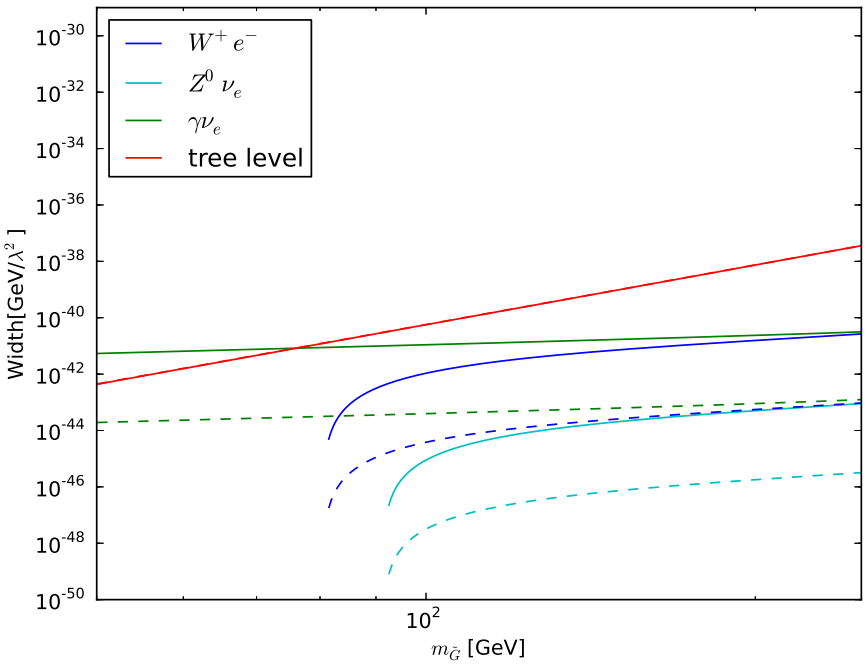

Figure 6.5: Width of decay channels for the gravitino plotted as a function of the gravitino mass, comparing λ_{133} (solid lines) to λ_{122} (dashed lines). Here all sfermions have a mass $m_s = 1$ TeV.

range of masses where the $W\tau$ decay mode is biggest. One can again observe that the range of masses where the $W^+\tau^-$ is biggest is larger for the case where $m_{\tilde{b}R} > m_{\tilde{b}L}$ if the splitting is of the same size. Figure 6.9 on page 76 shows the width of the decay channels $\tilde{G} \to Z^0\nu$ and $\tilde{G} \to W^+l^-$ for $m_{\tilde{\tau}R} = 1$ TeV compared to $m_{\tilde{\tau}R} = 100$ TeV for λ_{233} where $m_{\tilde{\tau}L} = 1$ TeV. Here the loop contains leptons. In this case the massive boson decays are not enhanced enough give the biggest contribution to the width in any region. A similar result can be found for $m_{\tilde{\tau}L} > m_{\tilde{\tau}R}$.

After inspecting the mass and flavor dependence of the calculated processes, it is found that for λ_{i11}, λ_{i22}, λ'_{i11} and λ'_{i22} tree level or $\gamma\nu$ processes dominate over the radiative decay modes containing massive vector bosons for all gravitino masses as long as the sfermion masses are on the TeV scale. For λ_{i33} these decay modes are subdominant, but not insignificant at large sfermion masses and splittings. Finally it is found that for λ'_{i33} there are gravitino masses where the processes containing

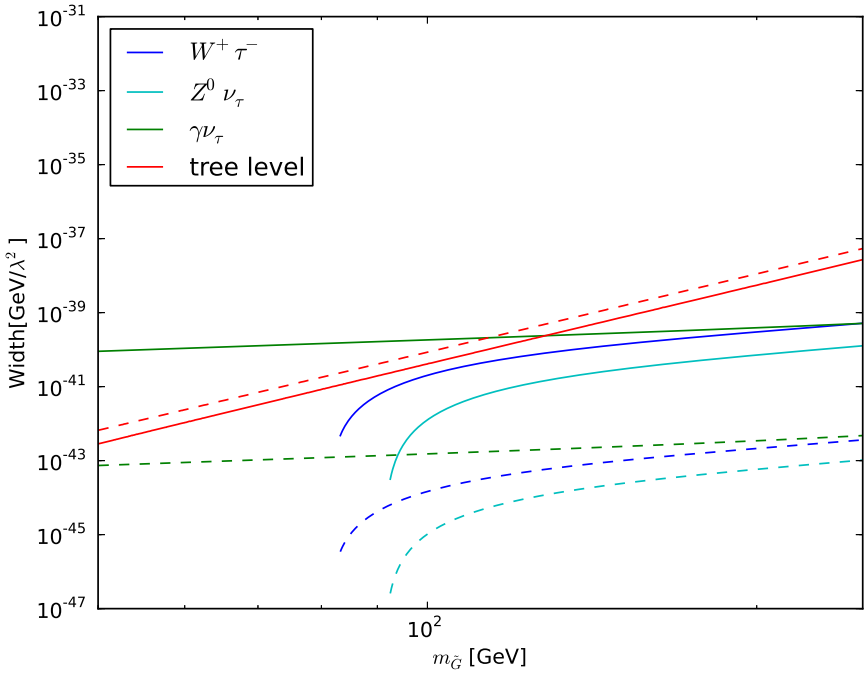

Figure 6.6: Width of decay channels for the gravitino as a function of the gravitino mass, comparing λ'_{333} (solid lines) to λ'_{233} (dashed lines). Here all sfermions have a mass $m_s = 1$ TeV.

massive vector bosons give the biggest contribution to the width, as long as $m_{\tilde{b}R} \geq 3 \times m_{\tilde{b}L}$ or $m_{\tilde{b}L} \geq 3 \times m_{\tilde{b}R}$. In the following two sections scenarios where λ'_{333} is the dominating coupling and where $m_{\tilde{b}R} = 10$ TeV and $m_{\tilde{b}L} = 1$ TeV are investigated. In these scenarios, the decay mode $\tilde{G} \to W^+\tau^-$ has the largest width for 100 GeV $< m_{\tilde{G}} <$ 170 GeV.

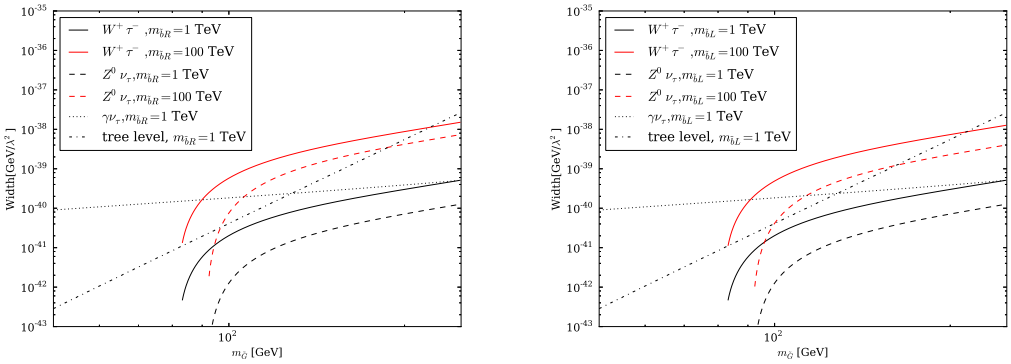

(a) $m_{\tilde{b}L} \leq m_{\tilde{b}R}$ (b) $m_{\tilde{b}R} \leq m_{\tilde{b}L}$

Figure 6.7: Width of decay channels for the gravitino with a dominant λ'_{333} as a function of the gravitino mass, the left figure for $m_{\tilde{b}L} = 1$ TeV and $m_{\tilde{b}R} = 1$ TeV (black lines) compared to $m_{\tilde{b}R} = 100$ TeV (red lines), the right figure for $m_{\tilde{b}R} = 1$ TeV and $m_{\tilde{b}L} = 1$ TeV (black lines) compared to $m_{\tilde{b}L} = 100$ TeV (red lines).

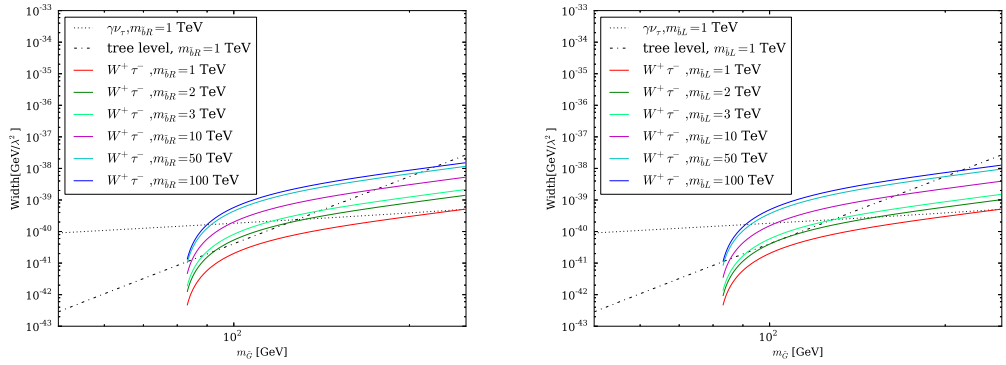

(a) $m_{\tilde{b}L} \leq m_{\tilde{b}R}$ (b) $m_{\tilde{b}R} \leq m_{\tilde{b}L}$

Figure 6.8: Width of decay channel $\tilde{G} \to W^+\tau^-$ with a dominant λ'_{333} as a function of the gravitino mass, right figure for $m_{\tilde{b}R} = 1$ TeV and a range of values for $m_{\tilde{b}L}$, left figure for $m_{\tilde{b}L} = 1$ TeV and a range of values for $m_{\tilde{b}R}$. The channel $\gamma\nu$ and the tree level processes are plotted for comparison.

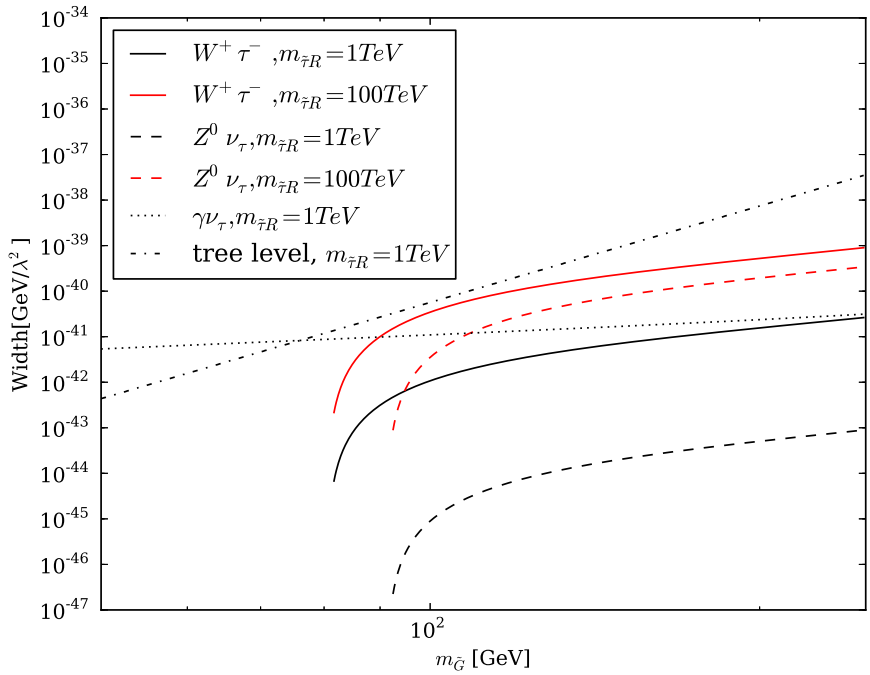

Figure 6.9: Width of decay channels for the gravitino with a dominant λ_{133} as a function of the gravitino mass for $m_{\tilde{\tau}L} = 1$ TeV and $m_{\tilde{\tau}R} = 1$ TeV (black lines) compared to $m_{\tilde{\tau}R} = 100$ TeV (red lines).

6.2 Stability of the gravitino

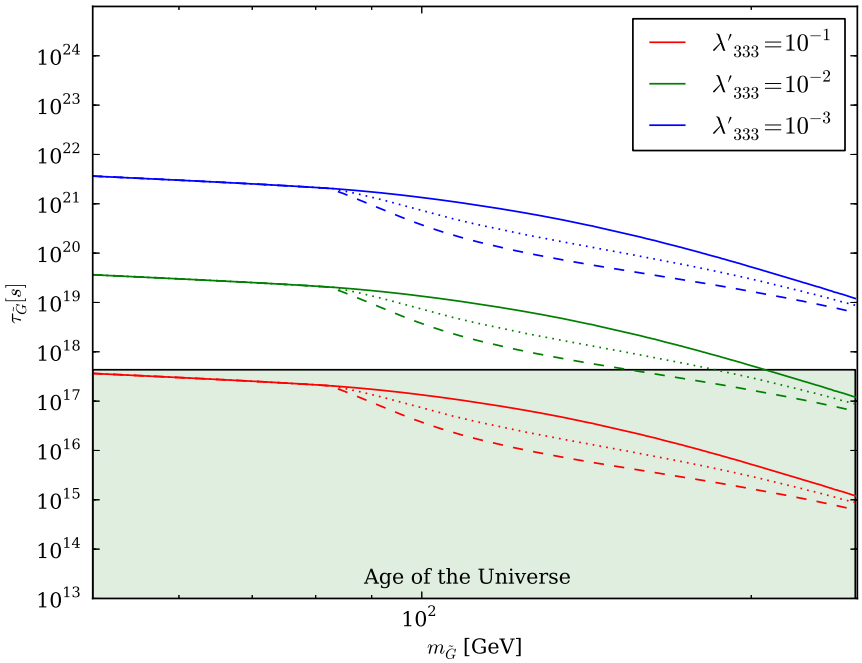

Figure 6.10: The total lifetime of the gravitino plotted against the gravitino mass for scenarios where λ'_{333} dominates. The sfermion mass scale is $m_s = 1$ TeV. $m_{\tilde{b}L} = m_{\tilde{b}R} = 1$ TeV (solid lines) is compared to $m_{\tilde{b}L} = 1$ TeV and $m_{\tilde{b}R} = 10$ TeV (dotted lines) and $m_{\tilde{b}L} = 1$ TeV and $m_{\tilde{b}R} = 100$ TeV (dashed lines). The green area indicates that the lifetime is less then the age of the universe.

In the previous section it was found that decays involving massive vector bosons in the final state are suppressed in most considered scenarios. It was, however, found that these processes can dominate for large left-right mass splitting in the case where λ'_{i33} is the dominant coupling and where the lighter sfermion has a mass of around 1 TeV. Figure 6.10 shows the lifetime of the gravitino for different values of the R-parity breaking coupling λ'_{333}. One can see that gravitino is stable enough to constitute dark matter for $\lambda'_{333} < 10^{-3}$ in the whole mass range considered, while a coupling of ten times this value, $\lambda'_{333} \sim 10^{-2}$, leads to cosmologically unstable gravitinos for $m_{\tilde{G}} \geq 210$ GeV for the case where $m_{\tilde{f}L} = m_{\tilde{f}R}$, and for $m_{\tilde{G}} \geq 150$ GeV in the case where $100 \times m_{\tilde{f}L} = m_{\tilde{f}R}$. When the left handed sbottom is heavier, the change in the lifetime

is very similar. In scenarios with somewhat smaller splitting where $m_{\tilde{b}R} = 10$ TeV and $m_{\tilde{b}L} = 1$ TeV, the gravitino is cosmologically stable for $\lambda'_{333} \leq 10^{-2}$ for gravitino masses bigger than 180 GeV.

6.3 The decay spectrum and limits

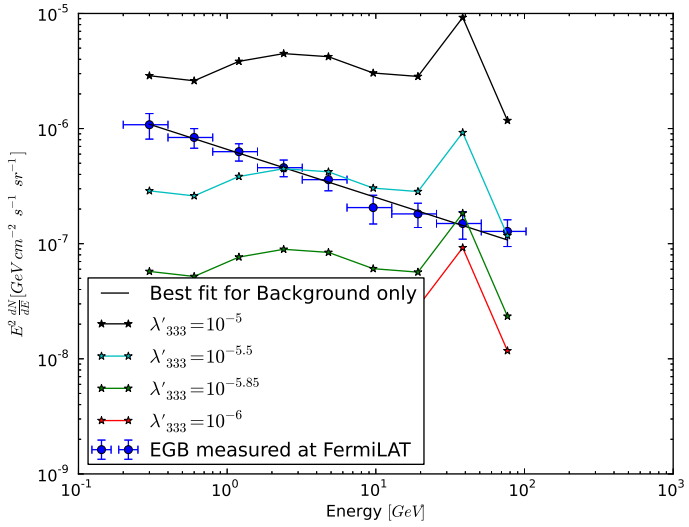

Figure 6.11: Extra galactic gamma-ray spectrum for $m_{\tilde{G}} = 120$ GeV, where $m_{\tilde{b}L} = 1$ TeV and $m_{\tilde{b}R} = 10$ TeV, plotted for $\lambda'_{333} = 10^{-5}$, $10^{-5.5}$, $10^{-5.85}$ and 10^{-6}. The extra galactic background flux measured by Fermi-LAT, and the best fit background, see Section 5.2, is superimposed for comparison.

To get an impression of what kind of spectrum and exclusions we get from decays to vector bosons, the case $m_{\tilde{G}} = 120$ GeV where $m_{\tilde{b}L} = 1$ TeV and $m_{\tilde{b}R} = 10$ TeV is investigated. For these values the branching ratios are $BR(\tilde{G} \to W^{\pm}\tau^{\mp}) = 52\%$, $BR(\tilde{G} \to \gamma\nu_{\tau}/\gamma\overline{\nu}_{\tau}) = 18\%$, $BR(\tilde{G} \to Z^0\nu_{\tau}/Z^0\overline{\nu}_{\tau}) = 16\%$ and $BR(\tilde{G} \to \text{tree-level}) = 14\%$. Figure 6.11 shows the theoretical spectrum for this model for $\lambda'_{333} = 10^{-5}$, $10^{-5.5}$, $10^{-5.85}$ and 10^{-6} with the measured extra galactic background flux from Fermi-LAT [33] superimposed for comparison. Additionally the best fit for the power-law background only is plotted in. Here the spike in one of the bins is due to the redshifted monochromatic photons from the $\gamma\nu$ channel, while the wide distribution is due to the massive vector boson processes. One can easily see that $\lambda'_{333} > 10^{-5.85}$ is excluded from

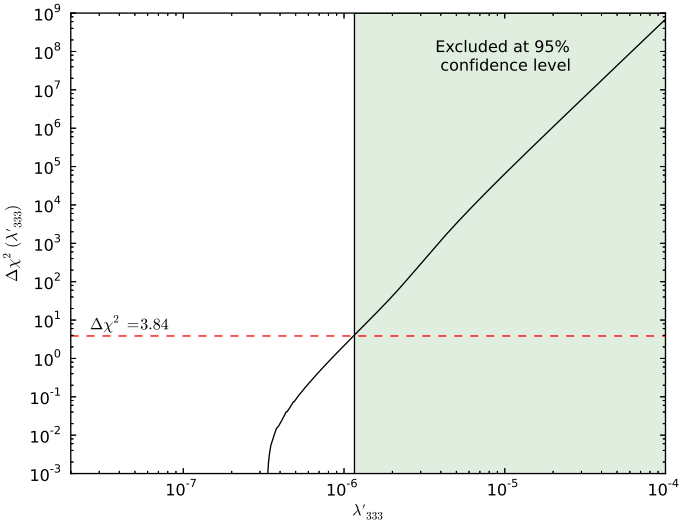

Figure 6.12: The $\Delta\chi^2(\lambda'_{333})$ distribution for $m_{\tilde{G}} = 120$ GeV, where $m_{\tilde{b}L} = 1$ TeV and $m_{\tilde{b}R} = 10$ TeV, plotted against λ'_{333}. The colored region is excluded at 95% confidence level.

requiring the theoretical spectrum to be less than the measured spectrum within the experimental uncertainties.

Figure 6.12 shows the more sophisticated method of least square fitting described in Section 5.2. One can see that in this scenario values of $\lambda'_{333} > 1.148 \times 10^{-6}$ are excluded. Studying the spectrum in Fig. 6.11 one can see that the spike from the gamma process hits a bin that has a small excess compared to the best fit for the background, such that one expects very good chi-squared values for small couplings. This is seen in Fig. 6.12, with a dramatic decrease in $\Delta\chi^2$ for couplings less than $4 \cdot 10^{-7}$.

Figure 6.13 on the next page shows the limits obtained by finding the maximum values of λ'_{333} for a range of masses at 95% confidence level, using the same method applied in Fig. 6.12. For comparison the limit not including the decay channels $\tilde{G} \to W^{\pm}l^{\mp}$ and $\tilde{G} \to Z^0\nu/Z^0\overline{\nu}$ are shown as well. All the limits are much harder then the limits one gets from requiring the gravitino to be cosmologically stable shown in Section 6.2 in the mass regions considered. The limit is driven by the $\gamma\nu$ process in the low end of the gravitino mass spectrum, as the red-shifted γ line dominates over all other contributions to the spectrum up to gravitino masses $m_{\tilde{G}} \sim 200$ GeV. Because of this one gets worse limits for masses where the red-shifted monochromatic line from

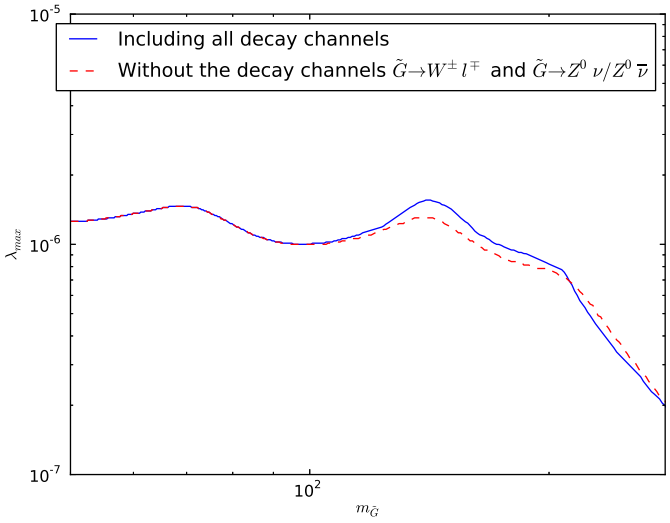

Figure 6.13: Plot of the limits on λ'_{333} as a function of $m_{\tilde{G}}$ for $m_{\tilde{b}L} = 1$ TeV and $m_{\tilde{b}R} = 10$ TeV. Values of λ'_{333} above the lines are excluded at 95% confidence level. The exclusion without the decay channels $\tilde{G} \to W^{\pm}l^{\mp}$ and $\tilde{G} \to Z^0\nu/Z^0\overline{\nu}$ is plotted for comparison.

this channel is split between two bins compared to the case where most of the line is inside one bin. This leads to the two tops seen in the exclusion plot.

One can also see that including massive vector boson processes leads to weaker limits in the region where the γ process dominates the exclusion. The reason for this is that the branching-ratio to $\gamma\nu$ is decreased compared to the case without massive vector bosons, and that the contribution from massive vector bosons to the spectrum is mainly in the lower energy regions compared to the γ line. For masses bigger than $m_{\tilde{G}} = 200$ GeV the photons from the $\gamma\nu$ process become harder then 100 GeV in the rest frame of the gravitino. As the highest energy bin sums over photons from 51.2–102.4 GeV, there is little sensitivity to photons from the $\tilde{G} \to \gamma\nu$ process for gravitino masses higher than 200 GeV. Because of this the exclusion line is driven by the tree-level processes at high gravitino masses. Both the tree level processes and the massive vector bosons produce a broad top as shown in Fig. 6.11. Because of this the limit is harder when one includes the massive vector bosons, even though the branching ratio to massive vector bosons is comparably small in this mass region. In total the contribution to the exclusion limit is small, even in regions where the massive vector

boson decays are the dominant channel.

The exclusions for λ'_{133} and λ'_{233} have been checked as well, and it was found that the same limits as shown in Fig. 6.13 apply in these channels in the mass range considered. Additionally exclusion limits for $m_s = 10$ TeV without splitting were checked and it was found that the inclusion of massive vector boson decay channels does not improve the limits.

7

Conclusion and Outlook

In this thesis the importance of the gravitino decay channels $\tilde{G} \to Z^0\nu$ and $\tilde{G} \to W^+l^-$ in scenarios with significant trilinear R-parity violating couplings was considered. The spin-polarization tensor $\Pi_{\mu\nu}$ for spin-3/2 particles was found and used to calculate the width of the gravitino in the decay channels $\tilde{G} \to Z^0\nu$ and $\tilde{G} \to W^+l^-$ expressed in the Passarino-Veltman formalism. It was found that, in scenarios with third generation fermions in the loops, radiative decay channels can dominate over tree-level decay channels for the gravitino for high sfermion masses, and that because the channels $\tilde{G} \to Z^0\nu$ and $\tilde{G} \to W^+l^-$ mix left and right handed diagrams, they are very sensitive to the mass splitting between the left and right handed sparticles involved. Furthermore it was found that the decay channels to massive vector bosons can be the biggest contribution to the gravitino width in scenarios where λ'_{i33} is the dominant RPV coupling, for a large splitting between left and right handed sbottom squarks, for a range of gravitino masses between 100 GeV $< m_{\tilde{G}} <$ 170 GeV. However, the contribution to the gamma-ray spectrum leads only to minor changes in exclusion limits on the R-parity violating couplings, even scenarios where decays to massive vector bosons give the largest contribution to the gravitino decay width.

There are further possibilities how to use and extend this result, that could not be part of this thesis because of time constraints. Here some of them will be mentioned.

- One could calculate these decays including virtual W and Z bosons. This leads to a small enhancement for gravitino masses around the boson masses, and it allows the processes to be calculated in all mass regions. However, this approach leads

to much more complicated final states with at least three final state particles, and the calculations are very complicated.

- One could extend the analysis to galactic gamma-rays. This is a difficult exercise, as the galactic backgrounds are complicated and large compared to the flux from gravitino decays.

- The results found can also be used to calculate the amount of antimatter or neutrinos produced. The cosmological background for anti-matter is much more limited than the photon backgrounds, and this approach might lead to better exclusion limits. One can compare the results to measured anti-matter spectra from astro-physical experiments and set limits in much the same way as done in this work. This would also mean that processes with massive vector bosons could be important for scenarios where the $\tilde{G} \to \gamma\nu$ process dominates over the massive vector boson processes for high scalar mass scales m_s, as they would be the dominant source of anti-matter in gravitino decays. However, this is much harder to do, as doing this would need a detailed study of anti-matter propagation through the galaxy and a much more complicated detection efficiency evaluation in the detector used.

Appendix A

Conventions and Feynman Rules

Here the necessary Feynman rules for this thesis and conventions for traces and calculations are found. The Feynman rules are closely modeled on Appendix A in Bolz [27]. In this thesis reading direction rules for Feynman diagrams as defined by Denner *et al.* [40] are used. The indices i, j and k are used as the generational indices of the (s)fermions, while s and t are used for gauge group matrix representation indices.

A.1 Conventions

Throughout this thesis the metric is assumed to be $(+---)$. Natural units are used where $\hbar = c = 1$. Additionally the value of the gravitational constant used is $G = 6.70881 \times 10^{-39} \hbar c/\ \mathrm{GeV}^2$. The gamma matrices are defined by the Clifford algebra

$$\{\gamma^\mu, \gamma^\nu\} = 2g^{\mu\nu}. \tag{A.1}$$

One can construct an additional gamma matrix γ^5

$$\gamma^5 \equiv i\gamma^0\gamma^1\gamma^2\gamma^3 \tag{A.2}$$

which leads to

$$\{\gamma^\mu, \gamma^5\} = 0. \tag{A.3}$$

From γ_5 one can construct projection operators $\mathrm{P_R}$ and $\mathrm{P_L}$

$$\mathrm{P_{R/L}} = \frac{1}{2}(1 \pm \gamma_5). \tag{A.4}$$

Using the commutation relation defined in Eq. (A.3) one finds that these operators satisfy the projection relations

$$\mathrm{P}_{\mathrm{R/L}}^2 = \mathrm{P}_{\mathrm{R/L}}, \quad \mathrm{P}_{\mathrm{L}} + \mathrm{P}_{\mathrm{R}} = 1 \quad \text{and} \quad \mathrm{P}_{\mathrm{L}}\mathrm{P}_{\mathrm{R}} = 0. \tag{A.5}$$

The anti-commuting Grassmann numbers θ_A and $\overline{\theta}^{\dot{A}}$, where $A \in 1,2$ and $\dot{A} \in \dot{1},\dot{2}$, are defined by the commutation relations

$$[x^\mu, \theta^A] = [x^\mu, \overline{\theta}^{\dot{A}}] = \{\theta^A, \theta^B\} = \{\theta^A, \overline{\theta}^{\dot{B}}\} = \{\overline{\theta}^{\dot{A}}, \theta^B\} = \{\overline{\theta}^{\dot{A}}, \overline{\theta}^{\dot{B}}\} = 0. \tag{A.6}$$

Indices can be lowered and raised with

$$\epsilon_{AB} = \epsilon_{\dot{A}\dot{B}} = \begin{pmatrix} 0 & -1 \\ 1 & 0 \end{pmatrix}, \tag{A.7}$$

$$\epsilon^{AB} = \epsilon^{\dot{A}\dot{B}} = \begin{pmatrix} 0 & 1 \\ -1 & 0 \end{pmatrix}. \tag{A.8}$$

These two properties lead to

$$\theta_A\theta_A = 0, \quad \theta\theta \equiv \theta_A\theta^A = -2\theta_1\theta_2 \quad \text{and} \quad \overline{\theta\theta} \equiv \overline{\theta}_{\dot{A}}\overline{\theta}^{\dot{A}} = 2\overline{\theta}^{\dot{1}}\overline{\theta}^{\dot{2}}. \tag{A.9}$$

One defines differentiation and integration for Grassmann numbers as

$$\partial_A\theta^B \equiv \delta_A{}^B, \quad \int d\theta_A \equiv 0 \quad \text{and} \quad \int d\theta_A\theta_A \equiv 1. \tag{A.10}$$

Because of the anti-commutation, one can write a general function of θ_A as

$$f(\theta_A) = f_0 + f_1\theta_A, \tag{A.11}$$

as all higher order terms are zero. One can then define volume elements

$$d^2\theta = -\frac{1}{4}d\theta^A d\theta_A, \quad d^2\overline{\theta} = -\frac{1}{4}d\overline{\theta}_{\dot{A}}d\overline{\theta}^{\dot{A}} \quad \text{and} \quad d^4\theta = d^2\theta d^2\overline{\theta}, \tag{A.12}$$

such that

$$\int d^4\theta(\theta\theta)(\overline{\theta\theta}) = 1. \tag{A.13}$$

The boson polarization vector $\epsilon^\nu(k)$ in the Feynman-'t-Hooft gauge for a massive spin-1 boson with mass M and momentum k satisfies

$$\sum_{pol.} \epsilon^\nu(k)\epsilon^{*\rho}(k) = -(g^{\nu\rho} - k^\nu k^\rho/M^2). \tag{A.14}$$

The spin–1/2 fermion spinor for a massive fermion with mass m and momentum p satisfies

$$\sum_{spin} u(p)\overline{u}(p) = \not{p} + m. \tag{A.15}$$

A.2 Initial states, final states and propagators

All momenta are in the following running from left to right. As all initial and final colorless scalar particles contribute only trivially with a factor of one, their Feynman rules are not written down here. Particles that have color charge contribute with a color wave function which is ignored here as it is of no consequence in the couplings considered, however, one has to remember that there exist three copies of all colored particles, and that therefore any diagram containing such particles must be multiplied with a color factor 3. The dots designate vertices. The external lines represent the reading direction, while the arrows on the lines represent fermion number flow.

This gives the following Feynman rules:

- Initial and final vector bosons with the momentum P and the polarization vectors $\epsilon_\mu(P)$ in Fig. A.1.

Figure A.1: Feynman rule for initial and final vector bosons with the momentum P and the polarization vectors $\epsilon_\mu(P)$

- Initial and final spin-1/2 fermions with the momentum P and the standard fermion spinors u, $\overline{u}$, v and $\overline{v}$ in Fig. A.2 on the next page.
- Initial and final gravitinos with momentum P and the spinor vector $\psi_\mu(P)$ in Fig. A.3 on the following page.
- The propagator for a scalar particle with momentum P and the mass m_s in Fig. A.4 on the next page.
- The propagator for a spin-1/2 fermion with momentum P and the mass m_f in Fig. A.5 on the following page.

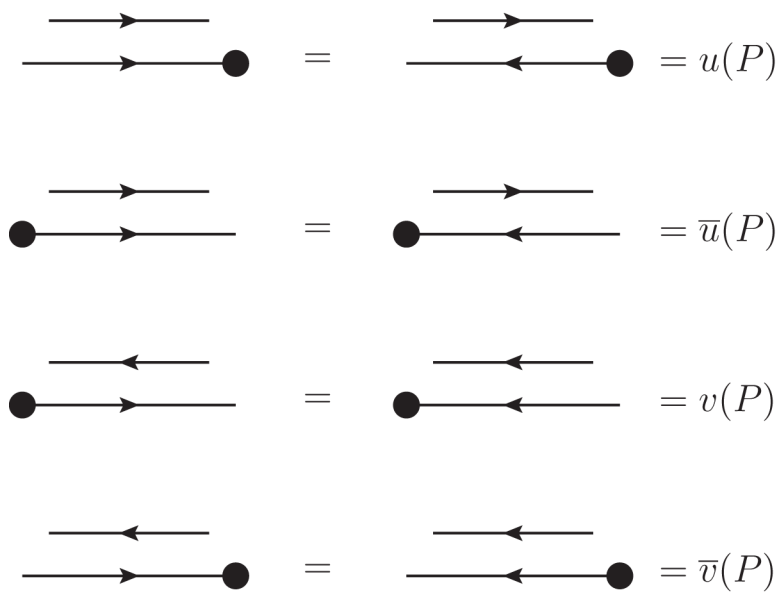

Figure A.2: Feynman rule for initial and final spin-1/2 fermions with the momentum P and the standard fermion spinors u, $\overline{u}$, v and $\overline{v}$.

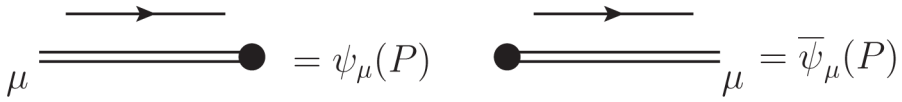

Figure A.3: Feynman rule for initial and final gravitinos with momentum P and the spinor vector $\psi_\mu(P)$.

Figure A.4: Feynman propagator for scalar particles with momentum P and the mass m_s.

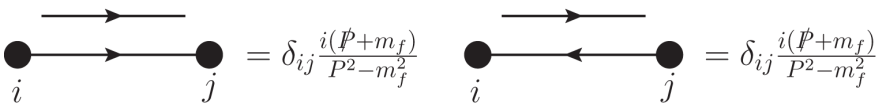

Figure A.5: Feynman propagator for spin-1/2 fermions with momentum P and the mass m_f.

A.3 Vertices

The following section contains all the vertices used in this work. All the momenta are defined running left to right.

A.3.1 The RPV couplings

The LLE part of the superpotential is given by

$$\mathbf{W}_{LLE} = \frac{1}{2}\lambda_{ijk} L_i i\sigma_2 L_j \overline{E}_k, \tag{A.16}$$

or written as the SU(2) components ν_i and l_i

$$\mathbf{W}_{LLE} = \frac{1}{2}\lambda_{ijk} (\nu_i l_j - l_i \nu_j) \overline{E}_k, \tag{A.17}$$

where $\lambda_{ijk} = -\lambda_{jik}$.

The superfield l_i contains the left handed fermion field l_{iL} and the scalar field $\tilde{l}_{iL}$, while $\overline{E}_k$ contains the left handed fermion field $\overline{l}_{kR}$ and the scalar field $\tilde{l}^*_{kR}$ and ν_i contains the left handed fermion field ν_{iL} and the scalar field $\tilde{\nu}_{iL}$. Here the R-s and L-s are part of the name of the field, and do not designate handedness. In the same way the bar does not contain any conjugation, but is part of the name of the field.

To find the Lagrangian terms from this superpotential term that give us a coupling between two leptons and one slepton, we use the part of the Lagrangian that reads $-\frac{1}{2}W_{ab}\psi_a\psi_b - \frac{1}{2}W^*_{ab}\psi^\dagger_a\psi^\dagger_b$ and the results of Section 2.1.5 where

$$W_{ab} = \frac{\partial W[A_1, ..., A_n]}{\partial A_a \partial A_b}, \tag{A.18}$$

so using only the LLE part of the superpotential one gets

$$\begin{aligned} \frac{1}{2}W_{ab}\psi_a\psi_b &= \frac{\lambda_{ijk}}{2}\Big[(\tilde{l}_{jL}\nu_{iL} + \tilde{\nu}_{iL}l_{jL} - \tilde{\nu}_{jL}l_{iL} - \tilde{l}_{iL}\nu_{jL})\overline{l}_{kR} \\ &\quad + \tilde{l}^*_{kR}(l_{jL}\nu_{iL} - \nu_{jL}l_{iL})\Big] \end{aligned} \tag{A.19}$$

and using that $\lambda_{ijk} = -\lambda_{jik}$ and writing it only for $i < j$ simplifies to

$$\frac{1}{2}W_{ij}\psi_i\psi_j = \lambda_{ijk}\left[\tilde{l}_{jL}\nu_{iL}\overline{l}_{kR} + \tilde{\nu}_{iL}l_{jL}\overline{l}_{kR} + \tilde{l}^*_{kR}\nu_{iL}l_{jL}\right]. \tag{A.20}$$

Similarly

$$\frac{1}{2}W^*_{ij}\psi^\dagger_i\psi^\dagger_j = \lambda^*_{ijk}\left[\tilde{l}^*_{jL}\nu^\dagger_{iL}\overline{l}^\dagger_{kR} + \tilde{\nu}^*_{iL}l^\dagger_{jL}\overline{l}^\dagger_{kR} + \tilde{l}_{kR}\nu^\dagger_{iL}l^\dagger_{jL}\right]. \tag{A.21}$$

Dirac spinors for two fields ψ_1 and ψ_2 can in the chiral basis for the γ matrices be written in terms of Weyl spinors as

$$\psi_1 = \begin{pmatrix} \psi_L^1 \\ \overline{\psi}_R^1 \end{pmatrix}, \quad \psi_2 = \begin{pmatrix} \psi_L^2 \\ \overline{\psi}_R^2 \end{pmatrix}, \tag{A.22}$$

and can thus replace the following combinations of Weyl spinors

$$\overline{\psi}_1 P_L \psi_2 = \overline{\psi}_R^1 \psi_L^2, \quad \overline{\psi}_2 P_R \psi_1 = \psi_R^1 \overline{\psi}_L^2.$$

Writing down the Dirac spinors of the particles using the chiral representation of the gamma matrices gives

$$l_i = \begin{pmatrix} l_{iL} \\ \overline{l}_{iR}^\dagger \end{pmatrix}, \quad l_i^c = \begin{pmatrix} \overline{l}_{iR} \\ l_{iL}^\dagger \end{pmatrix}, \tag{A.23}$$

$$\nu_i = \begin{pmatrix} \nu_{iL} \\ 0 \end{pmatrix}, \quad \nu_i^c = \begin{pmatrix} 0 \\ \nu_{iL}^\dagger \end{pmatrix}. \tag{A.24}$$

This can be used to replace the Weyl spinors in the Eq. (A.20) above by corresponding Dirac spinors. The Lagrangian term is then

$$\begin{aligned} \mathcal{L}_{LLE} = & -\lambda_{ijk} \Big[\tilde{l}_{jL} \overline{l}_k P_L \nu_i + \tilde{\nu}_{iL} \overline{l}_k P_L l_j + \tilde{l}_{kR}^* \overline{\nu}_i^c P_L l_j \\ & + \tilde{l}_{jL}^* \overline{\nu}_i P_R l_k + \tilde{\nu}_{iL}^* \overline{l}_j P_R l_k + \tilde{l}_{kR} \overline{l}_j P_R \nu_i^c \Big]. \end{aligned} \tag{A.25}$$

From this one can directly write down the two RPV couplings that have an outgoing neutrino in the final state, which come from the two terms $-\lambda_{ijk} \tilde{l}_{kR} \overline{l}_j P_R \nu_i^c$ and $-\lambda_{ijk} \tilde{l}_{jL}^* \overline{\nu}_i P_R l_k$ respectively in Fig. A.6.

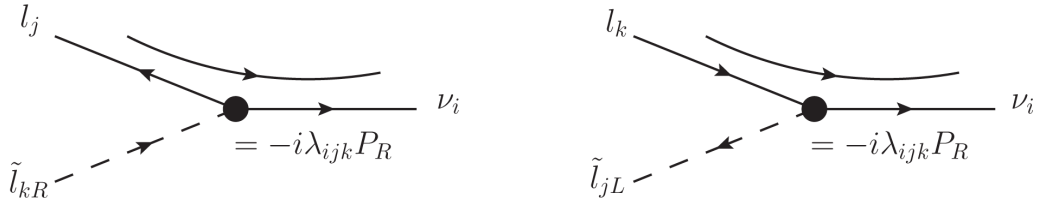

Figure A.6: The vertices that have an outgoing neutrino in the final state from the LLE part of the superpotential.

The two RPV couplings that have an outgoing charged lepton in the final state must have the same generational index on both charged leptons in order to contribute to the process $\tilde{G} \to W^+ l^-$. Since $\lambda_{iik} = 0$ we choose all couplings where the lepton has index

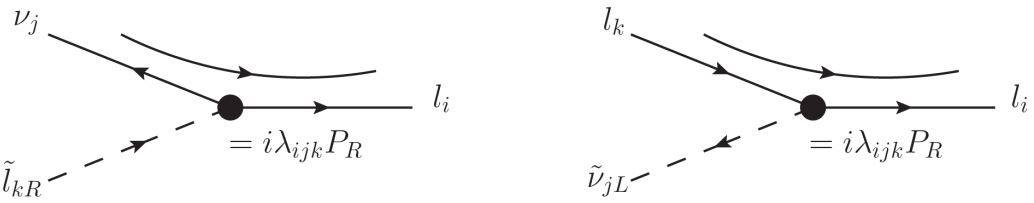

Figure A.7: The two vertices that have an outgoing lepton in the final state from the LLE part of the superpotential.

i or j, which come from the two terms $\lambda_{ijk}\tilde{l}_{kR}\overline{l}_i P_R \nu_j^c$ and $\lambda_{ijk}\tilde{\nu}^*_{jL}\overline{l}_i P_R l_k$ respectively in Fig. A.7.

An equivalent argument can be carried out for the LQD part of the superpotential given by

$$\mathbf{W}_{LQD} = \lambda'_{ijk} L_i i\sigma_2 Q_j \overline{D}_k, \tag{A.26}$$

or written as the SU(2) components ν_i, l_i, u_j and d_j

$$\mathbf{W}_{LQD} = \lambda'_{ijk}(\nu_i u_j - l_i d_j)\overline{D}_k. \tag{A.27}$$

The superfield u_i contains the left handed fermion field u_{iL} and the scalar field $\tilde{u}_{iL}$, while $\overline{D}_k$ contains the left handed fermion field $\overline{d}_{kR}$ and the scalar field $\tilde{d}^*_{kR}$ and d_i contains the left handed fermion field d_{iL} and the scalar field $\tilde{d}_{iL}$.

Using the same construction as above, one can find the Lagrangian density to be

$$\begin{aligned}
\mathcal{L}_{LQD} \;=\; & -\lambda'_{ijk}\Big[\tilde{d}^*_{kR}\overline{\nu}^c_i P_L d_j - \tilde{d}^*_{kR}\overline{l}^c_i P_L u_j + \tilde{d}_{jL}\overline{d}_k P_L \nu_i \\
& -\tilde{u}_{jL}\overline{d}_k P_L l_i + \tilde{\nu}_{iL}\overline{d}_k P_L d_j - \tilde{l}_{iL}\overline{d}_k P_L u_j \\
& +\tilde{d}_{kR}\overline{d}_j P_R \nu^c_i - \tilde{d}_{kR}\overline{u}_j P_R l^c_i + \tilde{d}^*_{jL}\overline{\nu}_i P_R d_k \\
& -\tilde{u}^*_{jL}\overline{l}_i P_R d_k + \tilde{\nu}^*_{iL}\overline{d}_j P_R d_k - \tilde{l}^*_{iL}\overline{u}_j P_L d_k\Big]
\end{aligned} \tag{A.28}$$

From this one can directly write down the two vertices that have an outgoing neutrino in the final state, which come from the two terms $-\lambda'_{ijk}\tilde{d}_{kR}\overline{d}_j P_R \nu^c_i$ and $-\lambda'_{ijk}\tilde{d}^*_{jL}\overline{\nu}_i P_R d_k$ respectively, in Fig. A.8 on the next page. The two vertices that have an outgoing lepton in the final state, which come from the two terms $\lambda'_{ijk}\tilde{u}^*_{jL}\overline{l}_i P_R d_k$ and $\lambda'_{ijk}\tilde{d}_{kR}\overline{u}_j P_R l^c_i$ respectively, are found in Fig. A.9 on the following page.

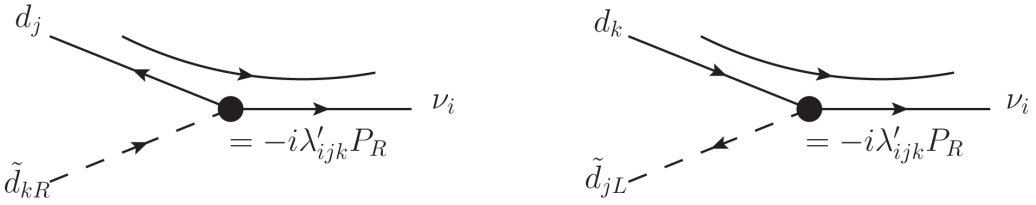

Figure A.8: The two vertices that have an outgoing neutrino in the final state from the LQD part of the superpotential.

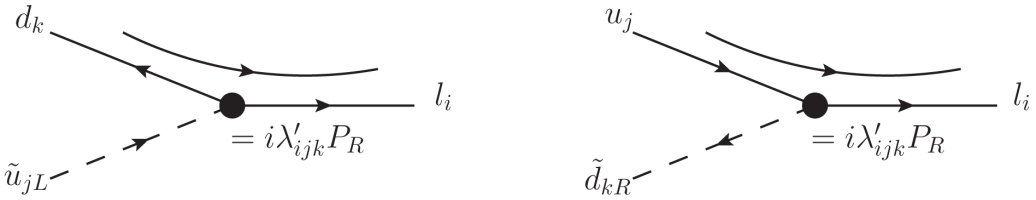

Figure A.9: The two vertices that have an outgoing lepton in the final state from the LQD part of the superpotential.

A.3.2 Gravitino couplings to a scalar and a fermion

The gravitino Lagrangian, given in Eq. (3.1), gives the two couplings between a gravitino, a sfermion with momentum P and a fermion found in Fig. A.10. Here we here choose the two combinations of reading direction and handedness of the sfermion that is used in writing down our amplitudes in Sections 4.4.1 and 4.5.1.

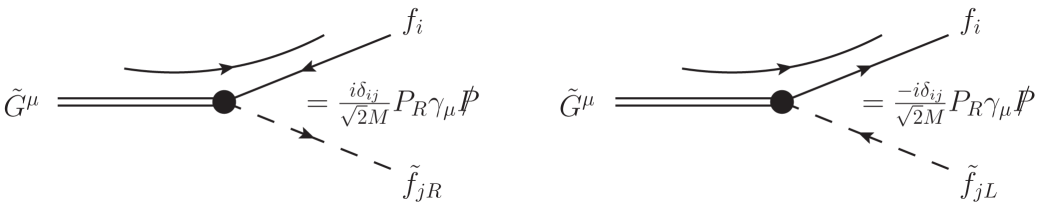

Figure A.10: The vertices for the coupling between a gravitino, a sfermion with momentum P and a fermion.

A.3.3 Z^0 couplings

To find the couplings of the Z^0 to the involved particles, we need to write down the explicit form of the covariant derivative D_μ that generates the coupling to the Z^0 boson for a general field ϕ. Here T^a_{st} is a generator for a gauge group with a boson A^a_μ, g is

the coupling constant and s and t designate indices of the matrix representation of T. This leads to

$$D_\mu \phi_s = \left(\partial_\mu \delta_{st} + igT^a_{st} A^a_\mu\right) \phi_t. \tag{A.29}$$

in the Standard Model the Z^0 boson is composed of the $SU(2)$ and $U(1)$ gauge bosons in the following way:

$$W^{3\mu} = \cos\theta_W Z^\mu + \sin\theta_W A^\mu, \tag{A.30}$$

$$B^\mu = -\sin\theta_W Z^\mu + \cos\theta_W A^\mu. \tag{A.31}$$

Here θ_W is the weak mixing angle where

$$\sin\theta_W = \frac{g'}{\sqrt{g^2 + g'^2}}, \tag{A.32}$$

$$\cos\theta_W = \frac{g}{\sqrt{g^2 + g'^2}}, \tag{A.33}$$

and

$$g \sin\theta_W = g' \cos\theta_W = e. \tag{A.34}$$

Here $W^{i\mu}$ are the SU(2) gauge bosons, and B^μ is the U(1) gauge boson. g and g' are the $SU(2)$ and $U(1)$ gauge bosons respectively. The covariant derivative for the $SU(2) \times U(1)$ group is given as

$$D^{U(1)\times SU(2)}_\mu \phi^i_s = \delta^{ij}\left(\partial_\mu \delta_{st} + i\frac{g}{2}\sigma^a_{st} W^a_\mu + ig'\frac{Y_{st}}{2} B_\mu\right)\phi^j_t. \tag{A.35}$$

Observe that Y_{st} and σ^3_{st} are zero for off diagonal terms and do therefore not change charges. Both designate neutral currents.

Looking at the part of the covariant derivative involving only for $W^{3\mu}$ we get

$$\begin{aligned} D^{W^3}_\mu \phi_s &= \left(\partial_\mu \delta^{st} + i\frac{g}{2}\sigma^3_{st} W^3_\mu\right)\phi_t \\ &= \left(\partial_\mu \delta^{st} + i\frac{g}{2}\sigma^3_{st}\cos\theta_W Z^\mu + i\frac{g}{2}\sigma^3_{st}\sin\theta_W A^\mu\right)\phi_t. \end{aligned} \tag{A.36}$$

And looking at the covariant derivative only for B_μ

$$\begin{aligned} D^B_\mu \phi_s &= \left(\partial_\mu \delta^{st} + ig'\frac{Y_{st}}{2} B_\mu\right)\phi_t \\ &= \left(\partial_\mu \delta^{st} - ig'\frac{Y_{st}}{2}\sin\theta_W Z^\mu + ig'\frac{Y_{st}}{2}\cos\theta_W A^\mu\right)\phi_t. \end{aligned} \tag{A.37}$$

Taking out the Z^μ part of both expressions we get part of the covariant derivative coupling the Z boson:

$$D^Z_\mu \phi_s = \left(\partial_\mu \delta^{st} + \frac{ie}{2\sin\theta_W \cos\theta_W}(\cos^2\theta_W \sigma^3_{st} - \sin^2\theta_W Y_{st}) Z^\mu\right)\phi_t. \quad \text{(A.38)}$$

This gives the following vertices:

- The coupling of two down type fermions to a Z^0 boson. Here the left handed fermions are contained in the lower part of a SU(2) doublet and have hypercharge Y_L, while the the right handed fermions are singlets in $SU(2)$ and have hypercharge Y_R, leading to:

$$D^Z_\mu f^i = \left(\partial_\mu - ie\frac{([1-(1-Y_L)\sin^2\theta_W]P_L + Y_R \sin^2\theta_W P_R)}{2\sin\theta_W\cos\theta_W} Z^\mu\right) f^i \quad \text{(A.39)}$$

  This leads to the vertices in Fig. A.11.

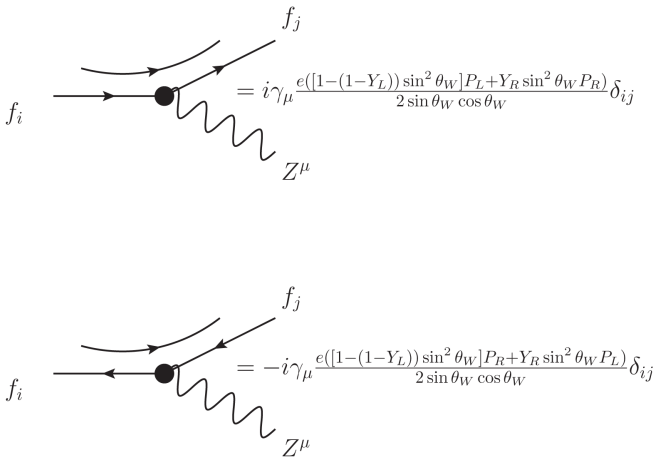

Figure A.11: The vertices of two down type fermions coupling to a Z^0 boson with both reading directions.

- The coupling of two down type sfermions to a Z^0 boson. The sfermions inherit their quantum numbers from their fermion Weyl partners in the superfield. The incoming sfermion has a momentum P while the outgoing has a momentum Q. For left handed sfermions this gives the covariant derivative

$$D^Z_\mu \tilde{f}^i_L = \left(\partial_\mu - \frac{ie(1-(1-Y_L)\sin^2\theta_W)}{2\sin\theta_W\cos\theta_W} Z^\mu\right)\tilde{f}^i_L, \quad \text{(A.40)}$$

while the right handed sfermion has

$$D_\mu^Z \tilde{f}_R^i = \left(\partial_\mu - \frac{Y_R ie \sin^2\theta_W}{2\sin\theta_W \cos\theta_W} Z^\mu\right) \tilde{f}_R^i. \tag{A.41}$$

This gives the vertices in Fig. A.12. To get the vertices for the corresponding antiparticles, one must change the sign of the momenta.

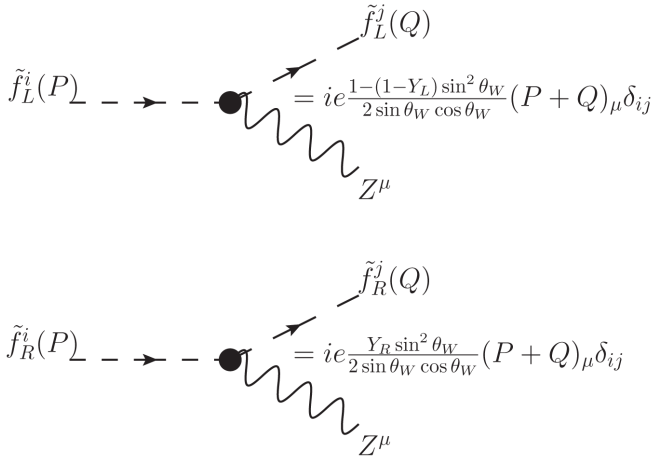

Figure A.12: The vertices for the coupling of two down type sfermions to a Z^0 boson.

- The 4-particle vertices containing one gravitino, one Z^0, one fermion and one sfermion are shown in Fig. A.13 on the following page. These are obtained from the combination of Eqs. (A.40), (A.41) and (3.1). Only the combinations of reading direction and handedness needed are listed.

A.3.4 W couplings

To find the couplings of the W to the involved particles, we need to write down the explicit form of the covariant derivative D_μ that generates the coupling to the W boson for a general field ϕ

$$D_\mu \phi_s^i = \delta^{ij}\left(\partial_\mu \delta_{st} + igT_{st}^a A_\mu^a\right)\phi_t^j. \tag{A.42}$$

The W boson is composed of the $SU(2)$ gauge bosons in the following way:

$$W^{+\mu} = \frac{1}{\sqrt{2}}[W^{1\mu} + iW^{2\mu}], \tag{A.43}$$

$$W^{-\mu} = \frac{1}{\sqrt{2}}[W^{1\mu} - iW^{2\mu}]. \tag{A.44}$$

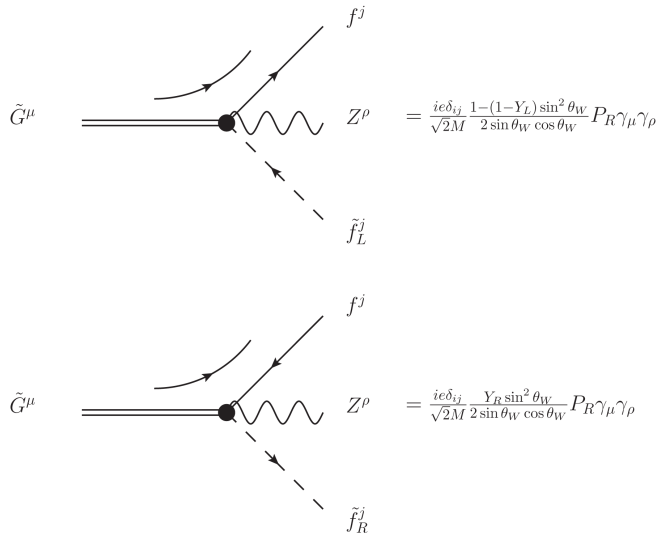

Figure A.13: The 4-particle vertices containing one gravitino, one Z, one fermion and one sfermion.

The covariant derivative for the $SU(2)$ group is given as

$$D_\mu^{SU(2)}\phi_s^i = \delta^{ij}\left(\partial_\mu\delta_{st} + i\frac{g}{2}\sigma_{st}^a W_\mu^a\right)\phi_t^j. \tag{A.45}$$

Since the Pauli matrices involved are

$$\sigma^1 = \begin{pmatrix} 0 & 1 \\ 1 & 0 \end{pmatrix}, \tag{A.46}$$

and

$$\sigma^2 = i\begin{pmatrix} 0 & -1 \\ 1 & 0 \end{pmatrix}, \tag{A.47}$$

one can write the covariant derivative as

$$D_\mu^{SU(2)}\phi^i = \left(\partial_\mu + i\frac{g}{\sqrt{2}}\begin{pmatrix} 0 & 1 \\ 0 & 0 \end{pmatrix}W_\mu^- + i\frac{g}{\sqrt{2}}\begin{pmatrix} 0 & 0 \\ 1 & 0 \end{pmatrix}W_\mu^+\right)\phi^i. \tag{A.48}$$

This gives the following vertices:

- The vertices with an up type fermion and a down type fermion to a W boson are given in Fig. A.14 on the next page. Here the left handed fermions are parts of an SU(2) doublet while the the right handed leptons are singlets in $SU(2)$ and do not couple.

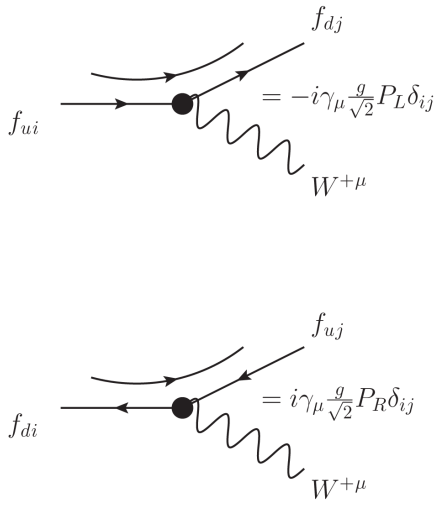

Figure A.14: The vertices for the coupling of a up type fermion and a down type fermion to a W boson.

- The vertiex for the coupling of an up type sfermion and a down type sfermion to a W boson are given in Fig. A.15. The sleptons inherit their quantum numbers from their fermion Weyl partners in the superfield. The incoming slepton has a momentum P while the outgoing sneutrino has a momentum Q.

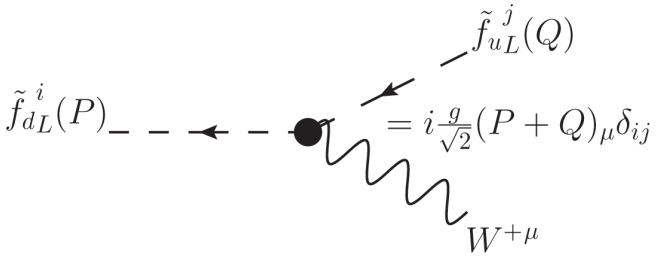

Figure A.15: The vertex of the coupling of an up type sfermion and a down type sfermion to a W boson.

- The 4-particle vertex containing one gravitino, one W, one fermion and one sfermion is given in Fig. A.16 on the next page. These are obtained from Eq. (3.1) and the explicit form of the covariant derivative. Only the combination of reading direction and handedness needed is shown.

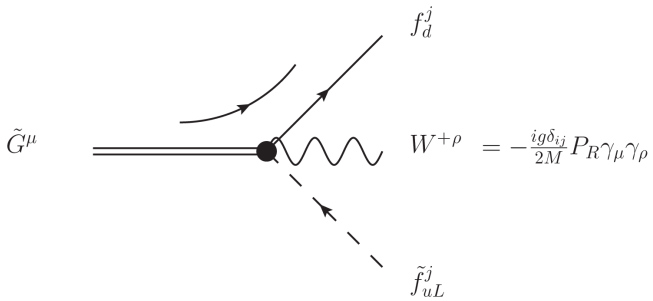

Figure A.16: The 4-particle vertex with one gravitino, one W boson, one fermion and one sfermion.

Appendix B

Passarino-Veltman Integrals

This document contains the decompositions of the integrals in Eqs. (4.9) and (4.10), for the kinematics $p_1 = -p$ and $p_2 = -k$ with $p^2 = m^2_{\tilde{G}}$, $k^2 = m^2_B$ and $(p-k)^2 = m^2_l$, into scalar components. The $m_\pm$ notation in Eq. (4.5) is used. All decompositions are done in Mathematica with the package FeynCalc [41]. All calculations are done in $d = 4 - \epsilon$ dimensions. In the calculations the following shorthands for the finite expressions will be used

$$
\begin{aligned}
C_0 &\equiv C_0(m^2_{\tilde{G}}, m^2_l, m^2_B, m^2_1, m^2_2, m^2_3), && \text{(B.1)}\\
\Delta B_0^{(a)} &\equiv B_0(m^2_{\tilde{G}}, m^2_1, m^2_2) - B_0(m^2_B, m^2_1, m^2_3), && \text{(B.2)}\\
\Delta B_0^{(b)} &\equiv B_0(m^2_{\tilde{G}}, m^2_1, m^2_2) - B_0(m^2_l, m^2_2, m^2_3), && \text{(B.3)}\\
\Delta B_0^{(c)} &\equiv B_0(m^2_B, m^2_1, m^2_3) - B_0(m^2_l, m^2_2, m^2_3), && \text{(B.4)}\\
\Delta B_0^{(d)} &\equiv B_0(m^2_G, m^2_1, m^2_2) - B_0(0, m^2_1, m^2_2), && \text{(B.5)}\\
\Delta B_0^{(e)} &\equiv B_0(m^2_B, m^2_1, m^2_3) - B_0(0, m^2_1, m^2_3), && \text{(B.6)}\\
\Delta B_0^{(f)} &\equiv B_0(m^2_l, m^2_2, m^2_3) - B_0(0, m^2_1, m^2_3) \quad \text{and} && \text{(B.7)}\\
\Delta B_0^{(g)} &\equiv B_0(m^2_l, m^2_2, m^2_3) - B_0(0, m^2_2, m^2_3). && \text{(B.8)}
\end{aligned}
$$

B.1 C^μ

The rank one tensor two point integral C^μ is given by Eq. (4.11) as

$$
C^\mu = \frac{(2\pi\mu)^{(\epsilon)}}{i\pi^2} \int \frac{q^\mu d^d q}{\left(q^2 - m^2_1\right)\left((q-p)^2 - m^2_2\right)\left((q-k)^2 - m^2_3\right)}, \qquad \text{(B.9)}
$$

which can be written as

$$C^\mu = p^\mu C_p + k^\mu C_k. \tag{B.10}$$

The constants are given by

$$\begin{aligned} C_p &= -\frac{1}{m_-^2 m_+^2} \\ &\times\{C_0[-m_1^2(m_{\tilde{G}}^2 - m_B^2 - m_l^2) - 2m_2^2 m_B^2 + m_3^2(m_{\tilde{G}}^2 + m_B^2 - m_l^2) \\ &+m_B^2(m_{\tilde{G}}^2 - m_B^2 + m_l^2)] \\ &+m_B^2(\Delta B_0^{(a)} - \Delta B_0^{(c)}) + (m_{\tilde{G}}^2 - m_l^2)\Delta B_0^{(b)}\}, \end{aligned} \tag{B.11}$$

and

$$\begin{aligned} C_k &= -\frac{1}{m_-^2 m_+^2} \\ &\times\{C_0[m_1^2(m_{\tilde{G}}^2 - m_B^2 + m_l^2) + m_2^2(m_{\tilde{G}}^2 + m_B^2 - m_l^2) - 2m_3^2 m_{\tilde{G}}^2 \\ &-m_{\tilde{G}}^2(m_{\tilde{G}}^2 - m_B^2 - m_l^2)] \\ &-m_{\tilde{G}}^2(\Delta B_0^{(a)} + \Delta B_0^{(b)}) + (m_B^2 - m_l^2)\Delta B_0^{(c)}\}. \end{aligned} \tag{B.12}$$

Both have mass dimension -2. One can define dimensionless versions C_p' and C_k' by multiplying by $-m_-^2 m_+^2/m_{\tilde{G}}^2$ and get

$$\begin{aligned} C_p' &= -\left\{C_0\left[m_1^2\left(1 - \frac{m_B^2 + m_l^2}{m_{\tilde{G}}^2}\right) + 2m_2^2\frac{m_B^2}{m_{\tilde{G}}^2} - m_3^2\left(1 + \frac{m_B^2 - m_l^2}{m_{\tilde{G}}^2}\right)\right.\right. \\ &\left.\left.-m_B^2\left(1 - \frac{m_B^2 - m_l^2}{m_{\tilde{G}}^2}\right)\right] \right. \\ &\left. -\frac{m_B^2}{m_{\tilde{G}}^2}(\Delta B_0^{(a)} - \Delta B_0^{(c)}) - \left(1 - \frac{m_l^2}{m_{\tilde{G}}^2}\right)\Delta B_0^{(b)}\right\} \end{aligned} \tag{B.13}$$

and

$$\begin{aligned} C_k' &= \left\{C_0\left[m_1^2\left(1 - \frac{m_B^2 - m_l^2}{m_{\tilde{G}}^2}\right) + m_2^2\left(1 + \frac{m_B^2 - m_l^2}{m_{\tilde{G}}^2}\right) - 2m_3^2\right.\right. \\ &\left.\left.-\left(m_{\tilde{G}}^2 - m_B^2 - m_l^2\right)\right] \right. \\ &\left. -(\Delta B_0^{(a)} + \Delta B_0^{(b)}) + \frac{m_B^2 - m_l^2}{m_{\tilde{G}}^2}\Delta B_0^{(c)}\right\}. \end{aligned} \tag{B.14}$$

As the constants C_p' and C_k' only contain linear combinations of the finite expressions defined in Eqs. (B.1)–(B.8), they are themselves finite.

B.2 $C^{\mu\nu}$

The rank two tensor two point integral $C^{\mu\nu}$ is given by Eq. (4.12) as

$$C^{\mu\nu} = \frac{(2\pi\mu)^{(4-d)}}{i\pi^2} \int \frac{q^\mu q^\nu d^d q}{\left(q^2 - m_0^2\right)\left((q-p)^2 - m_1^2\right)\left((q-k)^2 - m_2^2\right)}, \tag{B.15}$$

which can be written as

$$C^{\mu\nu} = g^{\mu\nu} C_{00} + p^\mu p^\nu C_{pp} + k^\mu k^\nu C_{kk} + (p^\mu k^\nu + k^\mu p^\nu) C_{pk}. \tag{B.16}$$

The constant C_{00} can be written as[1]

$$\begin{aligned}
C_{00} \;=\; & \frac{1}{4m_-^2 m_+^2} \\
& \times\{2C_0[-m_1^2 m_l^2(m_{\tilde{G}}^2 + m_B^2 - m_l^2 - m_1^2) - m_2^2 m_B^2(m_{\tilde{G}}^2 - m_B^2 + m_l^2 - m_2^2) \\
& + m_3^2 m_{\tilde{G}}^2(m_{\tilde{G}}^2 - m_B^2 - m_l^2 + m_3^2) + m_1^2 m_2^2(m_{\tilde{G}}^2 - m_B^2 - m_l^2) \\
& - m_1^2 m_3^2(m_{\tilde{G}}^2 - m_B^2 + m_l^2) - m_2^2 m_3^2(m_{\tilde{G}}^2 + m_B^2 - m_l^2) + m_{\tilde{G}}^2 m_B^2 m_l^2] \\
& - m_1^2((m_{\tilde{G}}^2 - m_B^2)\Delta B_0^{(a)} + m_l^2(\Delta B_0^{(b)} + \Delta B_0^{(c)})) \\
& - m_2^2((m_{\tilde{G}}^2 - m_l^2)\Delta B_0^{(b)} - m_B^2(\Delta B_0^{(c)} - \Delta B_0^{(a)})) \\
& + m_3^2(m_{\tilde{G}}^2(\Delta B_0^{(a)} + \Delta B_0^{(b)}) - (m_B^2 - m_l^2)\Delta B_0^{(c)}) \\
& + m_B^2(m_{\tilde{G}}^2 - m_B^2 + m_l^2)\Delta B_0^{(a)} + m_l^2(m_{\tilde{G}}^2 + m_B^2 - m_l^2)\Delta B_0^{(b)} \\
& + m_-^2 m_+^2 B_0(m_{\tilde{G}}^2, m_1^2, m_2^2)\}.
\end{aligned} \tag{B.17}$$

This scalar constant has mass dimension 0. It can be split into a finite part C'_{00} and a divergent part:

$$C_{00} \equiv C'_{00} + \frac{1}{4} B_0(m_{\tilde{G}}^2, m_1^2, m_2^2). \tag{B.18}$$

[1]This is the correct expression, using FeynCalc alone gives this plus an additional erroneous term $+1/4$.

The constant C_{pp} can be written as

$$
\begin{aligned}
C_{pp} \;=\; & \frac{1}{2m_+^4 m_-^4}\Bigg\{ 2C_0\left[(m_1^2+m_3^2-m_B^2)^2 m_+^2 m_-^2\right. \\
& +6m_B^2(m_2^4 m_B^2 + m_3^4 m_{\tilde{G}}^2 + m_1^4 m_l^2 - m_2^2 m_B^2(m_{\tilde{G}}^2 - m_B^2 + m_l^2) \\
& +m_3^2 m_{\tilde{G}}^2(m_{\tilde{G}}^2 - m_B^2 - m_l^2) - m_1^2 m_l^2(m_{\tilde{G}}^2 + m_B^2 - m_l^2) \\
& +m_1^2 m_2^2(m_{\tilde{G}}^2 - m_B^2 - m_l^2) - m_2^2 m_3^2(m_{\tilde{G}}^2 + m_B^2 - m_l^2)) \\
& \left.+6m_B^4 m_l^2 m_{\tilde{G}}^2 + 2m_1^2 m_3^2(m_B^4 + (m_{\tilde{G}}^2 + m_l^2)m_B^2 - 2(m_{\tilde{G}}^2 - m_l^2)^2)\right] \\
& -\frac{(m_1^2-m_2^2)}{m_{\tilde{G}}^2} m_+^2 m_-^2 (m_{\tilde{G}}^2 + m_B^2 - m_l^2)\Delta B_0^{(d)} \\
& +6m_B^2[(m_1^2-m_3^2)(m_{\tilde{G}}^2 - m_l^2) + (m_1^2 + 2m_2^2 + m_3^2)m_B^2]\Delta B_0^{(c)} \\
& +2m_1^2[m_+^2 m_-^2 + 2(m_{\tilde{G}}^2 - m_l^2)^2 + m_B^2(m_{\tilde{G}}^2 + m_B^2 + m_l^2)]\Delta B_0^{(b)} \\
& -6m_2^2 m_B^2(m_{\tilde{G}}^2 + m_B^2 - m_l^2)\Delta B_0^{(b)} \\
& +2m_3^2(m_B^4 + 2m_B^2(2m_{\tilde{G}}^2 - m_l^2) + (m_l^2 - m_{\tilde{G}}^2)^2)\Delta B_0^{(b)} \\
& -((m_{\tilde{G}}^2 - m_l^2)^3 - 5(m_{\tilde{G}}^4 - m_l^4)m_B^2 + m_B^4(3m_B^2 + (m_{\tilde{G}}^2 - 7m_l^2)))\Delta B_0^{(b)} \\
& +2m_B^4(3m_B^2 + 4(m_{\tilde{G}}^2 - m_l^2))\Delta B_0^{(c)} \\
& \left.+2m_+^2 m_-^2 m_B^2\right\} \\
& -\frac{(m_2^2-m_3^2)(m_{\tilde{G}}^2 - m_B^2 - m_l^2)}{2m_l^2 m_+^2 m_-^2}\Delta B_0^{(g)}. \qquad \text{(B.19)}
\end{aligned}
$$

This expression has mass dimension -2. One can define a dimensionless finite version C'_{pp} by multiplying by $m_-^2 m_+^2/m_{\tilde{G}}^2$ and splitting off the superficially divergent part ($m_l \to 0$) in the following way:

$$
C_{pp} \;\equiv\; \frac{m_{\tilde{G}}^2}{m_+^2 m_-^2} C'_{pp} - \frac{(m_2^2-m_3^2)(m_{\tilde{G}}^2 - m_B^2 - m_l^2)}{2m_+^2 m_-^2}\frac{\Delta B_0^{(g)}}{m_l^2}. \qquad \text{(B.20)}
$$

The constant C_{kk} can be written as

$$
\begin{aligned}
C_{kk} &= \frac{1}{2m_+^4 m_-^4} \\
&\times\{2C_0[m_+^2 m_-^2((m_1^2-m_2^2+m_{\tilde{G}}^2)^2-4m_1^2 m_{\tilde{G}}^2) \\
&+6m_{\tilde{G}}^2(m_1^4 m_l^2+m_2^4 m_B^2+m_3^4 m_{\tilde{G}}^2+m_l^2 m_B^2 m_{\tilde{G}}^2 \\
&-(m_1^2 m_l^2+m_2^2 m_3^2)(m_{\tilde{G}}^2+m_B^2-m_l^2) \\
&-(m_2^2 m_B^2+m_1^2 m_3^2)(m_{\tilde{G}}^2-m_B^2+m_l^2) \\
&+(m_3^2 m_{\tilde{G}}^2+m_1^2 m_2^2)(m_{\tilde{G}}^2-m_B^2-m_l^2))] \\
&+2m_-^2 m_+^2 m_{\tilde{G}}^2 \\
&-\frac{(m_1^2-m_3^2)}{m_B^2} m_-^2 m_+^2(m_{\tilde{G}}^2+m_B^2-m_l^2)\Delta B_0^{(e)} \\
&-2(m_1^2-m_2^2)m_-^2 m_+^2 \Delta B_0^{(c)} \\
&-6m_1^2 m_{\tilde{G}}^2[(m_{\tilde{G}}^2-m_B^2)\Delta B_0^{(a)}+m_l^2(\Delta B_0^{(b)}+\Delta B_0^{(c)})] \\
&-6m_2^2 m_{\tilde{G}}^2[(m_{\tilde{G}}^2+m_B^2-m_l^2)\Delta B_0^{(b)}-2m_B^2\Delta B_0^{(c)}] \\
&+6m_3^2 m_{\tilde{G}}^2(m_{\tilde{G}}^2(\Delta B_0^{(a)}+\Delta B_0^{(b)})-(m_B^2-m_l^2)\Delta B_0^{(c)}) \\
&+6m_{\tilde{G}}^2(m_{\tilde{G}}^2-m_B^2)(m_{\tilde{G}}^2\Delta B_0^{(a)}+(m_{\tilde{G}}^2-m_B^2)\Delta B_0^{(c)}) \\
&-6m_{\tilde{G}}^2 m_l^2(m_{\tilde{G}}^2\Delta B_0^{(a)}+(m_{\tilde{G}}^2+m_B^2)\Delta B_0^{(c)}) \\
&-m_-^2 m_+^2(3m_{\tilde{G}}^2+m_B^2-m_l^2)\Delta B_0^{(c)}\} \\
&+\frac{(m_2^2-m_3^2)(m_{\tilde{G}}^2-m_B^2+m_l^2)}{2m_+^2(m_{\tilde{G}}^2+(m_B-m_l)^2)}\frac{\Delta B_0^{(g)}}{m_l^2}.
\end{aligned}
\tag{B.21}
$$

This expression has mass dimension -2. One can again define a dimensionless finite version C'_{kk} by multiplying by $m_-^2 m_+^2/m_{\tilde{G}}^2$ and splitting off the superficially divergent part ($m_l \to 0$) in the following way:

$$
C_{kk} \equiv \frac{m_{\tilde{G}}^2}{m_+^2 m_-^2} C'_{kk} + \frac{(m_2^2-m_3^2)(m_{\tilde{G}}^2-m_B^2+m_l^2)}{2m_+^2(m_{\tilde{G}}^2+(m_B-m_l)^2)}\frac{\Delta B_0^{(g)}}{m_l^2}. \tag{B.22}
$$

The constant C_{pk} can be written as

$$\begin{aligned}
C_{pk} &= -\frac{1}{(2m_+^4 m_-^4)} \\
&\times\{2C_0[((m_1^2-2m_2^2-m_{\tilde{G}}^2)(m_1^2-2m_3^2-m_B^2)-m_1^2m_l^2+4m_1^2(m_2^2+m_3^2) \\
&-6m_2^2m_3^2)m_+^2m_-^2 \\
&+3(m_1^4m_l^2+m_2^4m_B^2+m_3^4m_{\tilde{G}}^2+m_B^2m_{\tilde{G}}^2m_l^2)(m_B^2-m_l^2+m_{\tilde{G}}^2) \\
&-6(m_1^2m_3^2+m_2^2m_B^2)m_{\tilde{G}}^2(m_{\tilde{G}}^2-m_B^2-m_l^2) \\
&+6(m_1^2m_2^2+m_3^2m_{\tilde{G}}^2)m_B^2(m_{\tilde{G}}^2-m_B^2+m_l^2)-12(m_2^2m_3^2+m_1^2m_l^2)m_{\tilde{G}}^2m_B^2] \\
&+m_-^2m_+^2(m_{\tilde{G}}^2+m_B^2-m_l^2) \\
&-2(m_1^2-m_3^2)m_-^2m_+^2\Delta B_0^{(f)} \\
&+m_-^2m_+^2[(m_1^2-m_2^2)\Delta B_0^{(b)}+(m_1^2-m_3^2)\Delta B_0^{(c)}] \\
&-6m_1^2((m_{\tilde{G}}^2-m_B^2)(m_{\tilde{G}}^2\Delta B_0^{(b)}-m_B^2\Delta B_0^{(c)})+m_l^2(m_{\tilde{G}}^2\Delta B_0^{(b)}+m_B^2\Delta B_0^{(c)})) \\
&+6m_2^2m_B^2[(m_{\tilde{G}}^2+m_B^2-m_l^2)\Delta B_0^{(c)}-2m_{\tilde{G}}^2\Delta B_0^{(b)}] \\
&+6m_3^2m_{\tilde{G}}^2[(m_{\tilde{G}}^2+m_B^2-m_l^2)\Delta B_0^{(b)}-2m_B^2\Delta B_0^{(c)}] \\
&-6m_B^2m_{\tilde{G}}^2[(m_{\tilde{G}}^2-m_B^2)(\Delta B_0^{(c)}-\Delta B_0^{(b)})-m_l^2(\Delta B_0^{(b)}+\Delta B_0^{(c)})] \\
&+m_-^2m_+^2(m_{\tilde{G}}^2\Delta B_0^{(b)}+m_B^2\Delta B_0^{(c)})\} \\
&-\frac{(m_2^2-m_3^2)(m_{\tilde{G}}^2-m_B^2-m_l^2)}{2m_+^2(m_{\tilde{G}}^2+(m_B-m_l)^2)}\frac{\Delta B_0^{(g)}}{m_l^2}.
\end{aligned} \tag{B.23}$$

This expression has mass dimension -2. One can define a dimensionless finite version C'_{kk} by multiplying by $m_-^2m_+^2/m_{\tilde{G}}^2$ and splitting off the superficially divergent part ($m_l \to 0$) in the following way:

$$C_{pk} \equiv -\frac{m_{\tilde{G}}^2}{m_+^2m_-^2}C'_{pk}-\frac{(m_2^2-m_3^2)(m_{\tilde{G}}^2-m_B^2-m_l^2)}{2m_+^2(m_{\tilde{G}}^2+(m_B-m_l)^2)}\frac{\Delta B_0^{(g)}}{m_l^2}. \tag{B.24}$$

Appendix C

Calculation of $T_{\rho\eta}$

This appendix contains the explicit calculation of the trace

$$\begin{aligned} T_{\rho\eta} &= \mathrm{Tr}[(\not{p} - \not{k} + m_s)\mathrm{P_R}\left\{(C_{Ppk}p_\rho + C_{P\gamma k}\gamma_\rho)k_\mu + C_{Pg}g_{\mu\rho}\right\}\left(\not{p} + m_{\tilde{G}}\right) \\ &\quad \times \left[\left(g^{\mu\pi} - \frac{p^\mu p^\pi}{m^2_{\tilde{G}}}\right) - \frac{1}{3}\left(g^{\mu\alpha} - \frac{p^\mu p^\alpha}{m^2_{\tilde{G}}}\right)\left(g^{\pi\beta} - \frac{p^\pi p^\beta}{m^2_{\tilde{G}}}\right)\gamma_\alpha\gamma_\beta\right] \\ &\quad \times \left\{(C^*_{Ppk}p_\eta + C^*_{P\gamma k}\gamma_\eta)k_\pi + C^*_{Pg}g_{\eta\pi}\right\}\mathrm{P_L}]. \end{aligned} \tag{C.1}$$

Using the cyclicity of the trace and that projection operators change handedness when commuting with gamma matrices one gets

$$\begin{aligned} T_{\rho\eta} &= \mathrm{Tr}[\mathrm{P_R}(\not{p} - \not{k})\left\{(C_{Ppk}p_\rho + C_{P\gamma k}\gamma_\rho)k_\mu + C_{Pg}g_{\mu\rho}\right\}\left(\not{p} + m_{\tilde{G}}\right) \\ &\quad \left[\left(g^{\mu\pi} - \frac{p^\mu p^\pi}{m^2_{\tilde{G}}}\right) - \frac{1}{3}\left(g^{\mu\alpha} - \frac{p^\mu p^\alpha}{m^2_{\tilde{G}}}\right)\left(g^{\pi\beta} - \frac{p^\pi p^\beta}{m^2_{\tilde{G}}}\right)\gamma_\alpha\gamma_\beta\right] \\ &\quad \left\{(C^*_{Ppk}p_\eta + C^*_{P\gamma k}\gamma_\eta)k_\pi + C^*_{Pg}g_{\eta\pi}\right\}]. \end{aligned} \tag{C.2}$$

C. CALCULATION OF THE TRACE

This can be split into traces over gamma matrices and constants in the following way:

$$
\begin{aligned}
T_{\rho\eta} &= (p^\sigma - k^\sigma)\left(g^{\mu\pi} - \frac{p^\mu p^\pi}{m_{\tilde{G}}^2}\right) \\
&\times \left\{ \left(C_{Ppk} p_\rho k_\mu + C_{Pg} g_{\mu\rho}\right)\left(C^*_{Ppk} p_\eta k_\pi + C^*_{Pg} g_{\eta\pi}\right) \mathrm{Tr}\left[\mathrm{P_R}\gamma_\sigma\left(\not{p} + m_{\tilde{G}}\right)\right] \right. \\
&+ C_{P\gamma k} k_\mu \left(C^*_{Ppk} p_\eta k_\pi + C^*_{Pg} g_{\eta\pi}\right) \mathrm{Tr}\left[\mathrm{P_R}\gamma_\sigma\gamma_\rho\left(\not{p} + m_{\tilde{G}}\right)\right] \\
&+ \left(C_{Ppk} p_\rho k_\mu + C_{Pg} g_{\mu\rho}\right) C^*_{P\gamma k} k_\pi \mathrm{Tr}\left[\mathrm{P_R}\gamma_\sigma\left(\not{p} + m_{\tilde{G}}\right)\gamma_\eta\right] \\
&\left. + C_{P\gamma k} C^*_{P\gamma k} k_\mu k_\pi \mathrm{Tr}\left[\mathrm{P_R}\gamma_\sigma\gamma_\rho\left(\not{p} + m_{\tilde{G}}\right)\gamma_\eta\right] \right\} \\
&- \frac{1}{3}(p^\sigma - k^\sigma)\left(g^{\mu\alpha} - \frac{p^\mu p^\alpha}{m_{\tilde{G}}^2}\right)\left(g^{\pi\beta} - \frac{p^\pi p^\beta}{m_{\tilde{G}}^2}\right) \\
&\times \left\{ \left(C_{Ppk} p_\rho k_\mu + C_{Pg} g_{\mu\rho}\right)\left(C^*_{Ppk} p_\eta k_\pi + C^*_{Pg} g_{\eta\pi}\right) \mathrm{Tr}\left[\mathrm{P_R}\gamma_\sigma\left(\not{p} + m_{\tilde{G}}\right)\gamma_\alpha\gamma_\beta\right] \right. \\
&+ C_{P\gamma k} k_\mu \left(C^*_{Ppk} p_\eta k_\pi + C^*_{Pg} g_{\eta\pi}\right) \mathrm{Tr}\left[\mathrm{P_R}\gamma_\sigma\gamma_\rho\left(\not{p} + m_{\tilde{G}}\right)\gamma_\alpha\gamma_\beta\right] \\
&+ \left(C_{Ppk} p_\rho k_\mu + C_{Pg} g_{\mu\rho}\right) C^*_{P\gamma k} k_\pi \mathrm{Tr}\left[\mathrm{P_R}\gamma_\sigma\left(\not{p} + m_{\tilde{G}}\right)\gamma_\alpha\gamma_\beta\gamma_\eta\right] \\
&\left. + C_{P\gamma k} C^*_{P\gamma k} k_\mu k_\pi \mathrm{Tr}\left[\mathrm{P_R}\gamma_\sigma\gamma_\rho\left(\not{p} + m_{\tilde{G}}\right)\gamma_\alpha\gamma_\beta\gamma_\eta\right] \right\}. \qquad \text{(C.3)}
\end{aligned}
$$

The traces in this expression can be calculated easily using the commutation relations for gamma matrices and following the relations for projection operators:

$$
\begin{aligned}
\mathrm{Tr}\left[\mathrm{P_R}\gamma_\sigma\left(\not{p} + m_{\tilde{G}}\right)\right] &= 2p_\sigma, & \text{(C.4)} \\
\mathrm{Tr}\left[\mathrm{P_R}\gamma_\sigma\gamma_\rho\left(\not{p} + m_{\tilde{G}}\right)\right] &= 2m_{\tilde{G}} g_{\sigma\rho}, & \text{(C.5)} \\
\mathrm{Tr}\left[\mathrm{P_R}\gamma_\sigma\left(\not{p} + m_{\tilde{G}}\right)\gamma_\eta\right] &= 2m_{\tilde{G}} g_{\eta\sigma}, & \text{(C.6)} \\
\mathrm{Tr}\left[\mathrm{P_R}\gamma_\sigma\gamma_\rho\left(\not{p} + m_{\tilde{G}}\right)\gamma_\eta\right] &= 2(g_{\eta\sigma}p_\rho - g_{\eta\rho}p_\sigma + p_\eta g_{\sigma\rho} + p^\tau i\epsilon_{\eta\sigma\rho\tau}), & \text{(C.7)} \\
\mathrm{Tr}\left[\mathrm{P_R}\gamma_\sigma\left(\not{p} + m_{\tilde{G}}\right)\gamma_\alpha\gamma_\beta\right] &= 2(g_{\alpha\beta}p_\sigma - g_{\alpha\sigma}p_\beta + p_\alpha g_{\beta\sigma} - p^\tau i\epsilon_{\alpha\beta\sigma\tau}), & \text{(C.8)} \\
\mathrm{Tr}\left[\mathrm{P_R}\gamma_\sigma\gamma_\rho\left(\not{p} + m_{\tilde{G}}\right)\gamma_\alpha\gamma_\beta\right] &= 2m_{\tilde{G}}(g_{\alpha\beta}g_{\sigma\rho} - g_{\alpha\sigma}g_{\beta\rho} + g_{\alpha\rho}g_{\beta\sigma} - i\epsilon_{\alpha\beta\sigma\rho}), & \text{(C.9)} \\
\mathrm{Tr}\left[\mathrm{P_R}\gamma_\sigma\left(\not{p} + m_{\tilde{G}}\right)\gamma_\alpha\gamma_\beta\gamma_\eta\right] &= 2m_{\tilde{G}}(g_{\alpha\beta}g_{\eta\sigma} - g_{\alpha\eta}g_{\beta\sigma} + g_{\alpha\sigma}g_{\beta\eta} - i\epsilon_{\alpha\beta\eta\sigma}), & \text{(C.10)}
\end{aligned}
$$

and

$$\begin{aligned}
\mathrm{Tr}\left[\mathrm{P_R}\gamma_\sigma\gamma_\rho\left(\not{p}+m_{\tilde{G}}\right)\gamma_\alpha\gamma_\beta\gamma_\eta\right] &= 2(g_{\alpha\beta}(g_{\eta\sigma}p_\rho - g_{\eta\rho}p_\sigma + g_{\rho\sigma}p_\eta) \\
&\quad -g_{\alpha\eta}(g_{\beta\sigma}p_\rho - g_{\beta\rho}p_\sigma + g_{\sigma\rho}p_\beta) \\
&\quad +g_{\alpha\sigma}(g_{\beta\eta}p_\rho - g_{\beta\rho}p_\eta + g_{\eta\rho}p_\beta) \\
&\quad -g_{\alpha\rho}(g_{\beta\eta}p_\sigma - g_{\beta\sigma}p_\eta + g_{\eta\sigma}p_\beta) \\
&\quad +p_\alpha(g_{\beta\eta}g_{\sigma\rho} - g_{\beta\sigma}g_{\eta\rho} + g_{\beta\rho}g_{\eta\sigma}) \\
&\quad +ip^\tau(g_{\alpha\beta}\epsilon_{\eta\sigma\rho\tau} - g_{\alpha\eta}\epsilon_{\beta\sigma\rho\tau} + g_{\alpha\sigma}\epsilon_{\beta\eta\rho\tau} \\
&\quad -g_{\alpha\rho}\epsilon_{\beta\eta\sigma\tau} + g_{\alpha\tau}\epsilon_{\beta\eta\sigma\rho} \\
&\quad +g_{\beta\eta}\epsilon_{\alpha\sigma\rho\tau} - g_{\beta\sigma}\epsilon_{\alpha\eta\rho\tau} + g_{\beta\rho}\epsilon_{\alpha\eta\sigma\tau} - g_{\beta\tau}\epsilon_{\alpha\eta\sigma\rho} \\
&\quad +g_{\eta\sigma}\epsilon_{\alpha\beta\rho\tau} - g_{\eta\rho}\epsilon_{\alpha\beta\sigma\tau} + g_{\eta\tau}\epsilon_{\alpha\beta\sigma\rho} \\
&\quad +g_{\sigma\rho}\epsilon_{\alpha\beta\eta\tau} - g_{\sigma\tau}\epsilon_{\alpha\beta\eta\rho} + g_{\rho\tau}\epsilon_{\alpha\beta\eta\sigma})). \qquad \text{(C.11)}
\end{aligned}$$

Some of these expressions are quite extensive. However, the following simple argument can remove all complex parts. $\epsilon_{\alpha\beta\pi\rho}$ is the completely antisymmetric tensor. This means that $g^{\alpha\beta}\epsilon_{\alpha\beta\pi\rho} = 0$, as well as $k^\alpha\epsilon_{\alpha\beta\pi\rho} = -k_\alpha\epsilon_{\beta\alpha\pi\rho}$, which yields $k^\alpha k^\beta\epsilon_{\alpha\beta\pi\rho} = -k^\alpha k^\beta\epsilon_{\beta\alpha\pi\rho} = k^{\alpha'}k^{\beta'}\epsilon_{\alpha'\beta'\pi\rho} = 0$ and similar for all pairs of indices. Since there are only two external four-momenta and the metric tensor left after doing all the traces, there is no possibility of contracting all indexes in the epsilon tensor without either contracting with a metric tensor, or two times the same four momentum. As a result we can remove all terms containing an epsilon tensor. Having done all the traces

the complete expression becomes

$$\begin{aligned}
T_{\rho\eta} &= 2(p^\sigma - k^\sigma)\left(g^{\mu\pi} - \frac{p^\mu p^\pi}{m^2_{\tilde{G}}}\right)\left\{\left(C_{Ppk}p_\rho k_\mu + C_{Pg}g_{\mu\rho}\right)\left(C^*_{Ppk}p_\eta k_\pi + C^*_{Pg}g_{\eta\pi}\right)p_\sigma\right. \\
&\quad + m_{\tilde{G}}C_{P\gamma k}k_\mu\left(C^*_{Ppk}p_\eta k_\pi + C^*_{Pg}g_{\eta\pi}\right)g_{\sigma\rho} \\
&\quad + m_{\tilde{G}}\left(C_{Ppk}p_\rho k_\mu + C_{Pg}g_{\mu\rho}\right)C^*_{P\gamma k}k_\pi g_{\eta\sigma} \\
&\quad \left. + C_{P\gamma k}C^*_{P\gamma k}k_\mu k_\pi(g_{\eta\sigma}p_\rho - g_{\eta\rho}p_\sigma + p_\eta g_{\sigma\rho})\right\} \\
&\quad - \frac{2}{3}(p^\sigma - k^\sigma)\left(g^{\mu\alpha} - \frac{p^\mu p^\alpha}{m^2_{\tilde{G}}}\right)\left(g^{\pi\beta} - \frac{p^\pi p^\beta}{m^2_{\tilde{G}}}\right) \\
&\quad \times\left\{\left(C_{Ppk}p_\rho k_\mu + C_{Pg}g_{\mu\rho}\right)\left(C^*_{Ppk}p_\eta k_\pi + C^*_{Pg}g_{\eta\pi}\right)\left(g_{\alpha\beta}p_\sigma - g_{\alpha\sigma}p_\beta + p_\alpha g_{\beta\sigma}\right)\right. \\
&\quad + m_{\tilde{G}}C_{P\gamma k}k_\mu\left(C^*_{Ppk}p_\eta k_\pi + C^*_{Pg}g_{\eta\pi}\right)\left(g_{\alpha\beta}g_{\sigma\rho} - g_{\alpha\sigma}g_{\beta\rho} + g_{\alpha\rho}g_{\beta\sigma}\right) \\
&\quad + m_{\tilde{G}}\left(C_{Ppk}p_\rho k_\mu + C_{Pg}g_{\mu\rho}\right)C^*_{P\gamma k}k_\pi(g_{\alpha\beta}g_{\eta\sigma} - g_{\alpha\eta}g_{\beta\sigma} + g_{\alpha\sigma}g_{\beta\eta}) \\
&\quad + C_{P\gamma k}C^*_{P\gamma k}k_\mu k_\pi\left[g_{\alpha\beta}(g_{\eta\sigma}p_\rho - g_{\eta\rho}p_\sigma + g_{\rho\sigma}p_\eta)\right. \\
&\quad - g_{\alpha\eta}(g_{\beta\sigma}p_\rho - g_{\beta\rho}p_\sigma + g_{\sigma\rho}p_\beta) + g_{\alpha\sigma}(g_{\beta\eta}p_\rho - g_{\beta\rho}p_\eta + g_{\eta\rho}p_\beta) \\
&\quad \left.\left. - g_{\alpha\rho}(g_{\beta\eta}p_\sigma - g_{\beta\sigma}p_\eta + g_{\eta\sigma}p_\beta) + p_\alpha(g_{\beta\eta}g_{\sigma\rho} - g_{\beta\sigma}g_{\eta\rho} + g_{\beta\rho}g_{\eta\sigma})\right]\right\}. \qquad \text{(C.12)}
\end{aligned}$$

To make it more manageable, one can split this into two expressions as follows

$$T_{\rho\eta} = 2(p^\sigma - k^\sigma)\left(T^1_{\rho\eta\sigma} - \frac{1}{3}T^2_{\rho\eta\sigma}\right). \qquad \text{(C.13)}$$

Taking a closer look at $T^2_{\rho\eta\sigma}$ where Eq. (4.22) is used to remove terms containing p_α, p_β, p_μ or p_π one gets

$$\begin{aligned}
T^2_{\rho\eta\sigma} &= \left(g^{\mu\alpha} - \frac{p^\mu p^\alpha}{m^2_{\tilde{G}}}\right)\left(g^{\pi\beta} - \frac{p^\pi p^\beta}{m^2_{\tilde{G}}}\right) \\
&\quad \times\left\{\left(C_{Ppk}p_\rho k_\mu + C_{Pg}g_{\mu\rho}\right)\left(C^*_{Ppk}p_\eta k_\pi + C^*_{Pg}g_{\eta\pi}\right)g_{\alpha\beta}p_\sigma\right. \\
&\quad + m_{\tilde{G}}C_{P\gamma k}k_\mu\left(C^*_{Ppk}p_\eta k_\pi + C^*_{Pg}g_{\eta\pi}\right)\left(g_{\alpha\beta}g_{\sigma\rho} - g_{\alpha\sigma}g_{\beta\rho} + g_{\alpha\rho}g_{\beta\sigma}\right) \\
&\quad + m_{\tilde{G}}\left(C_{Ppk}p_\rho k_\mu + C_{Pg}g_{\mu\rho}\right)C^*_{P\gamma k}k_\pi(g_{\alpha\beta}g_{\eta\sigma} - g_{\alpha\eta}g_{\beta\sigma} + g_{\alpha\sigma}g_{\beta\eta}) \\
&\quad + C_{P\gamma k}C^*_{P\gamma k}k_\mu k_\pi\left[g_{\alpha\beta}(g_{\eta\sigma}p_\rho - g_{\eta\rho}p_\sigma + g_{\rho\sigma}p_\eta) - g_{\alpha\eta}(g_{\beta\sigma}p_\rho - g_{\beta\rho}p_\sigma)\right. \\
&\quad \left.\left. + g_{\alpha\sigma}(g_{\beta\eta}p_\rho - g_{\beta\rho}p_\eta) - g_{\alpha\rho}(g_{\beta\eta}p_\sigma - g_{\beta\sigma}p_\eta)\right]\right\}. \qquad \text{(C.14)}
\end{aligned}$$

One can further simplify

$$\begin{aligned}
\left(g^{\mu\alpha} - \frac{p^\mu p^\alpha}{m^2_{\tilde{G}}}\right)\left(g^{\pi\beta} - \frac{p^\pi p^\beta}{m^2_{\tilde{G}}}\right)g_{\alpha\beta} &= \left(g^{\mu\alpha} - \frac{p^\mu p^\alpha}{m^2_{\tilde{G}}}\right)\left(g^{\pi}{}_{\alpha} - \frac{p^\pi p_\alpha}{m^2_{\tilde{G}}}\right) \\
&= \left(g^{\mu\pi} - \frac{p^\mu p^\pi}{m^2_{\tilde{G}}}\right). \qquad \text{(C.15)}
\end{aligned}$$

Inserting this in Eq. (C.14), one can write it as

$$\begin{aligned} T^2_{\rho\eta\sigma} &= T^1_{\rho\eta\sigma} + \left(g^{\mu\alpha} - \frac{p^\mu p^\alpha}{m^2_{\tilde{G}}}\right)\left(g^{\pi\beta} - \frac{p^\pi p^\beta}{m^2_{\tilde{G}}}\right) \\ &\times \left\{ m_{\tilde{G}} C_{P\gamma k}\left(C^*_{Ppk} p_\eta k_\pi + C^*_{Pg} g_{\eta\pi}\right) k_\mu (g_{\alpha\rho} g_{\beta\sigma} - g_{\alpha\sigma} g_{\beta\rho}) \right. \\ &+ m_{\tilde{G}} C^*_{P\gamma k}\left(C_{Ppk} p_\rho k_\mu + C_{Pg} g_{\mu\rho}\right) k_\pi (g_{\alpha\sigma} g_{\beta\eta} - g_{\alpha\eta} g_{\beta\sigma}) \\ &+ C_{P\gamma k} C^*_{P\gamma k} k_\mu k_\pi \left[-g_{\alpha\eta}(g_{\beta\sigma} p_\rho - g_{\beta\rho} p_\sigma) \right. \\ &\left. \left. + g_{\alpha\sigma}(g_{\beta\eta} p_\rho - g_{\beta\rho} p_\eta) - g_{\alpha\rho}(g_{\beta\eta} p_\sigma - g_{\beta\sigma} p_\eta) \right] \right\}. \end{aligned} \tag{C.16}$$

By explicitly contracting indexes one can write Eq. (C.16) as

$$\begin{aligned} T^2_{\rho\eta\sigma} - T^1_{\rho\eta\sigma} &= \left\{ m_{\tilde{G}} C_{P\gamma k}\left(C^*_{Ppk} p_\eta k_\pi + C^*_{Pg} g_{\eta\pi}\right) \left(k_\rho \left(g^\pi{}_\sigma - \frac{p^\pi p_\sigma}{m^2_{\tilde{G}}} \right) \right. \right. \\ &- k_\sigma \left(g^\pi{}_\rho - \frac{p^\pi p_\rho}{m^2_{\tilde{G}}} \right) - g^\pi{}_\sigma \frac{k\cdot p}{m^2_{\tilde{G}}} p_\rho + g^\pi{}_\rho \frac{k\cdot p}{m^2_{\tilde{G}}} p_\sigma \Big) \\ &+ m_{\tilde{G}} C^*_{P\gamma k}\left(C_{Ppk} p_\rho k_\mu + C_{Pg} g_{\mu\rho}\right) \left(g^\mu{}_\sigma \left(k_\eta - \frac{k\cdot p}{m^2_{\tilde{G}}} p_\eta \right) \right. \\ &- g^\mu{}_\eta \left(k_\sigma - \frac{k\cdot p}{m^2_{\tilde{G}}} p_\sigma \right) - k_\eta \frac{p^\mu p_\sigma}{m^2_{\tilde{G}}} + k_\sigma \frac{p^\mu p_\eta}{m^2_{\tilde{G}}} \Big) \\ &+ C_{P\gamma k} C^*_{P\gamma k} [-k_\eta \left(k_\sigma p_\rho - k_\rho p_\sigma \right) \\ &\left. \left. + k_\sigma \left(k_\eta p_\rho - k_\rho p_\eta \right) - k_\rho \left(k_\eta p_\sigma - k_\sigma p_\eta \right)] \right\}. \end{aligned} \tag{C.17}$$

In Section 4.3 it was explained that parts of $T_{\rho\eta}$ that contain k_ρ or k_η will not contribute and can be removed. This leads to

$$\begin{aligned} T^2_{\rho\eta\sigma} - T^1_{\rho\eta\sigma} &= \left\{ m_{\tilde{G}} C_{P\gamma k}\left(C^*_{Ppk} p_\eta k_\pi + C^*_{Pg} g_{\eta\pi}\right) \right. \\ &\times \left[- g^\pi{}_\sigma \frac{k\cdot p}{m^2_{\tilde{G}}} p_\rho - g^\pi{}_\rho \left(k_\sigma - \frac{k\cdot p}{m^2_{\tilde{G}}} p_\sigma \right) + k_\sigma \frac{p^\pi p_\rho}{m^2_{\tilde{G}}} \right] \\ &+ m_{\tilde{G}} C^*_{P\gamma k}\left(C_{Ppk} p_\rho k_\mu + C_{Pg} g_{\mu\rho}\right) \\ &\left. \times \left[-g^\mu{}_\sigma \frac{k\cdot p}{m^2_{\tilde{G}}} p_\eta - g^\mu{}_\eta \left(k_\sigma - \frac{k\cdot p}{m^2_{\tilde{G}}} p_\sigma \right) + k_\sigma \frac{p^\mu p_\eta}{m^2_{\tilde{G}}} \right] \right\}. \end{aligned} \tag{C.18}$$

Contracting the remaining free index (π for the first term, μ for the second term) one

can write this as

$$\begin{aligned} T^2_{\rho\eta\sigma} - T^1_{\rho\eta\sigma} &= \Bigg\{ m_{\tilde{G}} C_{P\gamma k} \Bigg[- C^*_{Ppk} (k_\sigma - \frac{k\cdot p}{m^2_{\tilde{G}}} p_\sigma) p_\eta k_\rho \\ &\quad - C^*_{Pg} \left((g_{\eta\sigma} p_\rho - g_{\eta\rho} p_\sigma) \frac{k\cdot p}{m^2_{\tilde{G}}} + \left(g_{\eta\rho} - \frac{p_\eta p_\rho}{m^2_{\tilde{G}}} \right) k_\sigma \right) \Bigg] \\ &\quad + m_{\tilde{G}} C^*_{P\gamma k} \Bigg[- C_{Ppk} \left(k_\sigma - \frac{k\cdot p}{m^2_{\tilde{G}}} p_\sigma \right) p_\rho k_\eta \\ &\quad - C_{Pg} \left(\left(g_{\sigma\rho} p_\eta - g_{\eta\rho} p_\sigma \right) \frac{k\cdot p}{m^2_{\tilde{G}}} + \left(g_{\eta\rho} - \frac{p_\rho p_\eta}{m^2_{\tilde{G}}} \right) k_\sigma \right) \Bigg] \Bigg\}. \end{aligned} \tag{C.19}$$

Here one can again remove occurrences of k_ρ and k_η and get

$$\begin{aligned} T^2_{\rho\eta\sigma} - T^1_{\rho\eta\sigma} &= - m_{\tilde{G}} C_{P\gamma k} C^*_{Pg} \left[(g_{\eta\sigma} p_\rho - g_{\eta\rho} p_\sigma) \frac{k\cdot p}{m^2_{\tilde{G}}} + \left(g_{\eta\rho} - \frac{p_\eta p_\rho}{m^2_{\tilde{G}}} \right) k_\sigma \right] \\ &\quad - m_{\tilde{G}} C^*_{P\gamma k} C_{Pg} \left[(g_{\sigma\rho} p_\eta - g_{\eta\rho} p_\sigma) \frac{k\cdot p}{m^2_{\tilde{G}}} + \left(g_{\eta\rho} - \frac{p_\rho p_\eta}{m^2_{\tilde{G}}} \right) k_\sigma \right]. \end{aligned} \tag{C.20}$$

This is put into Eq. (C.13) and gives

$$\begin{aligned} T_{\rho\eta} &= \frac{4}{3}(p^\sigma - k^\sigma) T^1_{\rho\eta\sigma} + \frac{2 m_{\tilde{G}}}{3}(p^\sigma - k^\sigma) \\ &\quad \times \Bigg[C_{P\gamma k} C^*_{Pg} \left(k_\sigma \left(g_{\eta\rho} - \frac{p_\eta p_\rho}{m^2_{\tilde{G}}} \right) + \frac{k\cdot p}{m^2_{\tilde{G}}} (g_{\eta\sigma} p_\rho - g_{\eta\rho} p_\sigma) \right) \\ &\quad + C^*_{P\gamma k} C_{Pg} \left(k_\sigma \left(g_{\rho\eta} - \frac{p_\rho p_\eta}{m^2_{\tilde{G}}} \right) + \frac{k\cdot p}{m^2_{\tilde{G}}} (g_{\rho\sigma} p_\eta - g_{\rho\eta} p_\sigma) \right) \Bigg]. \end{aligned} \tag{C.21}$$

Now one can contract the last index σ in the second term of this expression and get

$$\begin{aligned} T_{\rho\eta} &= \frac{4}{3}(p^\sigma - k^\sigma) T^1_{\rho\eta\sigma} + \frac{2}{3 m_{\tilde{G}}} [(C_{P\gamma k} C^*_{Pg} + C^*_{P\gamma k} C_{Pg}) \\ &\quad \times (g_{\eta\rho} ((k\cdot p)^2 - k^2 p^2) + p_\eta p_\rho k^2) \\ &\quad - k\cdot p (C_{P\gamma k} C^*_{Pg} k_\eta p_\rho - C^*_{P\gamma k} C_{Pg} k_\rho p_\eta)], \end{aligned} \tag{C.22}$$

where one can again remove k_ρ and k_η which yields

$$T_{\rho\eta} = \frac{4}{3}(p^\sigma - k^\sigma) T^1_{\rho\eta\sigma} + \frac{4}{3 m_{\tilde{G}}} \mathrm{Re}\{ C_{P\gamma k} C^*_{Pg} \} [g_{\eta\rho} ((k\cdot p)^2 - k^2 p^2) + p_\eta p_\rho k^2]. \tag{C.23}$$

To calculate the whole trace $T_{\rho\eta}$ we now only need to calculate $T^1_{\rho\eta\sigma}$. It is given by

$$\begin{aligned} T^1_{\rho\eta\sigma} &= \left(g^{\mu\pi} - \frac{p^\mu p^\pi}{m^2_{\tilde{G}}}\right) \left\{ \left(C_{Ppk} p_\rho k_\mu + C_{Pg} g_{\mu\rho}\right) \left(C^*_{Ppk} p_\eta k_\pi + C^*_{Pg} g_{\eta\pi}\right) p_\sigma \right. \\ &+ m_{\tilde{G}} C_{P\gamma k} k_\mu \left(C^*_{Ppk} p_\eta k_\pi + C^*_{Pg} g_{\eta\pi}\right) g_{\sigma\rho} \\ &+ m_{\tilde{G}} \left(C_{Ppk} p_\rho k_\mu + C_{Pg} g_{\mu\rho}\right) C^*_{P\gamma k} k_\pi g_{\eta\sigma} \\ &\left. + |C_{P\gamma k}|^2 k_\mu k_\pi (g_{\eta\sigma} p_\rho - g_{\eta\rho} p_\sigma + p_\eta g_{\sigma\rho}) \right\}. \end{aligned} \tag{C.24}$$

Contracting over the index μ one gets

$$\begin{aligned} T^1_{\rho\eta\sigma} &= \frac{1}{m^2_{\tilde{G}}} \left(C_{Ppk} p_\rho \left(p^2 k^\pi - (k\cdot p) p^\pi\right) + C_{Pg} (p^2 g^\pi{}_\rho - p_\rho p^\pi)\right) \\ &\times \left(C^*_{Ppk} p_\eta k_\pi + C^*_{Pg} g_{\eta\pi}\right) p_\sigma \\ &+ \frac{1}{m_{\tilde{G}}} C_{P\gamma k} \left(p^2 k^\pi - (k\cdot p) p^\pi\right) \left(C^*_{Ppk} p_\eta k_\pi + C^*_{Pg} g_{\eta\pi}\right) g_{\sigma\rho} \\ &+ \frac{1}{m_{\tilde{G}}} \left(p^2 k^\mu - (k\cdot p) p^\mu\right) \left(C_{Ppk} p_\rho k_\mu + C_{Pg} g_{\mu\rho}\right) C^*_{P\gamma k} g_{\eta\sigma} \\ &+ \frac{1}{m^2_{\tilde{G}}} |C_{P\gamma k}|^2 (k^2 p^2 - (p\cdot k)^2)(g_{\eta\sigma} p_\rho - g_{\eta\rho} p_\sigma + p_\eta g_{\sigma\rho}). \end{aligned} \tag{C.25}$$

The first term (in the following called $t^1_{\rho\eta} p_\sigma$) can be written

$$\begin{aligned} m^2_{\tilde{G}} t^1_{\rho\eta} &= |C_{Ppk}|^2 p_\rho p_\eta \left(p^2 k^\pi - (k\cdot p) p^\pi\right) k_\pi \\ &+ C_{Ppk} C^*_{Pg} p_\rho \left(p^2 k^\pi - (k\cdot p) p^\pi\right) g_{\eta\pi} \\ &+ C_{Pg} C^*_{Ppk} p_\eta \left(p^2 g^\pi{}_\rho - p_\rho p^\pi\right) k_\pi \\ &+ |C_{Pg}|^2 \left(p^2 g^\pi{}_\rho - p_\rho p^\pi\right) g_{\eta\pi}. \end{aligned} \tag{C.26}$$

Contracting over π one gets

$$\begin{aligned} m^2_{\tilde{G}} t^1_{\rho\eta} &= |C_{Ppk}|^2 p_\rho p_\eta \left(p^2 k^2 - (k\cdot p)^2\right) \\ &+ C_{Ppk} C^*_{Pg} p_\rho \left(p^2 k_\eta - (k\cdot p) p_\eta\right) \\ &+ C_{Pg} C^*_{Ppk} p_\eta \left(p^2 k_\rho - (k\cdot p) p_\rho\right) \\ &+ |C_{Pg}|^2 \left(p^2 g_{\rho\eta} - p_\rho p_\eta\right). \end{aligned} \tag{C.27}$$

One can again remove k_ρ and k_η, and get

$$\begin{aligned} m^2_{\tilde{G}} t^1_{\rho\eta} &= |C_{Ppk}|^2 \left(p^2 k^2 - (k\cdot p)^2\right) p_\rho p_\eta \\ &- 2\mathrm{Re}\{C_{Ppk} C^*_{Pg}\} (k\cdot p) p_\rho p_\eta \\ &+ |C_{Pg}|^2 \left(p^2 g_{\rho\eta} - p_\rho p_\eta\right). \end{aligned} \tag{C.28}$$

C. CALCULATION OF THE TRACE

The second and third term in Eq. (C.25), in the following collectively called $t^{23}_{\rho\eta\sigma}$, is

$$\begin{aligned} t^{23}_{\rho\eta\sigma} &= \frac{1}{m_{\tilde{G}}} C_{P\gamma k} C^*_{Ppk} \left(p^2 k^\pi - (k\cdot p) p^\pi\right) k_\pi g_{\sigma\rho} p_\eta \\ &+ \frac{1}{m_{\tilde{G}}} C_{P\gamma k} C^*_{Pg} \left(p^2 k^\pi - (k\cdot p) p^\pi\right) g_{\eta\pi} g_{\sigma\rho} \\ &+ \frac{1}{m_{\tilde{G}}} C^*_{P\gamma k} C_{Ppk} \left(p^2 k^\mu - (k\cdot p) p^\mu\right) k_\mu g_{\sigma\eta} p_\rho \\ &+ \frac{1}{m_{\tilde{G}}} C^*_{P\gamma k} C_{Pg} \left(p^2 k^\mu - (k\cdot p) p^\mu\right) g_{\mu\rho} g_{\sigma\eta}. \end{aligned} \tag{C.29}$$

Contracting over π one gets

$$\begin{aligned} t^{23}_{\rho\eta\sigma} &= \frac{1}{m_{\tilde{G}}} [\left(p^2 k^2 - (k\cdot p)^2\right) \left[C_{P\gamma k} C^*_{Ppk} g_{\sigma\rho} p_\eta + C^*_{P\gamma k} C_{Ppk} g_{\sigma\eta} p_\rho\right] \\ &+ C_{P\gamma k} C^*_{Pg} \left(p^2 k_\eta - (k\cdot p) p_\eta\right) g_{\sigma\rho} + C^*_{P\gamma k} C_{Pg} \left(p^2 k_\rho - (k\cdot p) p_\rho\right) g_{\sigma\eta}], \end{aligned} \tag{C.30}$$

where one can remove k_η and k_ρ

$$\begin{aligned} t^{23}_{\rho\eta\sigma} &= \frac{1}{m_{\tilde{G}}} [\left(p^2 k^2 - (k\cdot p)^2\right) \left[C_{P\gamma k} C^*_{Ppk} g_{\sigma\rho} p_\eta + C^*_{P\gamma k} C_{Ppk} g_{\sigma\eta} p_\rho\right] \\ &- C_{P\gamma k} C^*_{Pg} (k\cdot p) p_\eta g_{\sigma\rho} - C^*_{P\gamma k} C_{Pg} (k\cdot p) p_\rho g_{\sigma\eta}]. \end{aligned} \tag{C.31}$$

Inserting Eqs. (C.28) and (C.31) in Eq. (C.25) and multiplying both sides by $(p^\sigma - k^\sigma)$ one gets

$$\begin{aligned} (p^\sigma - k^\sigma) T^1_{\rho\eta\sigma} &= \frac{(p^\sigma - k^\sigma) p_\sigma}{m^2_{\tilde{G}}} \Big[|C_{Ppk}|^2 \left(p^2 k^2 - (k\cdot p)^2\right) p_\rho p_\eta \\ &- 2\mathrm{Re}\{C_{Ppk} C^*_{Pg}\} (k\cdot p) p_\rho p_\eta + |C_{Pg}|^2 \left(p^2 g_{\rho\eta} - p_\rho p_\eta\right) \Big] \\ &+ \frac{1}{m_{\tilde{G}}} (p^\sigma - k^\sigma) [\left(p^2 k^2 - (k\cdot p)^2\right) \\ &\times [C_{P\gamma k} C^*_{Ppk} g_{\sigma\rho} p_\eta + C^*_{P\gamma k} C_{Ppk} g_{\sigma\eta} p_\rho] \\ &- C_{P\gamma k} C^*_{Pg} (k\cdot p) p_\eta g_{\sigma\rho} - C^*_{P\gamma k} C_{Pg} (k\cdot p) p_\rho g_{\sigma\eta}] \\ &+ \frac{1}{m^2_{\tilde{G}}} |C_{P\gamma k}|^2 (k^2 p^2 - (p\cdot k)^2) \\ &\times (p^\sigma - k^\sigma)(g_{\eta\sigma} p_\rho - g_{\eta\rho} p_\sigma + p_\eta g_{\sigma\rho}). \end{aligned} \tag{C.32}$$

Contracting σ this expression can be written as

$$\begin{aligned}(p^\sigma - k^\sigma)T^1_{\rho\eta\sigma} &= \frac{(p^2 - k\cdot p)}{m^2_{\tilde{G}}}\Big[|C_{Ppk}|^2\left(p^2k^2 - (k\cdot p)^2\right)p_\rho p_\eta \\ &\quad -2\mathrm{Re}\{C_{Ppk}C^*_{Pg}\}(k\cdot p)p_\rho p_\eta + |C_{Pg}|^2\left(p^2 g_{\rho\eta} - p_\rho p_\eta\right)\Big] \\ &\quad +\frac{1}{m_{\tilde{G}}}\left(p^2k^2 - (k\cdot p)^2\right)[C_{P\gamma k}C^*_{Ppk}(p_\rho - k_\rho)p_\eta \\ &\quad +C^*_{P\gamma k}C_{Ppk}(p_\eta - k_\eta)p_\rho] \\ &\quad -\frac{1}{m_{\tilde{G}}}C_{P\gamma k}C^*_{Pg}(k\cdot p)p_\eta(p_\rho - k_\rho) \\ &\quad -\frac{1}{m_{\tilde{G}}}C^*_{P\gamma k}C_{Pg}(k\cdot p)p_\rho(p_\eta - k_\eta) \\ &\quad +\frac{1}{m^2_{\tilde{G}}}|C_{P\gamma k}|^2(k^2p^2 - (p\cdot k)^2) \\ &\quad \times((p_\eta - k_\eta)p_\rho - g_{\eta\rho}(p^2 - k\cdot p) + p_\eta(p_\rho - k_\rho)). \end{aligned} \tag{C.33}$$

Removing again k_η and k_ρ this becomes

$$\begin{aligned}(p^\sigma - k^\sigma)T^1_{\rho\eta\sigma} &= \frac{(p^2 - k\cdot p)}{m^2_{\tilde{G}}}(|C_{Ppk}|^2\left(p^2k^2 - (k\cdot p)^2\right)p_\rho p_\eta \\ &\quad -2\mathrm{Re}\{C_{Ppk}C^*_{Pg}\}(k\cdot p)p_\rho p_\eta + |C_{Pg}|^2\left(p^2 g_{\rho\eta} - p_\rho p_\eta\right)) \\ &\quad +\frac{2}{m_{\tilde{G}}}\mathrm{Re}\{C_{P\gamma k}C^*_{Ppk}\}\left(p^2k^2 - (k\cdot p)^2\right)p_\eta p_\rho \\ &\quad -\frac{2}{m_{\tilde{G}}}\mathrm{Re}\{C_{P\gamma k}C^*_{Pg}\}(k\cdot p)p_\rho p_\eta \\ &\quad +\frac{1}{m^2_{\tilde{G}}}|C_{P\gamma k}|^2(k^2p^2 - (p\cdot k)^2)(2p_\eta p_\rho - g_{\eta\rho}(p^2 - k\cdot p)). \end{aligned} \tag{C.34}$$

This can be inserted in Eq. (C.23). To remove a common factor the expression is

written as $\frac{3}{4}T_{\eta\rho}$, which is

$$\begin{aligned}
\frac{3}{4}T_{\rho\eta} &= |C_{Ppk}|^2\frac{p^2-(p\cdot k)}{m_{\tilde{G}}^2}\left[p^2k^2-(p\cdot k)^2\right]p_\rho p_\eta \\
&+|C_{P\gamma k}|^2\frac{[p^2k^2-(p\cdot k)^2]}{m_{\tilde{G}}^2}[[(p\cdot k)-p^2]g_{\rho\eta}+2p_\rho p_\eta] \\
&+|C_{Pg}|^2\frac{[p^2-(p\cdot k)]}{m_{\tilde{G}}^2}\left[p^2g_{\rho\eta}-p_\rho p_\eta\right] \\
&-2\mathrm{Re}\{C_{Ppk}C_{Pg}^*\}\frac{[p^2-(p\cdot k)]}{m_{\tilde{G}}^2}(p\cdot k)p_\rho p_\eta \\
&+\frac{2}{m_{\tilde{G}}}\mathrm{Re}\{C_{P\gamma k}C_{Ppk}^*\}\left[p^2k^2-(p\cdot k)^2\right]p_\rho p_\eta \\
&+\frac{1}{m_{\tilde{G}}}\mathrm{Re}\{C_{P\gamma k}C_{Pg}^*\}[[k^2-2(p\cdot k)]p_\rho p_\eta-[p^2k^2-(p\cdot k)^2]g_{\rho\eta}]. \qquad \text{(C.35)}
\end{aligned}$$

Appendix D

Programs

Subroutines to evaluate the constants in Eqs. (B.12), (B.17), (B.21) and (B.23) :

```
C...Subrutine to calculate Cmk in the PaVe decomposition used
      SUBROUTINE PAVEKDC(P1SQ,P12SQ,P2SQ,M1SQ,M2SQ,M3SQ,PAVEKM)
      IMPLICIT NONE
C...Include LoopTools
#include "looptools.h"
C...Input parameters
      DOUBLE PRECISION P1SQ,P12SQ,P2SQ,M1SQ,M2SQ,M3SQ
      DOUBLE COMPLEX PAVEKM
C...Differences between Two Point functions
      DOUBLE COMPLEX DBA, DBB, DBC
C...The Three point function
      DOUBLE COMPLEX CSC
C...Calculation of the scalar functions
      DBA = B0(P1SQ,M1SQ,M2SQ)-B0(P2SQ,M1SQ,M3SQ)
      DBB = B0(P1SQ,M1SQ,M2SQ)-B0(P12SQ,M2SQ,M3SQ)
      DBC = B0(P2SQ,M1SQ,M3SQ)-B0(P12SQ,M2SQ,M3SQ)
      CSC = C0(P1SQ,P12SQ,P2SQ,M1SQ,M2SQ,M3SQ)

C...Calculation of the constants
      PAVEKM = 0
      PAVEKM = CSC*(M1SQ*(1D0-(P2SQ-P12SQ)/P1SQ)
     & + M2SQ*(1D0+(P2SQ-P12SQ)/P1SQ)
     &-2D0*M3SQ - P1SQ+P2SQ+P12SQ)
     & - (DBA+DBB)+(P2SQ/P1SQ-P12SQ/P1SQ)*DBC
      END


C...Subrutine to calculate Cm00 in the PaVe decomposition used
      SUBROUTINE PAVE00DC(P1SQ,P12SQ,P2SQ,M1SQ,M2SQ,M3SQ,PAVE00M)
```

```
      IMPLICIT NONE
C...Include LoopTools
#include "looptools.h"
C...Input parameters
      DOUBLE PRECISION P1SQ, P2SQ, P12SQ, M1SQ, M2SQ, M3SQ
      DOUBLE COMPLEX PAVE00M
C...Differences between Two Point functions
      DOUBLE COMPLEX DBA, DBB, DBC
C...The Three point function
      DOUBLE COMPLEX CSC
      DOUBLE COMPLEX A,B,C1,C2,C,D1
      DOUBLE COMPLEX D2,D,E1,E2,E,F,G,H
C... Denominator
      DOUBLE PRECISION DENOM
      DENOM =(P2SQ**2-2D0*P2SQ*(P1SQ+P12SQ)+(P1SQ-P12SQ)**2)
C...Calculation of the scalar functions
      DBA = B0(P1SQ,M1SQ,M2SQ)-B0(P2SQ,M1SQ,M3SQ)
      DBB = B0(P1SQ,M1SQ,M2SQ)-B0(P12SQ,M2SQ,M3SQ)
      DBC = B0(P2SQ,M1SQ,M3SQ)-B0(P12SQ,M2SQ,M3SQ)
      CSC = C0(P1SQ,P12SQ,P2SQ,M1SQ,M2SQ,M3SQ)

C...Calculation of the constant
      PAVE00M = 0
      A =CSC* ( - M1SQ*P12SQ*(P1SQ+P2SQ-P12SQ)
     & - M2SQ*P2SQ*(P1SQ-P2SQ+P12SQ)
     & + M3SQ*P1SQ*(P1SQ-P2SQ-P12SQ) + P1SQ*P2SQ*P12SQ
     &)/DENOM/2D0
      B =  (1D0/4D0)*P2SQ*(P1SQ-P2SQ+P12SQ)*DBA/DENOM
     & + (1D0/4D0)*P12SQ*(P1SQ+P2SQ-P12SQ)*DBB/DENOM
      C1 = CSC*M1SQ*P12SQ
      C2 = - (1D0/2D0)*((P1SQ-P2SQ)*DBA
     &+P12SQ*(DBB+DBC))
      C = (C1+C2)*M1SQ/2D0/DENOM
      D1 = CSC*M2SQ*P2SQ
      D2 =  (1D0/2D0)*(P2SQ*(DBC-DBA)-(P1SQ-P12SQ)*DBB)
      D = (D1+D2)*M2SQ/2D0/DENOM
      E1 = CSC*M3SQ*P1SQ
      E2 = (1D0/2D0)*(P1SQ*(DBA+DBB)-(P2SQ-P12SQ)*DBC)
      E = (E1+E2)*M3SQ/2D0/DENOM
      F = CSC/2D0*(M1SQ*M2SQ*(P1SQ-P2SQ-P12SQ)
     & - M2SQ*M3SQ*(P1SQ+P2SQ-P12SQ)
     & - M1SQ*M3SQ*(P1SQ-P2SQ+P12SQ))/DENOM
      PAVE00M = PAVE00M + A + B + C+D+E+F
      END
```

```
75
C...Subrutine to calculate Cmkk in the PaVe decomposition used
77        SUBROUTINE PAVEKKDC(P1SQ,P12SQ,P2SQ,M1SQ,M2SQ,M3SQ,PAVEKKM)
          IMPLICIT NONE
79C...Include LoopTools
#include "looptools.h"
81C...Input parameters
          DOUBLE PRECISION P1SQ,P12SQ,P2SQ,M1SQ,M2SQ,M3SQ
83        DOUBLE COMPLEX PAVEKKM
C...Differences between Two Point functions
85        DOUBLE COMPLEX DBA, DBB, DBC, DBE
C...The Three point function
87        DOUBLE COMPLEX CSC
          DOUBLE COMPLEX A,B,C1,C2,C,D1,D2,D,E1,E2,E,F1,F2,F
89C...Squares of the masses and denominator
          DOUBLE PRECISION DENOM
91        DENOM =(P2SQ**2-2D0*P2SQ*(P1SQ+P12SQ)+(P1SQ-P12SQ)**2)
C...Calculation of the scalar functions
93        DBA = B0(P1SQ,M1SQ,M2SQ)-B0(P2SQ,M1SQ,M3SQ)
          DBB = B0(P1SQ,M1SQ,M2SQ)-B0(P12SQ,M2SQ,M3SQ)
95        DBC = B0(P2SQ,M1SQ,M3SQ)-B0(P12SQ,M2SQ,M3SQ)
          DBE = B0(P2SQ,M1SQ,M3SQ)-B0(0D0,M1SQ,M3SQ)
97        CSC = C0(P1SQ,P12SQ,P2SQ,M1SQ,M2SQ,M3SQ)
C...Calculation of the constant
99        PAVEKKM = 0
          A = 6D0*CSC*(P12SQ*P2SQ*P1SQ
101      & - (M1SQ*P12SQ+M2SQ*M3SQ)*(P1SQ-P12SQ+P2SQ)
         & - (M2SQ*P2SQ+M1SQ*M3SQ)*(P1SQ+P12SQ-P2SQ)
103      & + (M3SQ*P1SQ+M1SQ*M2SQ)*(P1SQ-P12SQ-P2SQ))
          B =  3D0*(P1SQ-P2SQ)*(P1SQ*DBA+(P1SQ-P2SQ)*DBC)
105      & - 3D0*P12SQ*(P1SQ*DBA+(P1SQ+P2SQ)*DBC)
          C1 = 2D0*CSC*M1SQ*P12SQ
107       C2 = -((P1SQ-P2SQ)*DBA+P12SQ*DBB+P12SQ*DBC)
          C = 3D0*(C1+C2)*M1SQ
109       D1 = 2D0*CSC*M2SQ*P2SQ
          D2 = -(P1SQ+P2SQ-P12SQ)*DBB+2D0*P2SQ*DBC
111       D = 3D0*(D1+D2)*M2SQ
          E1 = 2D0*CSC*M3SQ
113       E2 = (DBA+DBB-(P2SQ/P1SQ-P12SQ/P1SQ)*DBC)
          E = 3D0*(E1+E2)*M3SQ*P1SQ
115       PAVEKKM = (A+B+C+D+E)/DENOM
          F1 = CSC*((P1SQ+M1SQ-M2SQ)**2/P1SQ-4D0*M1SQ)
117       F2 = - (1D0/2D0)*((M1SQ-M3SQ)/P2SQ)
         &*(P1SQ+P2SQ-P12SQ)/P1SQ*DBE
119      & - (M1SQ-M2SQ)/P1SQ*DBC+1D0
```

```
     & - (3D0/2D0*P1SQ+P2SQ/2D0-P12SQ/2D0)/P1SQ*DBC
121       F = (F1+F2)
          PAVEKKM = PAVEKKM + F
123       END


125


127 C...Subrutine to calculate Cmpk in the PaVe decomposition used
          SUBROUTINE PAVEPKDC(P1SQ,P12SQ,P2SQ,M1SQ,M2SQ,M3SQ,PAVEPKM)
129       IMPLICIT NONE
    C...Include LoopTools
131 #include "looptools.h"
    C...Input parameters
133       DOUBLE PRECISION P1SQ, P12SQ, P2SQ, M1SQ, M2SQ, M3SQ
          DOUBLE COMPLEX PAVEPKM
135 C...Differences between Two Point functions
          DOUBLE COMPLEX DBB, DBC, DBF
137 C...The Three point function
          DOUBLE COMPLEX CSC
139       DOUBLE COMPLEX A,B,C1,C2,C,D1,D2,D,E1,E2,E,F1,F2,F
    C...Squares of the masses and the denominator
141       DOUBLE PRECISION DENOM
          DENOM =(P2SQ**2-2D0*P2SQ*(P1SQ+P12SQ)+(P1SQ-P12SQ)**2)
143 C...Calculation of the scalar functions
          DBB = B0(P1SQ,M1SQ,M2SQ)-B0(P12SQ,M2SQ,M3SQ)
145       DBC = B0(P2SQ,M1SQ,M3SQ)-B0(P12SQ,M2SQ,M3SQ)
          DBF = B0(P12SQ,M2SQ,M3SQ)-B0(0D0,M1SQ,M3SQ)
147       CSC = C0(P1SQ,P12SQ,P2SQ,M1SQ,M2SQ,M3SQ)
    C...Calculation of the constant
149       PAVEPKM = 0
          A = CSC*( 3D0*P12SQ*P2SQ*(P1SQ+P2SQ-P12SQ)
151      & - 6D0*(M1SQ*M3SQ+M2SQ*P2SQ)*(P1SQ-P2SQ-P12SQ)
         & + 6D0*(M1SQ*M2SQ+M3SQ*P1SQ)*P2SQ/P1SQ*(P1SQ-P2SQ+P12SQ)
153      & - 12D0*(M2SQ*M3SQ+M1SQ*P12SQ)*P2SQ)
          B = 3D0*P2SQ*((P2SQ-P1SQ)*(DBC-DBB)
155      &+P12SQ*(DBB+DBC))
          C1 = M1SQ*P12SQ*CSC*(P1SQ+P2SQ-P12SQ)
157       C2 = (P2SQ-P1SQ)*(P1SQ*DBB-P2SQ*DBC)
         &+P12SQ*(P1SQ*DBB+P2SQ*DBC)
159       C = 3D0*(C1+C2)*M1SQ/P1SQ
          D1 = CSC*M2SQ*(P1SQ+P2SQ-P12SQ)
161       D2 = (P2SQ-P12SQ+P1SQ)*DBC-2D0*P1SQ*DBB
          D = (D1+D2)*3D0*M2SQ*P2SQ/P1SQ
163       E1 = M3SQ*CSC*(P1SQ+P2SQ-P12SQ)
          E2 = (P2SQ-P12SQ+P1SQ)*DBB-2D0*P2SQ*DBC
```

```
      E = 3D0*(E1+E2)*M3SQ
      PAVEPKM = (A+B+C+D+E)/DENOM
      F1 = CSC*((M1SQ-2D0*M2SQ-P1SQ)*(M1SQ-2D0*M3SQ-P2SQ)
     &-M1SQ*P12SQ+4D0*M1SQ*(M2SQ+M3SQ)-6D0*M2SQ*M3SQ)/P1SQ
      F2 = (1D0/2D0+P2SQ/(2D0*P1SQ)-P12SQ/(P1SQ*2D0))
     & - (M1SQ-M3SQ)/P1SQ*DBF+(1D0/2D0)*((M1SQ-M2SQ)/P1SQ*DBB
     & + (M1SQ-M3SQ)/P1SQ*DBC)+(DBB/2D0 + (P2SQ/P1SQ)*DBC/2D0)
      F = F1+F2
      PAVEPKM = PAVEPKM+F
      END
```

Evaluation of the widths in the required channels as given in Eqs. (4.83) and (4.124):

```
C...Subroutine to calculate the width of the gravitino in the decay
    channel Z nu
      SUBROUTINE GRAVITINO2BZ(LAMBDA,YFERL,YFERR,MSFERL,MSFERR,MFER
     +, MLFIN,GAMMA)
      IMPLICIT NONE
C...Commonblocks declared in seperate include file
#include "DoG.h"
C...Include LoopTools
#include "looptools.h"
C...Input parameters
      DOUBLE PRECISION LAMBDA, YFERL, YFERR
      DOUBLE PRECISION MSFERL,MSFERR,MFER
      DOUBLE PRECISION GAMMA, MLFIN
C...For calculating matrix element
      DOUBLE PRECISION ASQ,MFERSQ,MSFLSQ,MSFRSQ,MGRAVSQ
      DOUBLE PRECISION COSTHETAW, MZSQ, MLFINSQ,GA,GB
      DOUBLE COMPLEX K1,K2,K3,K1A,K2A,K3A,K1B,K2B,K3B
      DOUBLE COMPLEX C1RZPK,C1LZPK,C2RZPK,C2LZPK,C1RZKK,C1LZKK
      DOUBLE COMPLEX C1RZK,C1LZK,C1RZ0,C1LZ0,C2RZ0,C2LZ0
      DOUBLE COMPLEX DBEXTRA,DBEXTRB, AAA
C...Initialize constants
      MFERSQ = MFER*MFER
      MSFLSQ = MSFERL*MSFERL
      MSFRSQ = MSFERR*MSFERR
      MGRAVSQ = MGRAV*MGRAV
      MZSQ = MZ*MZ
      MLFINSQ = MLFIN*MLFIN
      GA = 0
      GB = 0
      K1 = 0
      K1A = 0
      K1B = 0
```

```
      K2 = 0
      K2A = 0
      K2B = 0
      K3 = 0
      K3A = 0
      K3B = 0
      C1LZKK = 0
      C1RZKK = 0
      C1LZPK = 0
      C1RZPK = 0
      C2LZPK = 0
      C2RZPK= 0
      C1RZK = 0
      C1LZK = 0
      C1LZ0 = 0
      C1RZ0 = 0
      C2LZ0 = 0
      C2RZ0 = 0
      GAMMA = 0
C...Return 0 for for low Gravitino masses
      IF (MGRAV.LT.(MZ+MLFIN+GAMMAZ/2D0)) THEN
         RETURN
      END IF
C...Initializing couplings and 2-point functions
C...At the Z mass in the MSbar scheme
      COSTHETAW = SQRT(1D0-SINSQTHETAW)
      GA = (1D0-(1D0-YFERL)*SINSQTHETAW)/COSTHETAW
      GB = YFERR*SINSQTHETAW/COSTHETAW
      DBEXTRA = 2D0*B0(0D0,MFERSQ,MSFLSQ)-B0(MGRAVSQ,MFERSQ,MSFRSQ)
     &-B0(MGRAVSQ,MSFLSQ,MFERSQ)
      DBEXTRB = 2D0*B0(0D0,MFERSQ,MSFRSQ)-B0(MGRAVSQ,MFERSQ,MSFRSQ)
     &-B0(MGRAVSQ,MFERSQ,MSFLSQ)
C...Find the constants needed for the calculations
      CALL PAVEKKDC(MGRAVSQ,MLFINSQ,MZSQ,MFERSQ,MSFLSQ,MFERSQ,C1LZKK)
      CALL PAVEKKDC(MGRAVSQ,MLFINSQ,MZSQ,MFERSQ,MSFRSQ,MFERSQ,C1RZKK)
      CALL PAVEPKDC(MGRAVSQ,MLFINSQ,MZSQ,MFERSQ,MSFLSQ,MFERSQ,C1LZPK)
      CALL PAVEPKDC(MGRAVSQ,MLFINSQ,MZSQ,MFERSQ,MSFRSQ,MFERSQ,C1RZPK)
      CALL PAVEPKDC(MGRAVSQ,MLFINSQ,MZSQ,MSFLSQ,MFERSQ,MSFLSQ,C2LZPK)
      CALL PAVEPKDC(MGRAVSQ,MLFINSQ,MZSQ,MSFRSQ,MFERSQ,MSFRSQ,C2RZPK)
      CALL PAVEKDC(MGRAVSQ,MLFINSQ,MZSQ,MFERSQ,MSFLSQ,MFERSQ,C1LZK)
      CALL PAVEKDC(MGRAVSQ,MLFINSQ,MZSQ,MFERSQ,MSFRSQ,MFERSQ,C1RZK)
      CALL PAVE00DC(MGRAVSQ,MLFINSQ,MZSQ,MFERSQ,MSFLSQ,MFERSQ,C1LZ0)
      CALL PAVE00DC(MGRAVSQ,MLFINSQ,MZSQ,MFERSQ,MSFRSQ,MFERSQ,C1RZ0)
      CALL PAVE00DC(MGRAVSQ,MLFINSQ,MZSQ,MSFLSQ,MFERSQ,MSFLSQ,C2LZ0)
      CALL PAVE00DC(MGRAVSQ,MLFINSQ,MZSQ,MSFRSQ,MFERSQ,MSFRSQ,C2RZ0)
```

```
77 C...Calculate dimensionless the constants K_1, K_2 and K_3
       K1A = 4D0*(C1LZKK-C1RZKK+C1RZPK+C2LZPK-C1RZK)
79     K1B = 4D0*(C1RZKK-C1LZKK+C1LZPK+C2RZPK-C1LZK)
       K2A = 2D0*(C1RZKK-C1LZKK-C1RZPK+C1LZPK+C1RZK)
81     K2B = 2D0*(C1LZKK-C1RZKK-C1LZPK+C1RZPK+C1LZK)
       K3A = DBEXTRA-4D0*C1RZ0-4D0*C2LZ0
83     K3B = DBEXTRB-4D0*C1LZ0-4D0*C2RZ0

85     K1 = GA*K1A + GB*K1B
       K2 = GA*K2A + GB*K2B
87     K3 = GA*K3A + GB*K3B

89 C...Calculation of the squared matrix element
       ASQ = 1/96D0*DBLE(K1*CONJG(K1))*(MGRAVSQ/MZSQ-1D0)
91    & + 1/24D0*DBLE(K2*CONJG(K2))
      &*(MGRAVSQ/(MZSQ)+3D0*MGRAVSQ/(MGRAVSQ-MZSQ))
93    & + 1/24D0*DBLE(K3*CONJG(K3))*(1D0-MZSQ/MGRAVSQ)
      &*(MZSQ/MGRAVSQ + MGRAVSQ/MZSQ+10D0)
95    & + 1/24D0*DBLE(K1*CONJG(K3))*(MGRAVSQ/MZSQ-MZSQ/MGRAVSQ)
      & + 1/24D0*DBLE(K1*CONJG(K2))*MGRAVSQ/MZSQ
97    & + 1/12D0*DBLE(K2*CONJG(K3))*(3D0+MGRAVSQ/MZSQ)

99 C...Calculation of the prefactors
       GAMMA = ALPHA*LAMBDA**2*MFERSQ
101   &*(MGRAVSQ-MZSQ)
      &/(8192D0*PI**4*SINSQTHETAW*MGRAV*MP**2)
103
   C...Calculation of the Width
105    GAMMA = ASQ*GAMMA
       END
107


109 C...Subroutine to calculate the width of the gravitino in the decay
      channel Wl
       SUBROUTINE GRAVITINO2BW(LAMBDA,MSFERDL,MSFERDR,MSFERUL,MFERD
111   +,MFERU,MLFIN,GAMMA)
       IMPLICIT NONE
113 C...Commonblocks declared in seperate include file
   #include "DoG.h"
115 C...Include LoopTools
   #include "looptools.h"
117 C...Input parameters
       DOUBLE PRECISION LAMBDA
119    DOUBLE PRECISION MSFERDL,MSFERDR,MSFERUL,MSFERD,MFERU,MLFIN
       DOUBLE PRECISION GAMMA,MFERD
```

```
C...For calculating matrix element
      DOUBLE PRECISION ASQ,MFERDSQ,MFERUSQ,MSFDLSQ,MSFDRSQ,  MSFULSQ
      DOUBLE PRECISION MGRAVSQ,MLFINSQ,MWSQ
      DOUBLE COMPLEX K1,K2,K3,C1AWKK,C1BWKK,C1AWPK,C1BWPK
      DOUBLE COMPLEX C2WPK,C1BWK,C1BW0,C2W0
      DOUBLE COMPLEX DBEXDSU,DBEXUSD,DEXTRA
C...Initialize constants
      K1 = 0
      K2 = 0
      K3 = 0
      C1AWKK = 0
      C1BWKK = 0
      C1AWPK = 0
      C1BWPK = 0
      C2WPK = 0
      C1BWK = 0
      C1BW0 = 0
      C2W0 = 0
      MFERDSQ = MFERD*MFERD
      MFERUSQ = MFERU*MFERU
      MSFDLSQ = MSFERDL*MSFERDL
      MSFDRSQ = MSFERDR*MSFERDR
      MSFULSQ = MSFERUL*MSFERUL
      MGRAVSQ = MGRAV*MGRAV
      MLFINSQ = MLFIN*MLFIN
      GAMMA = 0
C...Return 0 for for low Gravitino masses
      IF (MGRAV.LT.(MW+MLFIN+GAMMAW/2D0)) THEN
         RETURN
      END IF
C...Initializing couplings and 2-point functions
      MWSQ = MW*MW
      DBEXUSD = B0(MLFINSQ,MFERUSQ,MSFDRSQ)-B0(0D0,MFERUSQ,MSFDRSQ)
      DBEXDSU = B0(MLFINSQ,MFERDSQ,MSFULSQ)-B0(0D0,MFERDSQ,MSFULSQ)
      DEXTRA = B0(MGRAVSQ,MFERDSQ,MSFDRSQ)+B0(MGRAVSQ,MSFDLSQ,MFERDSQ)
     &- 2D0*B0(MLFINSQ,MFERDSQ,MSFULSQ)
C...Find the constants needed for the calculations
      CALL PAVEKKDC(MGRAVSQ,MLFINSQ,MWSQ,MFERUSQ,MSFULSQ,MFERDSQ,C1AWKK)
      CALL PAVEKKDC(MGRAVSQ,MLFINSQ,MWSQ,MFERDSQ,MSFDRSQ,MFERUSQ,C1BWKK)
      CALL PAVEPKDC(MGRAVSQ,MLFINSQ,MWSQ,MFERUSQ,MSFULSQ,MFERDSQ,C1AWPK)
      CALL PAVEPKDC(MGRAVSQ,MLFINSQ,MWSQ,MFERDSQ,MSFDRSQ,MFERUSQ,C1BWPK)
      CALL PAVEPKDC(MGRAVSQ,MLFINSQ,MWSQ,MSFDLSQ,MFERDSQ,MSFULSQ,C2WPK)
      CALL PAVEKDC(MGRAVSQ,MLFINSQ,MWSQ,MFERDSQ,MSFDRSQ,MFERUSQ,C1BWK)
      CALL PAVE00DC(MGRAVSQ,MLFINSQ,MWSQ,MFERDSQ,MSFDRSQ,MFERUSQ,C1BW0)
      CALL PAVE00DC(MGRAVSQ,MLFINSQ,MWSQ,MSFDLSQ,MFERDSQ,MSFULSQ,C2W0)
```

```
C...Calculate dimensionless the constants K_1, K_2 and K_3
      K1 = 4D0*SQRT(2D0)*(-C1BWPK-C2WPK+C1BWKK-C1AWKK-C1BWK
     &+(MFERUSQ/MGRAVSQ-MSFDRSQ/MGRAVSQ)*DBEXUSD
     &-(MFERDSQ/MGRAVSQ-MSFULSQ/MGRAVSQ)*DBEXDSU)
      K2 = 2D0*SQRT(2D0)*(C1BWPK-C1AWPK+(C1AWKK-C1BWKK+C1BWK)
     &*(1D0 + MLFIN/MGRAV))
     &+SQRT(2D0)*(MSFULSQ-MFERDSQ)*(MWSQ-MLFINSQ-MGRAVSQ)*DBEXDSU
     &/(MLFIN*MGRAV*MGRAVSQ)
     &-SQRT(2D0)*(MSFDRSQ-MFERUSQ)*(MWSQ-MLFINSQ-MGRAVSQ)*DBEXUSD
     &/(MLFIN*MGRAV*MGRAVSQ)
     &+2D0*SQRT(2D0)*((MSFULSQ/MGRAVSQ-MFERDSQ/MGRAVSQ)*DBEXDSU
     &-(MSFDRSQ/MGRAVSQ-MFERUSQ/MGRAVSQ)*DBEXUSD)
      K3 = SQRT(2D0)*(4D0*C2W0+4D0*C1BW0+DEXTRA)

C...Calculation of the squared matrix element
      ASQ = 1/96D0*DBLE(K1*CONJG(K1))*((MGRAVSQ+MLFINSQ)/MWSQ -1D0)
     & + 1/24D0*DBLE(K2*CONJG(K2))*MGRAVSQ/MWSQ
     &*(1D0+3D0*(MGRAVSQ-MWSQ+MLFINSQ)*MWSQ
     &/((MGRAVSQ-(MW-MLFIN)**2)*(MGRAVSQ - (MW+MLFIN)**2)))
     & + 1/24D0*DBLE(K3*CONJG(K3))*(1D0-MWSQ/MGRAVSQ+MLFINSQ/MGRAVSQ)
     &*((MW/MGRAV-MLFINSQ/(MGRAV*MW))**2
     &+10D0+MGRAVSQ/MWSQ-2D0*MLFINSQ/MWSQ)
     & + 1/24D0*DBLE(K1*CONJG(K3))*(MGRAVSQ/MWSQ
     &-(MW/MGRAV-MLFINSQ/(MGRAV*MW))**2)
     & + 1/24D0*DBLE(K1*CONJG(K2))*MGRAVSQ/MWSQ
     & + 1/12D0*DBLE(K2*CONJG(K3))*(MGRAVSQ/MWSQ+3D0-MLFINSQ/MWSQ)
C...Calculation of the coupling
      GAMMA = ALPHA*LAMBDA**2*MFERDSQ
     &*SQRT(MGRAVSQ - (MW+MLFIN)**2)*SQRT(MGRAVSQ - (MW-MLFIN)**2)
     &/(8192D0*PI**4*SINSQTHETAW*MGRAV*MP**2)
C...Calculation of the Width
      GAMMA = ASQ*GAMMA
      END
```

References

[1] G. Moreau and M. Chemtob, "R-parity Violation and the Cosmological Gravitino Problem," *Phys.Rev.* **D65** (2002) 024033, arXiv:hep-ph/0107286 [hep-ph]. ii, 1, 27, 61, 64, 67

[2] S. Lola, P. Osland, and A. Raklev, "Radiative gravitino decays from R-parity violation," *Phys.Lett.* **B656** (2007) 83–90, arXiv:0707.2510 [hep-ph]. ii, 1, 27, 61, 64, 67

[3] T. Hahn and M. Perez-Victoria, "Automatized One Loop Calculations in Four-Dimensions and D-Dimensions," *Comput.Phys.Commun.* **118** (1999) 153–165, arXiv:hep-ph/9807565 [hep-ph]. http://www.feynarts.de/looptools/. 1, 33, 61

[4] T. Sjostrand, S. Mrenna, and P. Skands, "Pythia 6.4 physics and manual," *JHEP* **0605** (2006) 026. doi:10.1088/1126-6708/2006/05/026. 1, 63

[5] S. P. Martin, "A Supersymmetry primer," arXiv:hep-ph/9709356 [hep-ph]. 3, 14, 18

[6] H. J. W. Müller-Kirsten and A. Wiedemann, *Introduction to Supersymmetry.* World Scientific Publishing Co. Pte. Ldt., second ed., 2010. 3, 7, 10, 11, 12

[7] R. Haag, J. T. Lopuszanski, and M. Sohnius, "All Possible Generators of Supersymmetries of the S Matrix," *Nucl.Phys.* **B88** (1975) 257. 4

[8] A. Salam and J. Strathdee, "On Superfields and Fermi-Bose Symmetry," *Phys.Rev.* **D11** (1975) 1521–1535. 7

[9] S. Ferrara and B. Zumino, "Supergauge Invariant Yang-Mills Theories," *Nucl.Phys.* **B79** (1974) 413. 10

[10] J. Bagger and J. Wess, "Partial Breaking of Extended Supersymmetry," *Phys.Lett.* **B138** (1984) 105. 10

[11] S. Ferrara, L. Girardello, and F. Palumbo, "A General Mass Formula in Broken Supersymmetry," *Phys.Rev.* **D20** (1979) 403. 11

[12] D. Z. Freedman, P. van Nieuwenhuizen, and S. Ferrara, "Progress Toward a Theory of Supergravity," *Phys.Rev.* **D13** (1976) 3214–3218. 12, 21

[13] **Particle Data Group** Collaboration, K. Nakamura *et al.*, "Review of Particle Physics," *J.Phys.G* **G37** (2010) 075021. 17, 64

[14] P. Fayet, "Spontaneous Supersymmetry Breaking Without Gauge Invariance," *Phys.Lett.* **B58** (1975) 67. 17

[15] H. K. Dreiner, "An Introduction to Explicit R-Parity Violation," `arXiv:hep-ph/9707435 [hep-ph]`. Published in '*Perspectives on Supersymmetry*', Ed. by G.L. Kane, World Scientific. 17

[16] L. E. Ibanez and G. G. Ross, "Discrete Gauge Symmetries and the Origin of Baryon and Lepton Number Conservation in Supersymmetric Versions of the Standard Model," *Nucl.Phys.* **B368** (1992) 3–37. 17

[17] S. Lola and G. G. Ross, "Baryon and lepton number (non)conservation in supersymmetric theories," *Phys.Lett.* **B314** (1993) 336–344. 17

[18] F. Zwicky, "Spectral Displacement of Extra Galactic Nebulae," *Helv.Phys.Acta* **6** (1933) 110–127. 18

[19] **WMAP** Collaboration, D. N. Spergel *et al.*, "First Year Wilkinson Microwave Anisotropy Probe (WMAP) Observations: Determination of Cosmological Parameters," *Astrophys. J. Suppl.* **148** (2003) 175–194, `arXiv:astro-ph/0302209`. 18

[20] G. Bertone, D. Hooper, and J. Silk, "Particle Dark Matter: Evidence, Candidates and Constraints," *Phys.Rept.* **405** (2005) 279–390, `arXiv:hep-ph/0404175 [hep-ph]`. 18

[21] G. Jungman, M. Kamionkowski, and K. Griest, "Supersymmetric Dark Matter," *Phys.Rept.* **267** (1996) 195–373, `arXiv:hep-ph/9506380 [hep-ph]`. 18

[22] **ATLAS** Collaboration, G. Aad *et al.*, "Search for the Standard Model Higgs Boson in the Decay Channel H→ZZ(*)→4l with 4.8 fb^{-1} of pp Collision Data at sqrt(s) = 7 TeV with ATLAS," *Phys. Lett.* **B710** (2012) 383–402, `arXiv:1202.1415 [hep-ex]`. 18

[23] **ATLAS** Collaboration, G. Aad *et al.*, "Search for the Standard Model Higgs boson in the Diphoton Decay Channel with 4.9 fb^{-1} of pp Collisions at sqrt(s)=7 TeV with ATLAS," *Phys.Rev.Lett.* **108** (2012) 111803, `arXiv:1202.1414 [hep-ex]`. 18

[24] **ATLAS** Collaboration, G. Aad *et al.*, "Combined Search for the Standard Model Higgs Boson using up to 4.9 fb^{-1} of pp Collision Data at sqrt(s) = 7 TeV with the ATLAS Detector at the LHC," *Phys.Lett.* **B710** (2012) 49–66, `arXiv:1202.1408 [hep-ex]`. 18

[25] E. Cremmer, S. Ferrara, L. Girardello, and A. Van Proeyen, "Yang-Mills Theories with Local Supersymmetry: Lagrangian, Transformation Laws and SuperHiggs Effect," *Nucl. Phys.* **B212** (1983) 413. 21

[26] W. Rarita and J. Schwinger, "On a Theory of Particles with Half Integral Spin," *Phys.Rev.* **60** (1941) 61. 22

[27] M. Bolz, "Thermal production of gravitinos,". Ph.D. Thesis (Advisor: W. Buchmuller). 22, 85

[28] M. Bolz, A. Brandenburg, and W. Buchmuller, "Thermal Production of Gravitinos," *Nucl.Phys.* **B606** (2001) 518–544, arXiv:hep-ph/0012052 [hep-ph]. 26

[29] M. Fukugita and T. Yanagida, "Baryogenesis Without Grand Unification," *Phys.Lett.* **B174** (1986) 45. 27

[30] F. D. Steffen, "Gravitino Dark Matter and Cosmological Constraints," *JCAP* **0609** (2006) 001, arXiv:hep-ph/0605306 [hep-ph]. 27

[31] A. Ibarra and D. Tran, "Gamma Ray Spectrum from Gravitino Dark Matter Decay," *Phys. Rev. Lett.* **100** (2008) 061301, arXiv:0709.4593 [astro-ph]. 28

[32] A. R. Raklev, "Massive Metastable Charged (S)Particles at the LHC," *Mod. Phys. Lett.* **A24** (2009) 1955–1969, arXiv:0908.0315 [hep-ph]. 28

[33] **Fermi-LAT** Collaboration, A. Abdo *et al.*, "The Spectrum of the Isotropic Diffuse Gamma-Ray Emission Derived From First-Year Fermi Large Area Telescope Data," *Phys.Rev.Lett.* **104** (2010) 101101, arXiv:1002.3603 [astro-ph.HE]. 28, 63, 65, 66, 78

[34] G. Passarino and M. Veltman, "One Loop Corrections for e+ e- Annihilation Into mu+ mu- in the Weinberg Model," *Nucl.Phys.* **B160** (1979) 151. 33

[35] A. Raklev, "Dog - a program for the decay of gravitinos.." private code, 2012. 61

[36] P. Z. Skands, B. Allanach, H. Baer, C. Balazs, G. Belanger, *et al.*, "SUSY Les Houches Accord: Interfacing SUSY Spectrum Calculators, Decay Packages, and Event Generators," *JHEP* **0407** (2004) 036, arXiv:hep-ph/0311123 [hep-ph]. 63

[37] A. Ibarra and D. Tran, "Antimatter Signatures of Gravitino Dark Matter Decay," *JCAP* **0807** (2008) 002, arXiv:0804.4596 [astro-ph]. 64

[38] **LAT** Collaboration, W. Atwood *et al.*, "The Large Area Telescope on the Fermi Gamma-Ray Space Telescope Mission," *Astrophys.J.* **697** (2009) 1071–1102, arXiv:0902.1089 [astro-ph.IM]. 64

[39] G. Cowan, *Statistical Data Analysis*. Oxford Science Publications. Clarendon Press, 1998. 65

[40] A. Denner, H. Eck, O. Hahn, and J. Kublbeck, "Feynman Rules for Fermion Number Violating Interactions," *Nucl.Phys.* **B387** (1992) 467–484. 85

REFERENCES

[41] R. Mertig, M. Bohm, and A. Denner, "FEYN CALC: Computer Algebraic Calculation of Feynman Amplitudes," *Comput.Phys.Commun.* **64** (1991) 345–359. `www.feyncalc.org`. 99